

Continuous Edit Distance, Geodesics and Barycenters of Time-varying Persistence Diagrams

Sebastien Tchitche, Mohamed Kissi, Julien Tierny

Abstract—We introduce the *Continuous Edit Distance* (CED), a geodesic and elastic distance for *time-varying persistence diagrams* (TVPDs). The CED extends edit-distance ideas to TVPDs by combining local substitution costs with penalized deletions/insertions, controlled by two parameters: α (trade-off between temporal misalignment and diagram discrepancy) and β (gap penalty). We also provide an explicit construction of CED-geodesics. Building on these ingredients, we present two practical barycenter solvers—one stochastic and one greedy—that monotonically decrease the CED Fréchet energy. Empirically, the CED is robust to additive perturbations (both temporal and spatial), recovers temporal shifts, and supports temporal pattern search. On real-life datasets, the CED achieves clustering performance comparable or better than standard elastic dissimilarities, while our clustering based on CED-barycenters yields superior classification results. Overall, the CED equips TVPD analysis with a principled distance, interpretable geodesics, and practical barycenters, enabling alignment, comparison, averaging, and clustering directly in the space of TVPDs. A C++ implementation is provided for reproducibility at the following address <https://github.com/sebastien-tchitche/ContinuousEditDistance>.

Index Terms—Topological data analysis, persistent homology, time-varying data.

I. INTRODUCTION

ADVANCEMENTS in data simulation and acquisition techniques have led to an ever-increasing data complexity and volume. Consequently, traditional analytical approaches often become inadequate, as they were not designed to handle such intricate and voluminous data. Thus, the introduction of abstractions capable of summarizing and interpreting this data becomes necessary to enable its analysis.

Topological data analysis (TDA) [1] provides a set of methods for the efficient encoding of the topological features of a dataset into concise topological representations, such as persistent diagrams [2], merge and contour trees [3], [4], Reeb graphs [5], [6], or Morse-Smale complexes [7], [8]. These representations have been successfully employed in a variety of applications such as combustion [9], [10], material sciences [11], [12], fluid dynamics [13], [14], chemistry [15], [16], astrophysics [17], [18], or geometry processing [19] and data science [20], [21]. Among the descriptors studied in TDA, we focus in this work on a very popular representation: the persistence diagram.

In addition to the increasing geometrical complexity and volume of datasets, users can face time-varying data, where a given phenomenon is represented not by a single dataset but

S. Tchitche, M. Kissi, and J. Tierny are with the CNRS and Sorbonne Université. E-mail: {sebastien.tchitche, mohamed.kissi}@etu.sorbonne-universite.fr, julien.tierny@sorbonne-universite.fr

Manuscript received XXXX XX, XXXX; revised XXXXX XX, XXXX.

by a succession of datasets. In the framework of persistent homology, if each dataset is converted into a persistence diagram, the user obtains a time-indexed family of persistence diagrams. We will refer to each such family as a time-varying persistence diagram (TVPD) hereafter.

In that context, TVPDs have recently found use as a means to study data that evolves over time. Some applications have been protein folding trajectory analysis [22], music classification [23], time-varying scalar field analysis [12], and analysis of dynamic functional brain connectivity [24].

However, to integrate TVPDs into traditional data analysis pipelines, additional tools are required for their study. In particular, essential components such as an elastic distance, geodesics, and barycenter computation methods are currently lacking. Indeed, a distance enables the use of specific search methods [25], piecewise constant approximations [26], and machine-learning methods with theoretical guarantees [27]–[29]. Geodesics allow, for example, principal geodesic analysis [30], [31] to facilitate variability analysis and visualization. Barycenters are necessary for performing k -means clustering and to obtain the corresponding centroids [32]. Equally important, to deal with the asynchronous nature of a given phenomenon over time, one needs an elastic distance—that is, a distance that remains robust to time shifts and time dilatation.

This paper addresses this problem by introducing a geodesic and elastic distance between TVPDs, called Continuous Edit Distance (CED), and whose barycenters can be computed. As its name suggests, the CED can be seen as an extension of the Edit distance with Real Penalty (ERP) [33], from numerical time series to TVPDs. Intuitively, our distance measures the minimal cost to transform one TVPD into another, through elementary operations—deletion, substitution, and insertion. Moreover, the CED can be used as a visual comparison tool, capturing similarities between two TVPDs.

A. Related work

The literature related to our work can be classified into two main families: (i) topological methods, and (ii) elastic dissimilarities.

(i) Topological methods: Several tools and methods have been developed for analysing persistence diagrams and TVPDs. Building on optimal-transport concepts [34]–[36] the Wasserstein distance is a popular metric for persistence diagrams. This distance exhibits stability properties that make it particularly well suited to the topological analysis scalar fields [37]. Based on the Wasserstein metric, several works have aimed to compute a representative barycenter for a persistence

diagram sample. The pioneering algorithm was proposed by Turner et al. with Frechet mean computation [38], while later Lacombe et al. [39] introduced an entropy-regularised optimal-transport variant, and Vidal et al. [32] presented a progressive computation method.

Cohen-Steiner et al. [22] introduced vineyards as the piecewise-linear trajectories traced by the points of a persistence diagram as the underlying data evolves piecewise-linearly over time. Vineyards, which reveal how individual birth-death pairs evolve through time, provide an interpretable topological summary for dynamic data [12], [22], with their piecewise-linear structure being exploited to track persistence pairs efficiently.

Turner [38] defines vineyards as equally long continuous TVPDs and, by encoding them as vineyard modules whose behaviour is captured by a matrix representation, furnishes under certain conditions a tractable framework for analysing their evolving topological structure.

Munch et al., [40] replace the classical Fréchet mean with a probabilistic Fréchet mean (PFM), a probability measure on diagram space. Evaluated along equal-length continuous vineyards, the PFM yields a continuous mean vineyard (avoiding the discontinuities of the classical mean) and can be stably computed on bootstrap samples of time-varying point clouds, making it a tool for statistical analysis.

(ii) Elastic dissimilarities: In this section, we briefly review the principal elastic dissimilarities proposed in the literature, from foundational works to more recent contributions.

Firstly, the Fréchet distance [41], [42] is originally defined as an elastic distance between curves by considering the minimal leash length required to traverse them in a continuous and monotonic fashion. Naturally suited for comparing time-parameterized trajectories, it captures both spatial proximity and ordering of points. However, the Fréchet distance is known to be sensitive to small perturbations, making it unstable in the presence of noise or irregular sampling [43]. This sensitivity limits its direct applicability in real-world time series analysis, especially in domains where robustness is essential.

Levenshtein et al. [44] introduce the edit distance as an elastic distance between character strings, defined as the minimum number of character insertions, deletions, and substitutions required to transform one string into another [45]. Initially designed for applications in error correction and computational linguistics, it has since been widely used in fields such as bioinformatics, natural language processing, and information retrieval [46].

Alternatively, Sakoe and Chiba [47] define dynamic time warping (DTW), an elastic dissimilarity between time series, as an approach to continuous speech recognition. Due to its efficiency it is extensively applied to other domains [48]–[50]. Subsequently, several methods of time series averaging for DTW have been developed and applied [51]–[54]. However, DTW is not a distance, as it does not satisfy the triangle inequality nor identity of indiscernibles.

Following [44], various extensions and approximations of the edit distance have been proposed to improve computational efficiency or adapt it to specific data types. Among these, the Edit distance with Real Penalty (ERP), introduced by Chen

and Ng [33] is an adaptation of the edit distance to time series [55], [56]. An arbitrary reference element is first fixed, then one seeks to transform a time series into another at minimal cost, through elementary operations — deletion, substitution, and insertion. A deletion or insertion of an element from a time series has a cost proportional to its deviation from the reference element. A substitution between two elements from different time series has a cost proportional to their difference.

Later, the Time Warp Edit Distance (TWED) is introduced by Marteau [26] as an elastic distance for time series that simultaneously accounts for both temporal distortions and amplitude variations. The TWED gives an alternative to the ERP by incorporating time stamps into the cost scheme, and by modifying the costs of the elementary operations. The TWED has been successfully applied in time series classification [26], [57], and clustering [58], particularly in contexts requiring metric consistency. However, the TWED, despite being a distance, is not well adapted to the geometry of the space of persistence diagrams. Indeed, even when the TWED is adapted to the persistence-diagram setting, the cost of deleting (or inserting) an element does not depend on its persistence. By contrast, in an ERP-based model, if the empty diagram is used as a reference, the deletion/insertion cost of an element becomes proportional to its persistence. This is consistent with the standard geometric interpretation in TDA, where more persistent features are both more significant and more expensive to remove.

Soft Dynamic Time Warping (Soft-DTW) is introduced by Cuturi and Blondel [59] as a smooth, differentiable relaxation of the classical DTW, obtained by replacing the hard-minimum operator in DTW's cost with a parameter-controlled soft-minimum. Controlled by this parameter $\gamma > 0$, Soft-DTW converges to the exact DTW distance as $\gamma \rightarrow 0$, while for a finite γ it yields a differentiable objective whose gradients can be efficiently computed. This differentiability enables seamless integration as a loss function in gradient-based optimisation pipelines, leading to applications in time-series averaging, prototype learning, and end-to-end neural network training [59]–[61]. Although Soft-DTW is an elastic dissimilarity, it does not constitute a distance, violating identity of indiscernibles and triangle inequality, but its smoothness provides favourable optimisation landscapes compared to the classical DTW [60].

B. Contributions

This paper makes the following new contributions:

- *A practical distance between TVPDs:* We extend the Edit Distance with Real penalty [33] to TVPDs. Unlike other state-of-the-art distances that can be adapted to TVPDs framework, our distance allows the computation of barycenters and geodesics between TVPDs.
- *An algorithm for computing geodesics between TVPDs:* Given our metric, we present a simple three-step approach for computing geodesics between TVPDs.
- *An approach for computing the barycenter of a set of TVPDs :* We extend two popular minimization schemes for computing barycenters of a set of TVPD : a deterministic scheme (imitating greedy subgradient descent), and a

stochastic one (imitating stochastic subgradient descent). Both versions are iterative with monotone improvement and come with practical stopping criteria.

- *An application to pattern matching:* We present an application to temporal pattern matching between TVPDs.
- *An application to clustering:* We illustrate the practical relevance of our barycenters in clustering problems.
- *Implementation:* We provide a C++ implementation of our algorithms that can be used for reproducibility (available at this address <https://github.com/sebastien-tchitchek/ContinuousEditDistance>).

II. PRELIMINARIES

This section presents the theoretical background required for the presentation our work. It formalizes our input data and introduces persistent diagrams and a typical metric for their comparison. We refer the reader to standard textbooks [1], [62] for an introduction to TDA.

A. Input data

We define a timed PL-scalar field as an ordered pair (f, t) , with $t \in \mathbb{R}$, and f a piecewise-linear (PL) scalar field $f : \mathcal{M}_f \rightarrow \mathbb{R}$ defined on a PL $(d_{\mathcal{M}_f})$ -manifold \mathcal{M}_f with $d_{\mathcal{M}_f} \leq 3$ in our applications.

Let $\Delta \in (0, +\infty)$. Each input in our study is a sequence of timed PL-scalar fields $U_n = ((f_n, t_n))_{0 \leq n \leq N_U}$, with $N_U \in \mathbb{N}^*$, such that $\Delta \mid (t_{N_U} - t_0)$ (i.e. $\exists k \in \mathbb{N}^*, (t_{N_U} - t_0) = k \cdot \Delta$). If $n \in \mathbb{N}$, for any threshold $w \in \mathbb{R}$, we write $L_w^-(f_n) = f_n^{-1}((-\infty, w])$ for the sub-level set of f_n at w . As w grows, the topology of $L_w^-(f_n)$ changes only at the critical values of f_n . The corresponding critical points $c \in \mathcal{M}_{f_n}$ can be classified by their Morse index $\mathcal{I}(c)$: 0 for minima, 1 for 1-saddles, $d_{\mathcal{M}_{f_n}} - 1$ for $(d_{\mathcal{M}_{f_n}} - 1)$ -saddles, and $d_{\mathcal{M}_{f_n}}$ for maxima. We assume, in practice [63], [64], that all critical points are isolated and non-degenerate. Following the Elder rule [1], every topological feature (i.e., connected components, cycles, and voids) that appears during the sweep $w : -\infty \rightarrow +\infty$ of $L_w^-(f_n)$ can be associated with a pair of critical points (c, c') such that $f_n(c) < f_n(c')$ and $\mathcal{I}(c) = \mathcal{I}(c') - 1$. The older point c marks the birth of the feature, whereas the younger point c' signals its death. The pair (c, c') is therefore called a persistence pair. For instance, when two connected components merge at a critical point c' , the component that appeared last (the youngest) vanishes while the oldest persists. Representing each persistence pair by the coordinates $(b, d) = (f_n(c), f_n(c'))$ produces a two-dimensional multiset known as the persistence diagram, denoted X_n . As shown in Fig. 1, prominent topological features correspond to pairs (b, d) far from the diagonal $\Lambda = \{(b, d) \in \mathbb{R}^2 \mid b = d\}$ —that is, pairs whose lifespan $d - b$ (called their persistence) is large—whereas pairs generated by small-amplitude noise accumulate near the diagonal. By repeating this procedure for each timed PL-scalar field (f_n, t_n) of $U_n = ((f_n, t_n))_{0 \leq n \leq N_U}$, we then obtain a sequence of timed persistence diagrams $V_n = ((X_n, t_n))_{0 \leq n \leq N_V}$, with $N_V = N_U$.

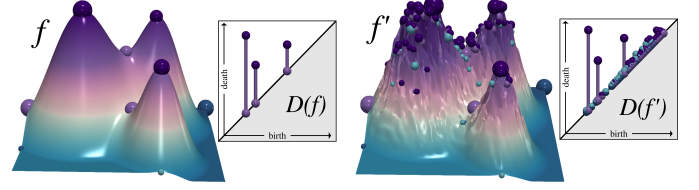


Fig. 1. Persistence diagrams $\mathcal{D}(f)$ and $\mathcal{D}(f')$ of a noise-free scalar field f (left), and of the same scalar field with an additive background noise f' (right). The persistence diagrams show the three main peaks as pairs with large persistence, whereas in the noise-corrupted diagram $\mathcal{D}(f')$ the many pairs with very small persistence capture only the background noise.

Although our applications focus on timed PL-scalar fields, the framework developed in this paper only takes as input such sequences of timed persistence diagrams. As a result, it is compatible directly with other types of input data that give rise to timed persistence diagrams (e.g., time-varying point clouds equipped with their associated Vietoris–Rips filtrations).

In what follows, we enumerate the K points of a persistence diagram X as $X = \{x^1, \dots, x^K\}$, and denote $X_\emptyset = \{\}$ the empty persistence diagram.

B. Metric for persistence diagrams

Let $X_1 = \{x_1^1, \dots, x_1^{K_1}\}$ and $X_2 = \{x_2^1, \dots, x_2^{K_2}\}$ be two persistence diagrams. To equalise their cardinalities, we augment each diagram with the diagonal projections of the off-diagonal points of the other diagram: $X_1^* = X_1 \cup \{\pi(x) \mid x \in X_2 \setminus \Lambda\}$, $X_2^* = X_2 \cup \{\pi(x) \mid x \in X_1 \setminus \Lambda\}$, where the projection $\pi(b, d)$ is defined by $\pi(b, d) = ((b+d)/2, (b+d)/2)$. The sizes of the augmented diagrams coincide, and we set $K := |X_1^*| = |X_2^*|$ and note $X_1^* = \{x_{*1}^1, \dots, x_{*1}^{K_1}\}$, and $X_2^* = \{x_{*2}^1, \dots, x_{*2}^{K_2}\}$.

Let $I_K = \{1, \dots, K\}$. A bijection $\psi : I_K \rightarrow I_K$ specifies a one-to-one matching between the points of X_1^* and X_2^* . We equip \mathbb{R}^2 with the cost $c(x, y) = 0$, if $x \in \Lambda$ and $y \in \Lambda$, and $c(x, y) = \|x - y\|_2^2$ otherwise, where $\|\cdot\|_2$ is the Euclidian distance in \mathbb{R}^2 . The 2-Wasserstein distance between the persistence diagrams X_1^* and X_2^* is defined by,

$$W_2(X_1^*, X_2^*) = \min_{\substack{\psi: \text{bijective} \\ I_K \rightarrow I_K}} \left(\sum_{j=1}^K c(x_{*1}^j, x_{*2}^{\psi(j)}) \right)^{1/2}. \quad (1)$$

Geometrically, W_2 is the least root-mean-square cost required to transport X_1^* to X_2^* while allowing any point to slide onto the diagonal at zero expense (see Fig. 2).

III. CONTINUOUS EDIT DISTANCE BETWEEN TVPDs

In this section, we introduce our distance. We begin by specifying the space of TVPDs. Next, we provide an overview of the CED and establish its basic properties. We conclude by explaining how to obtain a TVPD from our input data, and by presenting practical methods for computing the CED.

A. TVPDs

We introduce a subfamily of TVPDs—still referred to as TVPDs—defined by piecewise-measurable functions (cf.

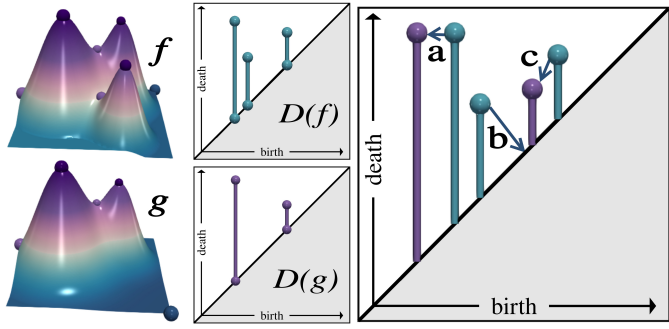


Fig. 2. Left: two toy scalar fields f (top) and g (bottom). Center: their persistence diagrams $D(f)$ and $D(g)$. Right: the optimal 2-Wasserstein matching ψ between $D(f)$ and $D(g)$, represented by arrows. For readability, only the persistence pairs of the unaugmented diagrams and the off-diagonal matchings are displayed. The sum $a^2 + b^2 + c^2$ of the arrow lengths equals $W_2(D(f), D(g))^2$.

Appendix A for measure-theoretic preliminaries) that satisfy certain conditions. Indeed, let (\mathcal{D}, W_2) be the metric space of persistence diagrams with the W_2 distance, provided with its Borel sigma-algebra $\mathcal{B}(\mathcal{D})$, and set a fixed non-empty subset $A \subsetneq \mathcal{D}$ (whose role and interpretation in the CED construction will be detailed in Sec. III-B). Fix a constant step $\Delta \in (0, +\infty)$, and let \mathcal{S}^Δ be the space of functions F from $\text{dom } F = \bigcup_{i \in \{1, \dots, N_F^\Delta\}} I_i^F \subset \mathbb{R}$ to \mathcal{D} , with $N_F^\Delta \in \mathbb{N}^*$, and $(I_i^F)_{i \in \{1, \dots, N_F^\Delta\}}$ a disjoint family of intervals of \mathbb{R} , such that:

- $\forall i \in \{1, \dots, N_F^\Delta\}$, $\sup I_i^F - \inf I_i^F = \Delta$,
- $\forall (i, i') \in \{1, \dots, N_F^\Delta\}^2$, $\forall (x, x') \in I_i^F \times I_{i'}^F$, $i < i' \Rightarrow x < x'$,
- $\forall t \in \text{dom } F$, $W_2(F(t), A) > 0$,
- $\forall i \in \{1, \dots, N_F^\Delta\}$, $F|_{I_i^F} : (I_i^F, \mathcal{B}(\mathbb{R})|_{I_i^F}) \rightarrow (\mathcal{D}, \mathcal{B}(\mathcal{D}))$ is Lebesgue-measurable,
- $\forall i \in \{1, \dots, N_F^\Delta\}$, $\sup\{W_2(a, b) \mid a \in \text{Im}(F|_{I_i^F}), b \in \text{Im}(F|_{I_i^F})\} < \infty$.

We will omit the superscript Δ in the notation N_F^Δ whenever no ambiguity arises. Let $(F, G) \in (\mathcal{S}^\Delta)^2$, $i \in \{1, \dots, N_F\}$, $j \in \{1, \dots, N_G\}$. We denote $F_i := F|_{I_i^F}$, and we call F_i a Δ -subdivision. We consider that two Δ -subdivisions F_i, G_j are equal if: $\inf I_i^F = \inf I_j^G$, $\sup I_i^F = \sup I_j^G$, and $\lambda(\{x \in I_i^F \cap I_j^G \mid F_i(x) \neq G_j(x)\}) = 0$. We denote \mathcal{S}^Δ the Δ -subdivision space.

In a similar way, let $(F, G) \in (\mathcal{S}^\Delta)^2$, with $N_F = N_G$, we consider that F, G are equal if, $\forall i \in \{1, \dots, N_F\}$, $F_i = G_i$. More generally, two measurable applications F and G from $\mathcal{X} \subset \mathbb{R}$ to \mathcal{D} are considered equal in our framework whenever $\lambda(\{x \in \mathcal{X}, F(x) \neq G(x)\}) = 0$.

Then, we call TVPDs elements of \mathcal{S}^Δ (see Fig. 3). Observe that, under this definition—and since every continuous map is Lebesgue-measurable (cf. Appendix A)—any mapping F that satisfies all the stated conditions, with the fourth condition replaced by, $\forall i \in \{1, \dots, N_F\}$, $F|_{I_i^F} : (I_i^F, |\cdot|) \rightarrow (\mathcal{D}, W_2)$ is continuous, belongs to \mathcal{S}^Δ and therefore is a TVPD. In the remaining, any such TVPD, with the additional conditions $\forall i \in \{1, \dots, N_F\}$, $\exists (l_i^+, l_i^-) \in \mathcal{D}^2$, $\lim_{t \rightarrow (\inf I_i^F) +} F|_{I_i^F} = l_i^+$ and $\lim_{t \rightarrow (\sup I_i^F) -} F|_{I_i^F} = l_i^-$, will be referred to as

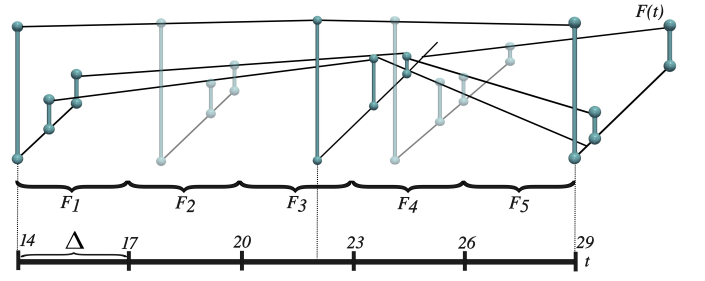


Fig. 3. Fix $A = \{X_\emptyset\} \subsetneq \mathcal{D}$ as the singleton containing the empty persistence diagram, and set $\Delta = 3$. The figure depicts a continuous function $F : \text{dom } F = [14, 29] = \bigcup_{i=1}^5 I_i^F \rightarrow \mathcal{D}$, $I_1^F = [14, 17]$, $I_2^F = [17, 20]$, $I_3^F = [20, 23]$, $I_4^F = [23, 26]$, $I_5^F = [26, 29]$, where every I_i^F has length $\Delta = 3$. Opaque diagrams correspond to the input timed persistence diagrams, whereas semi-transparent diagrams are intermediate diagrams inserted by interpolation along 2-Wasserstein geodesics between successive inputs (see Sec. III-F). Since F is continuous on $[14, 29]$, it is measurable on $[14, 29]$, and on each I_i^F . Then every F_i is measurable, which implies that each F_i is Lebesgue-measurable, and thus F is a TVPD.

continuous. We denote \mathcal{C}^Δ this subset of \mathcal{S}^Δ that contains all continuous TVPDs. Note that, as a result, every Cohen–Steiner [22] or Turner [38] vineyard is a continuous TVPD.

Finally, remark that for any $P \in \mathcal{S}^\Delta$, thanks to the imposed conditions, we can unambiguously denote P as a sequence $(P_i)_{1 \leq i < N_P}$. Moreover, if $N \in \{1, \dots, N_P\}$, then $(P_i)_{1 \leq i < N}$ stay obviously in \mathcal{S}^Δ .

B. Overview

Let $\alpha \in (0, 1)$ and $\beta \in (0, 1]$ be fixed parameters. In what follows, we present an overview of the $\text{CED}_{\alpha, \beta}^\Delta$ construction developed across Sec. III-C and Sec. III-D.

The $\text{CED}_{\alpha, \beta}^\Delta$ distance combines two conceptual layers.

(i) A local metric on Δ -subdivisions. Let two TVPDs $P = (P_1, \dots, P_{N_P}) \in \mathcal{S}^\Delta$ and $Q = (Q_1, \dots, Q_{N_Q}) \in \mathcal{S}^\Delta$. Sec. III-C defines a metric d_Δ^α on the space \mathcal{S}^Δ of Δ -subdivisions. For two elements $P_i \in \mathcal{S}^\Delta$ from P and $Q_j \in \mathcal{S}^\Delta$ from Q , $d_\Delta^\alpha(P_i, Q_j)$ blends spatial cost—the overall W_2 -distance between the corresponding images $\text{Im}(P_i) = \{P(t) : t \in I_i^P\}$ and $\text{Im}(Q_j) = \{Q(t) : t \in I_j^Q\}$ —with temporal cost—the shift between the intervals I_i^P and I_j^Q —weighted respectively by $1 - \alpha$ and α . Here, the parameter α controls the trade-off between temporal and spatial contributions to the local metric d_Δ^α . In this formulation, $d_\Delta^\alpha(P_i, Q_j)$ is interpreted as the cost of substituting P_i with Q_j (or vice versa). Additionally, $d_\Delta^\alpha(P_i, A)$ (resp. $d_\Delta^\alpha(Q_j, A)$) measures the overall W_2 -distance of the image of the Δ -subdivision P_i (resp Q_j) to the set A ; this value therefore represents the cost of deleting that Δ -subdivision into A (resp. inserting it from A). Therefore, A serves as a reference modeling deletions and insertions; for example, a typical choice is $A = \{X_\emptyset\}$.

(ii) A global edit distance with penalty between entire time varying persistence diagrams. Sec. III-D lifts the local metric d_Δ^α to whole TVPDs via a Δ -partial assignment $f : \text{dom } f \subset \{1, \dots, N_P^\Delta\} \rightarrow \text{Im } f \subset \{1, \dots, N_Q^\Delta\}$, required to be strictly increasing. Such an assignment realises three elementary operations: Substitution of P_i by Q_j (if $f(i) = j$) with cost $d_\Delta^\alpha(P_i, Q_{f(i)})$; Deletion of P_i (if $i \notin \text{dom } f$) with

cost $\beta \cdot d_{\Delta}^{\alpha}(P_i, A)$; Insertion of Q_j (if $j \notin \text{Im } f$) with cost $\beta \cdot d_{\Delta}^{\alpha}(Q_j, A)$; where the parameter β controls the penalty for unmatched Δ -subdivisions. $\text{CED}_{\alpha, \beta}^{\Delta}(P, Q)$ is the minimum total cost over all Δ -partial assignments. Here, $\text{CED}_{\alpha, \beta}^{\Delta}(P, Q)$ is interpreted as the minimal cost of converting P into Q (or vice versa) by means of a Δ -partial assignment.

Key properties. The pair $(\mathcal{S}^{\Delta}, \text{CED}_{\alpha, \beta}^{\Delta})$ is a metric space (see Appendix B.10). An $\mathcal{O}(N_P^{\Delta} \cdot N_Q^{\Delta})$ dynamic-programming scheme (Sec. III-E) evaluates the distance and produces an optimal partial assignment. Finally, continuous TVPDs can be approximated arbitrarily well (in CED, Sec. III-G) by piecewise-constant ones, so the metric is amenable to practical computation on sampled data (Sec. III-F).

C. Distance between Δ -subdivisions

Let $(p, q) \in (s^{\Delta})^2$, then $\exists (P, Q) \in (\mathcal{S}^{\Delta})^2$, $\exists (i, j) \in \{1, \dots, N_P\} \times \{1, \dots, N_Q\}$, such that $p = P_i$ and $q = Q_j$. Denoting $a_i = \inf(I_i^P)$, $b_i = \sup(I_i^P)$, $c_j = \inf(I_j^Q)$, $d_j = \sup(I_j^Q)$, we define $d_{\Delta}^{\alpha}(p, q) = d_{\Delta}^{\alpha}(P_i, Q_j) := \int_{a_i}^{b_i} (1 - \alpha) \cdot W_2(P(t), Q(t + c_j - a_i)) + \alpha \cdot |(t + c_j - a_i) - (t)| dt = \int_{a_i}^{b_i} (1 - \alpha) \cdot W_2(P(t), Q(t + c_j - a_i)) + \alpha \cdot |c_j - a_i| dt$. With this definition, we have the result that $(s^{\Delta}, d_{\Delta}^{\alpha})$ is a metric space, and so d_{Δ}^{α} is a distance on s^{Δ} (see Appendix B.4). Intuitively, the distance d_{Δ}^{α} can be understood as the successive sum of spatial and temporal distances between the elements composing each Δ -subdivision. The relative contribution of the spatial part is weighted by the parameter $1 - \alpha$, while that of the temporal part is weighted by α .

Moreover, with the same notation, we define $d_{\Delta}^{\alpha}(p, A) = d_{\Delta}^{\alpha}(P_i, A) := \int_{a_i}^{b_i} (1 - \alpha) \cdot W_2(P(t), A) dt$, with $\forall x \in \mathcal{D}$, $W_2(x, A) = \inf(W_2(x, y), y \in A)$. In this case, $d_{\Delta}^{\alpha}(P_i, A)$ can be viewed as the successive sum of spatial distances from the elements of the Δ -subdivision P_i to the set A . Then we have, as a result, that $d_{\Delta}^{\alpha}(P_i, Q_j) + d_{\Delta}^{\alpha}(Q_j, A) \geq d_{\Delta}^{\alpha}(P_i, A)$ (see Appendix B.5).

D. From distance between subdivisions to distance between TVPDs

Set $(P, Q) \in (\mathcal{S}^{\Delta})^2$. We call Δ -partial assignment (we omit the Δ when the context is clear) between P and Q any function f from $\text{dom } f \subset \{1, 2, \dots, N_P\}$ to $\text{Im } f \subset \{1, 2, \dots, N_Q\}$, such that f is strictly increasing, i.e. $\forall (i, j) \in (\text{dom } f)^2$, $i < j \Rightarrow f(i) < f(j)$. We denote $\mathcal{A}^{\Delta}(P, Q)$ the set of the partial assignments between P and Q in \mathcal{S}^{Δ} , we can see that specifying an $f \in \mathcal{A}^{\Delta}(P, Q)$ directly yields an assignment $f^{-1} \in \mathcal{A}^{\Delta}(Q, P)$.

Then, the $\text{CED}_{\alpha, \beta}^{\Delta}$ between $P = (P_i)_{1 \leq i \leq N_P}$ and $Q = (Q_j)_{1 \leq j \leq N_Q}$ is defined as:

$$\text{CED}_{\alpha, \beta}^{\Delta}(P, Q) = \min_{f \in \mathcal{A}^{\Delta}(P, Q)} \text{cost}_{(P, Q)}^{\Delta}(f) := \min_{f \in \mathcal{A}^{\Delta}(P, Q)} \left(\sum_{i \in \text{dom } f} d_{\Delta}^{\alpha}(P_i, Q_{f(i)}) \right) \quad (2)$$

$$+ \sum_{i \notin \text{dom } f} \beta \cdot d_{\Delta}^{\alpha}(P_i, A) \quad (3)$$

$$+ \sum_{j \notin \text{Im } f} \beta \cdot d_{\Delta}^{\alpha}(Q_j, A) \quad (4)$$

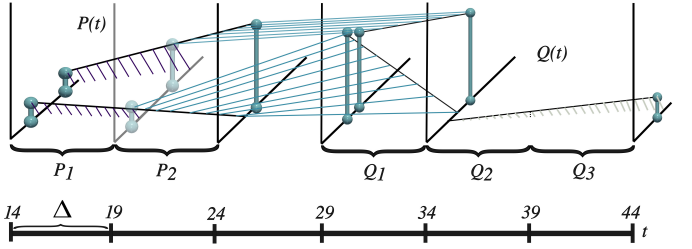


Fig. 4. Schematic illustration of the $\text{CED}_{\alpha, \beta}^{\Delta}$, with $A = \{X_{\emptyset}\}$ and $\Delta = 5$, between two TVPDs P and Q . The optimal Δ -partial assignment is the function $f : \text{dom } f = \{2\} \rightarrow \{1\}$. Accordingly, $\text{CED}_{\alpha, \beta}^{\Delta}(P, Q)$ decomposes into deletion of P_1 (purple hatched strip, cost $\beta \cdot d_{\Delta}^{\alpha}(P_1, A)$); substitution of P_2 by Q_1 (blue hatched strip, cost $d_{\Delta}^{\alpha}(P_2, Q_1)$); insertions of Q_2 and Q_3 (gray hatched strips, cost $\beta \cdot (d_{\Delta}^{\alpha}(Q_2, A) + d_{\Delta}^{\alpha}(Q_3, A))$). The colored and hatched regions therefore sum to $\text{CED}_{\alpha, \beta}^{\Delta}(P, Q)$.

Through this definition, the $\text{CED}_{\alpha, \beta}^{\Delta}$ between two TVPDs is the minimal cost to transform the first TVPD into the second (see Fig. 4), via a partial assignment, and three elementary operation types—substitution (line 2), deletion (line 3), and insertion (line 4). A substitution replaces a subdivision of the first TVPD with the subdivision assigned to it in the second TVPD, at a cost equal to the distance d_{Δ}^{α} between the two subdivisions. A deletion removes a subdivision from the first TVPD, at a cost equal to β times the distance d_{Δ}^{α} of that subdivision to the set A . An addition inserts, into the first TVPD, a subdivision from the second TVPD, at a cost equal to β times the distance d_{Δ}^{α} of that subdivision to the set A .

We observe that, if $N_P = N_Q = N$, a direct consequence of the definition is $\text{CED}_{\alpha, \beta}^{\Delta}(P, Q) \leq \sum_{i \in \{1, \dots, N\}} d_{\Delta}^{\alpha}(P_i, Q_i)$. Indeed, the identity function $Id : \{1, \dots, N\} \rightarrow \{1, \dots, N\}$, $i \rightarrow i$ is a partial assignment (i.e., $Id \in \mathcal{A}^{\Delta}(P, Q)$), then $\text{CED}_{\alpha, \beta}^{\Delta}(P, Q) \leq \text{cost}_{(P, Q)}^{\Delta}(Id) = \sum_{i \in \{1, \dots, N\}} d_{\Delta}^{\alpha}(P_i, Q_i)$.

Note also that for any $(\Delta_1, \Delta_2) \in (0, \infty)^2$, such that $\Delta_1 \mid \Delta_2$, if $(P, Q) \in \mathcal{S}^{\Delta_2} \times \mathcal{S}^{\Delta_2}$ then as a result $(P, Q) \in \mathcal{S}^{\Delta_1} \times \mathcal{S}^{\Delta_1}$, and $\text{CED}_{\alpha, \beta}^{\Delta_1}(P, Q) \leq \text{CED}_{\alpha, \beta}^{\Delta_2}(P, Q)$. Roughly speaking, the inequality follows from the fact that the partial assignment $g : \text{dom } g \subset \{1, 2, \dots, N_P^{\Delta_2}\} \rightarrow \text{Im } g \subset \{1, 2, \dots, N_Q^{\Delta_2}\}$ that realises $\text{CED}_{\alpha, \beta}^{\Delta_2}(P, Q)$ (i.e., such that $\text{CED}_{\alpha, \beta}^{\Delta_2}(P, Q) = \text{cost}_{(P, Q)}^{\Delta_2}(g)$), possesses an equivalent partial assignment $g' : \text{dom } g' \subset \{1, 2, \dots, N_P^{\Delta_1}\} \rightarrow \text{Im } g' \subset \{1, 2, \dots, N_Q^{\Delta_1}\}$ that realises the same cost in \mathcal{S}^{Δ_1} (i.e., $\text{cost}_{(P, Q)}^{\Delta_1}(g') = \text{cost}_{(P, Q)}^{\Delta_2}(g)$; see Appendix B.7). Therefore, $\text{CED}_{\alpha, \beta}^{\Delta_1}(P, Q) = \min_{f \in \mathcal{A}^{\Delta_1}(P, Q)} \text{cost}_{(P, Q)}^{\Delta_1}(f) \leq \text{cost}_{(P, Q)}^{\Delta_1}(g') = \text{cost}_{(P, Q)}^{\Delta_2}(g) = \text{CED}_{\alpha, \beta}^{\Delta_2}(P, Q)$. Moreover, by identical reasoning, we observe that for every partial assignment $h \in \mathcal{A}^{\Delta_2}(P, Q)$, there exists a partial assignment $h' \in \mathcal{A}^{\Delta_1}(P, Q)$, such that $\text{cost}_{(P, Q)}^{\Delta_1}(h') = \text{cost}_{(P, Q)}^{\Delta_2}(h)$. Then, the set $\mathcal{A}^{\Delta_1}(P, Q)$ is at least as extensive as the set $\mathcal{A}^{\Delta_2}(P, Q)$; in the sense that $\{\text{cost}_{(P, Q)}^{\Delta_2}(f) \in \mathbb{R}_+ \mid f \in \mathcal{A}^{\Delta_2}(P, Q)\} \subsetneq \{\text{cost}_{(P, Q)}^{\Delta_1}(f) \in \mathbb{R}_+ \mid f \in \mathcal{A}^{\Delta_1}(P, Q)\}$. It is therefore informative to choose Δ small, since a lower parameter value can reveal new, finer assignments.

E. Computation via Dynamic Programming

We provide in this subsection a computation method by dynamic programming [65], illustrated in Fig. 5, for the $\text{CED}_{\alpha,\beta}^{\Delta}$ between two TVPDs: Let $P = (P_i)_{1 \leq i \leq N_P} \in \mathcal{S}^{\Delta}$, $Q = (Q_j)_{1 \leq j \leq N_Q} \in \mathcal{S}^{\Delta}$. In this subsection, we will note for $v = (x, y) \in \mathbb{R}^2$, $v_1 = x$, $v_2 = y$, $\delta_{\Delta}^{\alpha,\beta}(v) = \delta_{\Delta}^{\alpha,\beta}((P_i)_{0 \leq i \leq v_1}, (Q_j)_{0 \leq j \leq v_2})$. Then, we define recursively, $\forall K \in \{1, \dots, N_P\}$, $\forall K' \in \{1, \dots, N_Q\}$,

$$\begin{aligned} \delta_{\Delta}^{\alpha,\beta}(K, K') &= \min \left\{ \delta_{\Delta}^{\alpha,\beta}(K-1, K') + \beta \cdot d_{\Delta}^{\alpha}(P_K, A), \right. \\ &\quad \delta_{\Delta}^{\alpha,\beta}(K-1, K'-1) + d_{\Delta}^{\alpha}(P_K, Q_{K'}), \\ &\quad \left. \delta_{\Delta}^{\alpha,\beta}(K, K'-1) + \beta \cdot d_{\Delta}^{\alpha}(Q_{K'}, A) \right\} \end{aligned}$$

with initialization $\delta_{\Delta}^{\alpha,\beta}(0, 0) = 0, \forall K \in \{1, \dots, N_P\}$, $\delta_{\Delta}^{\alpha,\beta}(K, 0) = \delta_{\Delta}^{\alpha,\beta}(K-1, 0) + \beta \cdot d_{\Delta}^{\alpha}(P_K, A)$, and $\forall K' \in \{1, \dots, N_Q\}$, $\delta_{\Delta}^{\alpha,\beta}(0, K') = \delta_{\Delta}^{\alpha,\beta}(0, K'-1) + \beta \cdot d_{\Delta}^{\alpha}(Q_{K'}, A)$. With this definition in place, we have the result that $\text{CED}_{\alpha,\beta}^{\Delta}(P, Q) = \delta_{\Delta}^{\alpha,\beta}(N_P, N_Q)$ (see Appendix B.9).

Moreover, once the recursive computation of $\delta_{\Delta}^{\alpha,\beta}((P_i)_{0 \leq i \leq N_P}, (Q_j)_{0 \leq j \leq N_Q})$ has been carried out, another result is that the partial assignment f achieving the minimal cost defining $\text{CED}_{\alpha,\beta}^{\Delta}(P, Q)$, i.e. such that $\text{CED}_{\alpha,\beta}^{\Delta}(P, Q) = \text{cost}_{(P, Q)}^{\Delta}(f)$, can be determined by the following procedure:

We define recursively, with initializations $A_0 = \emptyset$, $B_0 = (N_P, N_Q)$,

- $B_{z+1} = B_z - (1, 0)$ if $\delta_{\Delta}^{\alpha,\beta}(B_z) = \delta_{\Delta}^{\alpha,\beta}(B_z - (1, 0)) + \beta \cdot d_{\Delta}^{\alpha}(P_{B_{z_1}}, A)$,
- $B_{z+1} = B_z - (1, 1)$ if $\delta_{\Delta}^{\alpha,\beta}(B_z) = \delta_{\Delta}^{\alpha,\beta}(B_z - (1, 1)) + d_{\Delta}^{\alpha}(P_{B_{z_1}}, Q_{B_{z_2}})$,
- $B_{z+1} = B_z - (0, 1)$ if $\delta_{\Delta}^{\alpha,\beta}(B_z) = \delta_{\Delta}^{\alpha,\beta}(B_z - (0, 1)) + \beta \cdot d_{\Delta}^{\alpha}(Q_{B_{z_2}}, A)$,
- $A_{z+1} = A_z \cup B_z$ if $B_{z+1} = B_z - (1, 1)$,
- $A_{z+1} = A_z$ if $B_{z+1} = B_z - (1, 0)$,
- $A_{z+1} = A_z$ if $B_{z+1} = B_z - (0, 1)$.

We stop when $B_Z = (0, 0)$ for some $Z \in \mathbb{N}$, and then we have as a result $f = A_Z$ (see Fig. 5 and Appendix B.11).

F. Construction of a TVPD from an input diagram sequence

In this subsection, we describe how to obtain a TVPD from an input sequence of persistence diagrams.

Let $V_n((X_n, t_n))_{0 \leq n \leq N_V}$ be the sequence of timed persistence diagrams (cf. Sec. II-A). We now turn this discrete sequence into a continuous application $F : ([t_0, t_{N_V}], |\cdot|) \rightarrow (\mathcal{D}, W_2)$ in three substeps.

1) *Contiguous geodesics*: For every $n \in \{0, \dots, N_V - 1\}$ we compute the 2-Wasserstein distance $W_2(X_n, X_{n+1})$ and select a W_2 -geodesic $\gamma_n : [0, 1] \rightarrow \mathcal{D}$ satisfying $\gamma_n(0) = X_n$ and $\gamma_n(1) = X_{n+1}$. Such a geodesic exists because (\mathcal{D}, W_2) is a geodesic metric space [38].

2) *Temporal interpolation*: We map each real time $t \in [t_n, t_{n+1})$ to the geodesic parameter $\lambda_n(t) = \frac{t - t_n}{t_{n+1} - t_n} \in [0, 1]$, and set $\mathcal{H}_n(t) = \gamma_n(\lambda_n(t))$. Consequently, $\mathcal{H}_n(t_n) = X_n$, $\lim_{t \rightarrow t_{n+1}} \mathcal{H}_n(t) = X_{n+1}$, and \mathcal{H}_n is continuous on $[t_n, t_{n+1})$ because geodesics are continuous by definition.

3) *Piecewise-geodesic application*: Gluing the segments together yields the piecewise-geodesic application

$$F : [t_0, t_{N_V}] \rightarrow \mathcal{D}, F(t) = \begin{cases} \mathcal{H}_0(t) & \forall t \in [t_0, t_1), \\ \mathcal{H}_1(t) & \forall t \in [t_1, t_2), \\ \vdots \\ \mathcal{H}_{N-1}(t) & \forall t \in [t_{N_V-1}, t_{N_V}), \end{cases}$$

and we define $F(t_{N_V}) = X_{N_V}$. By construction, F is continuous on $[t_0, t_{N_V}]$. Therefore, if $F(t) \notin A$ for every $t \in [t_0, t_{N_V}]$, then $F \in \mathcal{S}^{\Delta}$ (but also $F \in C^{\Delta}$), and consequently F is a TVPD in the sense of our definition. We refer to such TVPDs, derived from our input data type, as input TVPDs (see Fig. 6). We denote by I^{Δ} the set of input TVPDs, and we have $I^{\Delta} \subsetneq C^{\Delta} \subsetneq \mathcal{S}^{\Delta}$. It should be noted that the information contained in F includes not only the sequence of timed-persistence diagrams $V_n = ((X_n, t_n))_{0 \leq n \leq N_V}$, but also the intermediate interpolations $\{\gamma_n(\lambda_n(t))\} \in \mathcal{D}, n \in \{0, \dots, N_V - 1\}, t \in (0, 1)\}$. The application F is therefore richer in information than the original sequence.

G. Piecewise-constant approximation of input TVPDs for practical CED computation

In order to ease the practical computation of $\text{CED}_{\alpha,\beta}^{\Delta}$, and later $\text{CED}_{\alpha,1}^{\Delta}$ -geodesics, we introduce in this subsection piecewise-constant approximations of TVPDs (see Fig. 7).

Let $F : \text{dom } F = \bigcup_{i \in \{1, \dots, N_F^{\Delta}\}} I_i^F \rightarrow \mathcal{D}$, be one such continuous TVPD of \mathcal{S}^{Δ} , that is $F \in C^{\Delta}$. Let $\eta \mid \Delta$, and $M \in \mathbb{N}$, such that for every $i \in \{1, \dots, N_F^{\Delta}\}$, $\inf I_i^F + M \cdot \eta = \sup I_i^F$, and denote $\tilde{F}_i^{\eta} : I_i^F \rightarrow \mathcal{D}$ the piecewise-constant application defined by $\tilde{F}_i^{\eta}(t) = \lim_{t \rightarrow a_{i,n}} F_i(t), \forall t \in [a_{i,n}, a_{i,n+1}) \cap I_i^F$, with $a_{i,n} = \inf I_i^F + n \cdot \eta$, for $n = 0, \dots, M$. Gluing all the \tilde{F}_i^{η} together, for every $i \in \{1, \dots, N_F^{\Delta}\}$, we obtain the piecewise-constant approximation $\tilde{F}^{\eta} : \text{dom } F \rightarrow \mathcal{D}$ of F , with $\tilde{F}^{\eta} \in \mathcal{S}^{\Delta}$ as a simple function on each I_i^F . As a result (see Appendix B.12), the subset of \mathcal{S}^{Δ} consisting of piecewise-constant TVPDs, denoted PC^{Δ} , is dense in the set C^{Δ} of continuous TVPDs. Indeed, for every $F \in C^{\Delta}$ and any $\varepsilon > 0$, there exists $\eta(\varepsilon) \mid \Delta$ such that $\text{CED}_{\alpha,\beta}^{\Delta}(F, \tilde{F}^{\eta(\varepsilon)}) < \varepsilon$. Because $I^{\Delta} \subsetneq C^{\Delta}$, we have $I^{\Delta} \subsetneq C^{\Delta} \subsetneq \text{PC}^{\Delta}$, and then we got the same conclusions for I^{Δ} . In practice, if $F : [t_0, t_{N_V}] \rightarrow \mathcal{D}$ is an input TVPD obtained from a timed persistence diagram sequence $V_n = ((X_n, t_n))_{0 \leq n \leq N_V}$, it suffices to choose $\eta(\varepsilon) < \frac{\varepsilon}{(1-\alpha) \cdot K_V \cdot (t_{N_V} - t_0)}$, with $K_V = \max_{0 \leq n \leq N_V-1} \frac{W_2(X_n, X_{n+1})}{t_{n+1} - t_n}$ (cf. Appendix B.13).

Since $(\mathcal{S}^{\Delta}, \text{CED}_{\alpha,\beta}^{\Delta})$ is a metric space, applying the triangle inequality and using symmetry property, we obtain $\forall (F, G) \in (\mathcal{S}^{\Delta})^2, |\text{CED}_{\alpha,\beta}^{\Delta}(F, G) - \text{CED}_{\alpha,\beta}^{\Delta}(\tilde{F}^{\eta(\varepsilon)}, \tilde{G}^{\eta(\varepsilon)})| \leq \text{CED}_{\alpha,\beta}^{\Delta}(F, \tilde{F}^{\eta(\varepsilon)}) + \text{CED}_{\alpha,\beta}^{\Delta}(G, \tilde{G}^{\eta(\varepsilon)}) \leq 2 \cdot \varepsilon$. In conclusion, we can $(2 \cdot \varepsilon)$ -approximate the value of $\text{CED}_{\alpha,\beta}^{\Delta}$.

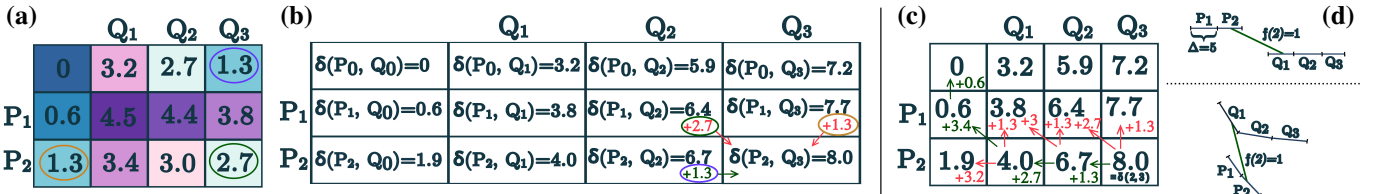


Fig. 5. (a) Cost matrix of the TVPDs $P = (P_1, P_2)$ and $Q = (Q_1, Q_2, Q_3)$ in Fig. 4: the first column and first row contain the initialization terms $d_{\Delta}^{\alpha}(\cdot, A)$; the remaining cells are the pairwise costs $d_{\Delta}^{\alpha}(P_i, Q_j)$. Cell color encodes the cost magnitude. (b) Dynamic programming computation of the $\text{CED}_{\alpha, \beta}^{\Delta}$ between TVPDs P and Q . For the example of the bottom right entry of the matrix, to compute $\delta_{\Delta}^{\alpha, \beta}((P_i)_{1 \leq i \leq 2}, (Q_j)_{1 \leq j \leq 3})$, we take the minimum among $\delta_{\Delta}^{\alpha, \beta}((P_i)_{1 \leq i \leq 1}, (Q_j)_{1 \leq j \leq 3}) + \beta \cdot d_{\Delta}^{\alpha}(P_2, A)$ (deletion, vertical arrow), $\delta_{\Delta}^{\alpha, \beta}((P_i)_{1 \leq i \leq 1}, (Q_j)_{1 \leq j \leq 2}) + d_{\Delta}^{\alpha}(P_2, Q_3)$ (substitution, diagonal arrow), and $\delta_{\Delta}^{\alpha, \beta}((P_i)_{1 \leq i \leq 2}, (Q_j)_{1 \leq j \leq 2}) + \beta \cdot d_{\Delta}^{\alpha}(Q_3, A)$ (insertion, horizontal arrow). Since the minimum is reached by the insertion term, $\delta_{\Delta}^{\alpha, \beta}((P_i)_{1 \leq i \leq 2}, (Q_j)_{1 \leq j \leq 3}) = \text{CED}_{\alpha, \beta}^{\Delta}(P, Q)$ is set to that value. (c) Procedure to recover the optimal partial assignment f that attains $\text{CED}_{\alpha, \beta}^{\Delta}(P, Q)$. Each cell of the table displays the value $\delta_{\Delta}^{\alpha, \beta}((P_i)_{1 \leq i \leq r}, (Q_j)_{1 \leq j \leq s})$; arrows indicate the three candidate predecessors (deletion \uparrow , substitution \nwarrow , insertion \leftarrow). A green arrow marks the predecessor realizing the minimum, so the reverse scan yields $f: \text{dom } f = \{2\} \rightarrow \{1\}$ with $f(2) = 1$. (d, top) Temporal representation of the TVPDs P and Q and their optimal partial assignment f (horizontal axis is time, ticks are the subdivision boundaries of length Δ). Each TVPD is represented by its domain of definition, and green straight line segments represent the optimal assignment f ; the vertical spacing between the TVPDs is solely to ease the visualization of f . (d, bottom) d_{Δ}^{α} -MDS (multidimensional scaling) embedding of TVPDs P and Q in \mathbb{R}^3 (each point along a curve represents a persistence diagram), with the optimal assignment f again drawn as green straight segment.

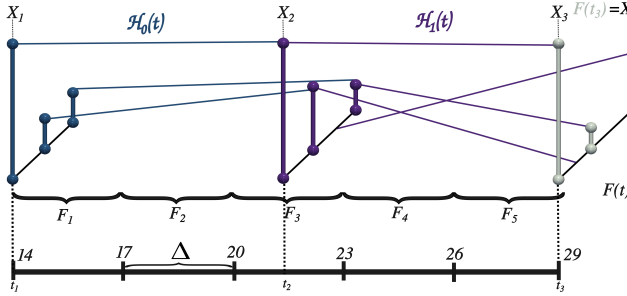


Fig. 6. Fix $A = \{X_{\emptyset}\}$. Illustration of constructing an input TVPD F from a sequence of timed persistence diagrams $V_n = ((X_1, t_1), (X_2, t_2), (X_3, t_3))$. In blue, the dilated W_2 -geodesic $\mathcal{H}_0(t) = \gamma_0(\lambda_0(t))$ joining X_1 to X_2 for $t \in [t_1, t_2]$. In purple, the dilated W_2 -geodesic $\mathcal{H}_1(t) = \gamma_1(\lambda_1(t))$ joining X_2 to X_3 for $t \in [t_2, t_3]$. In gray, $F(t_3)$ is defined to be X_3 . The input TVPD $F = (F_1, F_2, F_3, F_4, F_5)$ is then obtained by gluing the blue, purple, and gray parts (that is, $F(t) = \mathcal{H}_0(t)$ for $t \in [t_1, t_2]$, $F(t) = \mathcal{H}_1(t)$ for $t \in [t_2, t_3]$, $F(t_3) = X_3$).

between two input TVPDs F and G (or, more generally, between two continuous TVPDs), by the value of $\text{CED}_{\alpha, \beta}^{\Delta}$ computed between their piecewise-constant approximations $\tilde{F}^{\eta(\varepsilon)}$ and $\tilde{G}^{\eta(\varepsilon)}$. On a practical level, one may choose Δ to be as small as can be handled computationally, and set a common $\eta = \Delta$ for all the TVPDs whose pairwise $\text{CED}_{\alpha, \beta}^{\Delta}$ distances are to be computed, since it is advantageous for both of these parameters to be small. We then have $d_{\Delta}^{\alpha}(\tilde{F}_i^{\eta}, \tilde{G}_j^{\eta}) = \Delta \cdot \left(W_2(P_i(a_i), Q_j(c_j)) (1 - \alpha) + \alpha \cdot |c_j - a_i| \right)$, and $d_{\Delta}^{\alpha}(\tilde{P}_i^{\eta}, A) = \Delta \cdot (1 - \alpha) \cdot W_2(P_i(a_i), A)$.

IV. CONTINUOUS EDIT DISTANCE GEODESICS

This section formalizes geodesics for the $\text{CED}_{\alpha, 1}^{\Delta}$ metric on TVPDs. We discuss its existence under mild assumptions and describe an explicit three-step construction.

A. Definition and overview

In a metric space (\mathcal{X}, d) , a geodesic joining two points $(x, y) \in \mathcal{X}^2$ is a continuous application $\gamma: [0, d(x, y)] \rightarrow \mathcal{X}$ such that, $\gamma(0) = x$, $\gamma(d(x, y)) = y$, and $d(x, y) =$

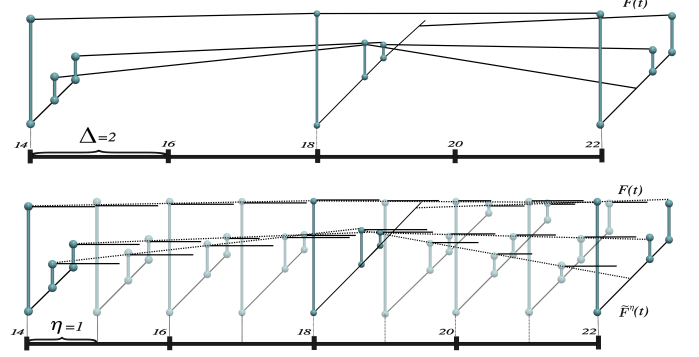


Fig. 7. Illustration of the approximation procedure of a continuous TVPD $F \in C^{\Delta}$ (top) by its piecewise-constant TVPD $\tilde{F}^{\eta} \in \text{PC}^{\Delta}$ of parameter $\eta = 1$ (bottom). A smaller η produces a correspondingly better approximation.

$\sup \sum_{i=0}^{k-1} d(\gamma(t_i), \gamma(t_{i+1}))$, where the supremum is taken over all $k \in \mathbb{N}^*$, and all sequences $t_0 = 0 < t_1 < \dots < t_k = d(x, y)$ in $[0, d(x, y)]$. A metric space is said to be geodesic if every pair of points can be joined by at least one geodesic.

As a result, if A closed and $\forall x \in \mathcal{D}, \{y \in A, d(x, y) = d(x, A)\}$ is non-empty, then $(s^{\Delta}, d_{\Delta}^{\alpha})$ and $(\mathcal{S}^{\Delta}, \text{CED}_{\alpha, 1}^{\Delta})$ are geodesics (see Appendix B.17 and B.18)

Many conditions allow the hypothesis, $\forall x \in \mathcal{D}, \{y \in A, d(x, y) = d(x, A)\}$ is non-empty, to be satisfied. Some examples are: A compact; $\forall x \in \mathcal{D}, A \cap \mathcal{B}(x, r + \epsilon)$ relatively compact (with any $\epsilon \in \mathbb{R}_+^*$, and $r = W_2(x, A)$).

Intuitively, a CED geodesic transforms a TVPD P into a TVPD Q by performing, in continuous time, the elementary operations specified by their optimal Δ -partial assignment $f \in \mathcal{A}^{\Delta}(P, Q)$: first, starting from P , deleting unmatched Δ -subdivisions of P ; then substituting each matched Δ -subdivision of P with its matched counterpart in Q ; and finally inserting the unmatched Δ -subdivisions of Q , yielding Q .

Setting. Fix two TVPDs $(P, Q) \in (\mathcal{S}^{\Delta})^2$ with optimal partial assignment $f \in \mathcal{A}^{\Delta}(P, Q)$. We decompose the index sets

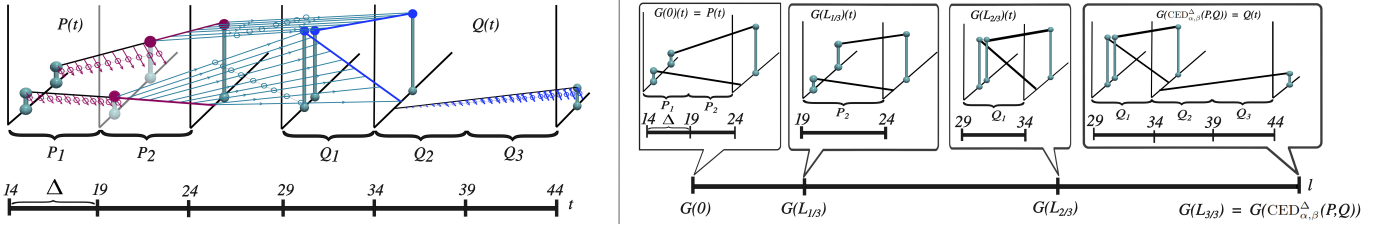


Fig. 8. Fix $A = \{X_\emptyset\}$. Left: The figure schematically illustrates the $\text{CED}_{\alpha,1}^\Delta$ -geodesic between two TVPDs $P = (P_1, P_2)$ and $Q = (Q_1, Q_2, Q_3)$, the optimal Δ -partial assignment being the map $f: \text{dom } f = \{2\} \rightarrow \{1\}$. Starting from P (that is, $G(0) = P$), we first perform the deletion step (in purple on the figure): P_1 is unmatched under f and therefore moves continuously toward A (the persistence diagrams constituting P_1 head toward the empty diagram), while P_2 remains fixed. At the end of this step only P_2 is left (that is, $G(L_{1/3}) = P_2$). Second, during the substitution step (in blue on the figure): the Δ -subdivision P_2 is matched to Q_1 by f , then P_2 travels along the d_Δ^α -geodesic to Q_1 . When this motion ends, the intermediate TVPD reduces to the single Δ -subdivision Q_1 (that is, $G(L_{2/3}) = Q_1$). Lastly, during the insertion step (in gray on the figure): the Δ -subdivisions Q_2 and Q_3 , which are unmatched by f , are inserted from A while Q_3 stays fixed. After both insertions are complete, the geodesic reaches the target TVPD $Q = (Q_1, Q_2, Q_3)$ (that is, $G(L_{3/3}) = Q$). Thus the $\text{CED}_{\alpha,1}^\Delta$ -geodesic from P to Q follows the delete \rightarrow substitute \rightarrow insert scheme encoded by the optimal assignment f . Right: The figure illustrates the intermediate TVPDs on the geodesic G between P and Q at the main stages, as the variable l varies from 0 to $\text{CED}_{\alpha,1}^\Delta(P, Q)$.

$\{1, \dots, N_P^\Delta\}$ and $\{1, \dots, N_Q^\Delta\}$ as

$$\begin{aligned} \mathcal{D}_P &= \{i \mid i \notin \text{dom } f\} && \text{(deletions),} \\ \mathcal{S}_P &= \text{dom } f && \text{(substitutions),} \\ \mathcal{I}_Q &= \{j \mid j \notin \text{Im } f\} && \text{(insertions).} \end{aligned}$$

The total CED cost splits accordingly

$$L = \text{CED}_{\alpha,1}^\Delta(P, Q) = L_{\mathcal{D}} + L_{\mathcal{S}} + L_{\mathcal{I}},$$

where $L_{\mathcal{D}} = \sum_{i \in \mathcal{D}_P} d_\Delta^\alpha(P_i, A)$, $L_{\mathcal{S}} = \sum_{i \in \mathcal{S}_P} d_\Delta^\alpha(P_i, Q_{f(i)})$, and $L_{\mathcal{I}} = \sum_{j \in \mathcal{I}_Q} d_\Delta^\alpha(Q_j, A)$. Define the break-points $L_{0/3} = 0$, $L_{1/3} = L_{\mathcal{D}}$, $L_{2/3} = L_{\mathcal{D}} + L_{\mathcal{S}}$, $L_{3/3} = L_{\mathcal{D}} + L_{\mathcal{S}} + L_{\mathcal{I}} = L$.

B. Steps of the geodesic

We construct a continuous path $G: [0, L] \rightarrow \mathcal{S}^\Delta$ by concatenating *three* uniformly-parameterised segments.

1) *First step of the geodesic* ($l \in [0, L_{1/3}]$): Starting from $G(0) = P$, only the Δ -subdivisions indexed by \mathcal{D}_P move, that is each P_i ($i \in \mathcal{D}_P$) follows a d_Δ^α -geodesic in s^Δ joining it to the set A . All other Δ -subdivisions of P stay fixed. At $l = L_{1/3}$ every deleted Δ -subdivision of P has collapsed onto A , yielding the intermediate TVPD

$$G(L_{1/3}) = P \setminus \{P_i \mid i \in \mathcal{D}_P\}.$$

2) *Second step of the geodesic* ($l \in (L_{1/3}, L_{2/3}]$): From $G(L_{1/3})$ we simultaneously transport each remaining Δ -subdivision P_i ($i \in \mathcal{S}_P$) along a d_Δ^α -geodesic to its counterpart $Q_{f(i)}$. At $l = L_{2/3}$ we reach

$$G(L_{2/3}) = \{Q_{f(i)} \mid i \in \mathcal{S}_P\},$$

that is, a sub-TVPD of Q lacking the subdivisions indexed by \mathcal{I}_Q .

3) *Third step of the geodesic* ($l \in (L_{2/3}, L_{3/3}]$): Finally, for each $j \in \mathcal{I}_Q$ we “spawn” the Δ -subdivision Q_j out of A , indeed each $j \in \mathcal{I}_Q$ is formed by following a d_Δ^α -geodesic from A to Q_j . At $l = L_{3/3} = L$ all insertions have finished and $G(L_{3/3}) = Q$.

Then G is a geodesic joining P to Q . The geodesic is not unique in general, but any optimal assignment yields at least one CED-geodesic that follows the **delete \rightarrow substitute \rightarrow insert** paradigm described above (see Fig. 8).

V. CONTINUOUS EDIT DISTANCE BARYCENTERS

In this section we seek to minimize the $\text{CED}_{\alpha,1}^\Delta$ -Fréchet energy of a TVPD X w.r.t. a sample $\{V_1, \dots, V_n\}$:

$$\mathcal{E}(X) = \sum_{i=1}^n \text{CED}_{\alpha,1}^\Delta(X, V_i)^2.$$

To this end, we use two simple, practical schemes that update X along CED-geodesics and keep the best candidate seen so far.

Stochastic geodesic descent: Let the initial step size be $\rho_s \in (0, 1)$; decrease it linearly over the first $\lfloor T/2 \rfloor$ iterations down to $0.1 \cdot \rho_s$, then hold it constant until iteration T .

- (i) Initialize by choosing $i \in \{1, \dots, n\}$ randomly and set $X \leftarrow V_i$; record $B \leftarrow X$ as the current best.
- (ii) Iterate: sample $j \in \{1, \dots, n\}$ randomly; move X a CED-geodesic step of length $\rho_s \cdot \text{CED}_{\alpha,1}^\Delta(X, V_j)$ from X toward V_j . If $\mathcal{E}(X) < \mathcal{E}(B)$, update $B \leftarrow X$. Decrease ρ_s .
- (iii) Stop when the relative energy decrease over the last M iterations is $< 1\%$, or after a fixed iteration cap T ; return B .

Greedy geodesic descent: Let the initial step size be $\rho_g = 1/k$, with $k \in \mathbb{N}, k > 1$.

- (i) Initialize by choosing $i \in \{1, \dots, n\}$ randomly and set $X \leftarrow V_i$; record $B \leftarrow X$ as the current best.
- (ii) Iterate: for every $j \in \{1, \dots, n\}$, sample candidates $C_{j,t}$ ($t \in \{0, \dots, k\}$) along the CED-geodesic from X to V_j with step $t \cdot \rho_g$; let X be the candidate with the smallest energy among all samples $C_{j,t}$. If $\mathcal{E}(X) < \mathcal{E}(B)$, set $B \leftarrow X$.
- (iii) Stop when the relative energy decrease over the last iteration is $< 1\%$, or after a fixed iteration cap T ; return B .

Both schemes are iterative and use monotone acceptance (the recorded best energy is non-increasing).

VI. APPLICATIONS

We illustrate two representative utilizations of our framework: (i) temporal pattern tracking via matching and (ii) topological clustering via barycenters, which respectively leverage the CED and the TVPD barycenter computations.

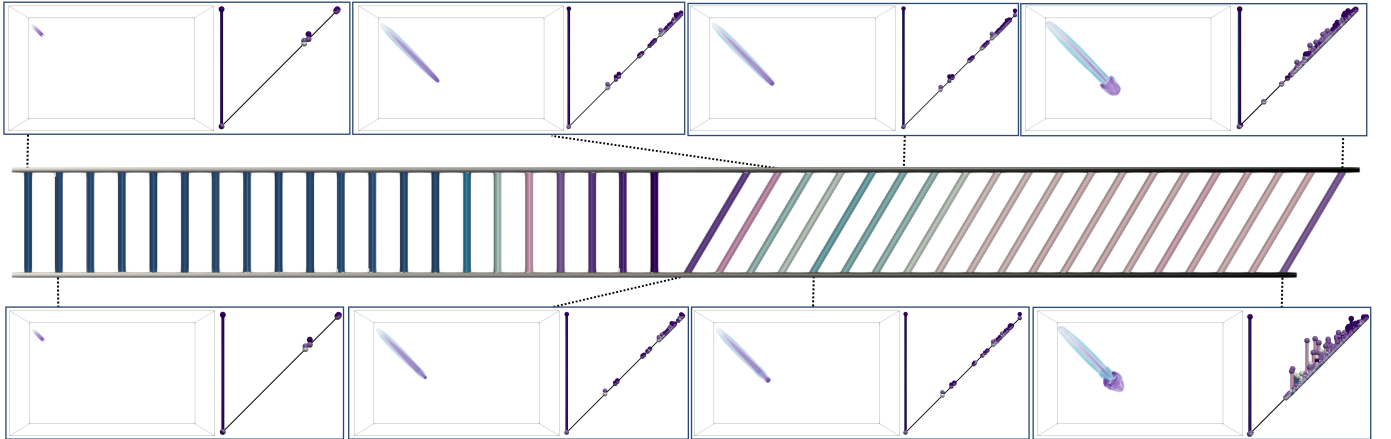


Fig. 9. Temporal-shift recovery between two input TVPDs, $YB11$ and $YC11$, from the *Asteroid Impact* dataset. Top/bottom rows show selected scalar fields and their persistence diagrams for $YB11$ (top) and $YC11$ (bottom). The middle strip shows the CED alignment: time is encoded in grayscale along each sequence (top= $YB11$, bottom= $YC11$); vertical connectors indicate the Δ -subdivision matchings, color-coded by assignment cost (from blue for low cost, through pink, to purple for high cost). The explosion occurs at different times—between time steps 6241–6931 in $YB11$ (top, 2nd–3rd snapshots) and 5335–6034 in $YC11$ (bottom, 2nd–3rd snapshots). The CED alignment correctly pairs pre- and post-explosion phases across the two sequences, thus recovering the temporal shift.

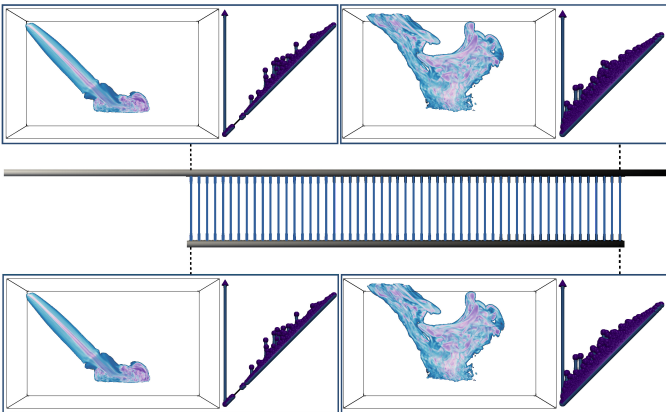


Fig. 10. Temporal pattern search between a TVPD, $YB11$, from the *Asteroid Impact* dataset and one of its sub-TVPDs. The top and bottom rows show snapshots of the scalar field and the corresponding persistence diagrams at selected time steps (top: full $YB11$ TVPD; bottom: candidate subsequence). The central strip visualizes the alignment computed by CED: both sequences are laid out along time ($YB11$ on top, subsequence on bottom), with time encoded in grayscale along each sequence; vertical connectors indicate the Δ -subdivision matchings, colored by assignment cost (in this figure uniformly blue, indicating zero cost because the target is an exact subsequence). Because the target is a true subsequence of the source, the alignment collapses to a one-to-one mapping on the selected window, effectively synchronizing the Δ -subdivisions (identical time stamps on both sides).

A. Temporal pattern tracking via matching

The CED (Sec. III) relies on the optimization of a partial assignment between two input TVPDs. Then, the resulting matchings can be used for pattern tracking between TVPDs. Fig. 9 and Fig. 10 illustrate this in two ways on input TVPDs from the asteroid impact dataset [66], [67]: (i) temporal-shift recovery by aligning two TVPDs with different event times, shown in Fig. 9; and (ii) pattern search by aligning a TVPD to one of its sub-TVPD, shown in Fig. 10. Above all, the CED matchings can be used as a visual comparison tool, allowing to represent where the similarities lie within two TVPDs. The performance of this tracking is discussed in Sec. VII-A.

B. Barycenters for topological clustering

Clustering partitions a dataset into subsets that are internally close and mutually well-separated under a task-relevant distance d . This yields a principled coarse-graining of the space: it reduces complexity, and exposes heterogeneity by delineating distinct regimes of behavior. When working with topological signatures, each cluster captures a typical topological behavior. To do so within the TVPD setting, we instantiate a k -means-style scheme [68], [69] adapted to the TVPD geometry: the centroid operator is given by our TVPD barycenter routine (stochastic or greedy; Sec. V), while pairwise dissimilarities are evaluated with the CED distance (Sec. III). Tab. 1 reports clustering results obtained with this strategy—using both the stochastic and the greedy barycenter variants—on several acquired datasets (sea-surface height [32], VESTEC [70] and asteroid impact). For comparison, we also report an MDS-based clustering baseline: for each dissimilarity (L2, Fréchet, TWED, DTW, CED), we compute the pairwise distance matrix between TVPDs, apply 2D MDS to this matrix, and then run k -means on the resulting embedding. The evaluation of the clustering performance is discussed at the end of Sec. VII-A.

Fig. 11 provides a qualitative view of the CED-based k -means on the sample of the four TVPDs from the VESTEC dataset. With $k = 2$ and the stochastic barycenter variant, the algorithm separates the TVPDs into two groups that coincide with the ground truth (runs 1–2 vs. 3–4). In the MDS embedding induced by the d_{Δ}^{α} distance, each cluster is organized around its CED barycenter, and the overlaid optimal partial matchings show that the TVPDs in a given group are consistently aligned with their centroid across time.

VII. RESULTS

This section reports experimental results executed on a workstation equipped with an Intel Xeon CPU (2.9 GHz; 16 cores; 64 GB RAM) and using TTK [71]–[73] for persistence diagram computation [74], [75] and matching [32]. Our method is implemented in C++ as TTK modules. We

Table 1. Comparison of two clustering pipelines on real TVPD datasets (SSH, VESTEC, Asteroid Impact). *MDS-clustering*: for each dissimilarities (L2, Fréchet, TWED, DTW, CED), we build the pairwise distance matrix, embed the data by classical MDS, then run k -means (with k equal to the number of classes). *CED-clustering*: our approach based on CED with two barycenter optimizers (stochastic and greedy). Entries are numbers of misclassified subsequences w.r.t. the ground truth (lower is better); – indicates not applicable. Within the MDS block, CED is competitive or superior, and on *Asteroid Impact* it is the only dissimilarity with zero error. For CED-clustering, one of the two variants reaches the ground truth on all datasets, whereas MDS-clustering makes an error on *VESTEC* for every dissimilarities.

Dataset	MDS-clustering				CED-clustering		
	L2	Fréchet	TWED	DTW	CED	CED-S	CED-G
SSH	2	0	0	0	0	0	0
VESTEC	2	2	1	1	1	0	0
Asteroid impact	–	2	1	1	0	0	1

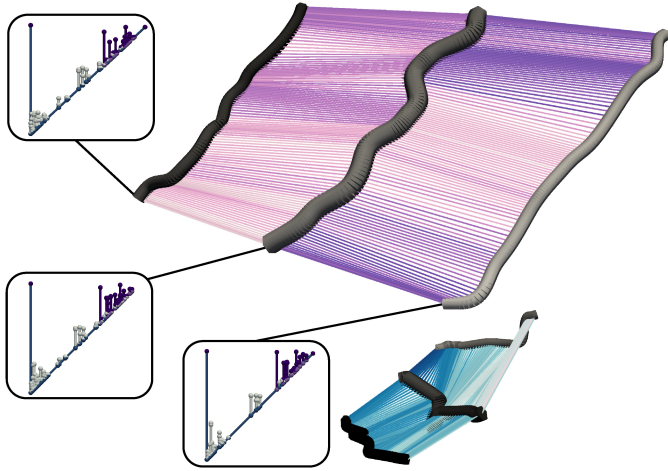


Fig. 11. 2-means clustering ($k = 2$) of the four VESTEC TVPDs (stochastic barycenter routine). Shown are the four TVPDs and the two cluster centroids returned. For visualization, TVPDs are embedded in \mathbb{R}^3 via an MDS embedding induced by d_Δ^α ; For each TVPD, time is encoded in grayscale, and its optimal CED partial matching to the assigned centroid is overlaid; with edge colors encoding assignment cost (from blue for low cost, through pink, to purple for high cost). Insets show, for the first cluster and at the initial time step, the persistence diagrams of the two input TVPDs and the persistence diagrams of their centroid, to which they are matched by CED. The two clusters correctly match the ground truth (runs 1–2 vs. 3–4).

performed the experiments on an ensemble of simulated and acquired 2D/3D datasets—some reused from prior work (sea-surface height [32], VESTEC [70]) and another drawn from the 2018 SciVis contest (asteroid impact [66], [67]). For each experiment whose results are reported in this section, we used $A = \{X_\emptyset\}$. Detailed specifications of these datasets are provided in Appendix C. The parameters α , Δ , η , and β in all our experiments are set according to the specifications detailed in Appendix D; these specifications can also be read as a practical guideline for choosing these parameters in applications of $\text{CED}_{\alpha,\beta}^\Delta$ to other TVPD datasets.

A. Framework quality

The CED is a metric (Sec. III). Fig. 12 empirically evaluates its robustness to additive noise (with one temporal-only noise experiment and one spatial-only noise experiment) for several values of parameter β . From a reference time series of timed

PL-scalar fields $U = ((f_n, t_n))_{n=0}^{N_U}$, we generate, for each experiment, 25 noisy sequences $U^{(\varepsilon)}$ with increasing values ε . For the temporal-only noise experiment, for each value of ε and each $n \in \{0, \dots, N_U\}$, we add uniform noise of amplitude ε to t_n , thereby obtaining $U^{(\varepsilon)}$. We then report $\text{CED}(\text{TVPD}(U), \text{TVPD}(U^{(\varepsilon)}))$ as a function of ε . The curves grow approximately linearly, indicating a stability of the CED to temporal jitter for reasonable noise levels. For the spatial-only noise experiment, for each value of ε and each $n \in \{0, \dots, N_U\}$, we add a uniform noise of amplitude ε to the values of f_n (that is, from f_n a noisy version f_n^ε is created such that $\|f_n - f_n^\varepsilon\| \leq \varepsilon$), yielding $U^{(\varepsilon)}$. As above, we report $\text{CED}(\text{TVPD}(U), \text{TVPD}(U^{(\varepsilon)}))$ versus ε ; empirically, the dependence on ε unfolds in four regimes. For small noise amplitude ($\varepsilon < 12\%$), the curve shows a near-linear baseline, the persistence pair birth and death times (of persistence diagrams CED-matched at the same time step) shift almost independently. For intermediate amplitudes ($12\% < \varepsilon < 20\%$), the curve becomes visibly convex as the first combinatorial events (argmax flips, elder inversions, changes of the killing cell) start to appear and increase in frequency, which steepens the slope. A threshold-crossing kink then emerges in a narrow window ($20\% < \varepsilon < 25\%$) when many pairs switch almost simultaneously. Beyond this, for $\beta = 1$ the growth becomes approximately linear as the typical W_2 contribution between diagrams matched by CED stabilizes, whereas for ($\beta < 1$) additional slope breaks appear, coinciding with switches of the CED matching regime (substitutions vs. deletions/insertions). Across both settings, β tunes tolerance to noise—the slopes and breakpoints shift as β decreases. These two experiments illustrate that, in practice, the CED varies smoothly and predictably under input perturbations, showing its robustness to additive noise.

Fig. 13 illustrates the decrease and convergence of the $\text{CED}_{\alpha,1}^\Delta$ -Fréchet energy during the iterative computation of a CED barycenter for 16 synthetic input TVPDs, using both the stochastic and the greedy variants. In both cases, the energy decreases monotonically and stabilizes.

Next, we illustrate on Fig. 9 the recovery of a temporal shift between two input TVPDs from the asteroid impact dataset (simulations of asteroid–ocean interactions with atmospheric airbursts). The two runs, YB11 and YC11, share the same early scenario but the airburst occurs markedly earlier in YC11 than in YB11. In the alignment strip, the CED produces a coherent block of matchings that follows the pre-explosion phase in both sequences, then shifts to align the post-explosion regime, rather than simply matching snapshots with similar time stamps. This behavior shows that the CED effectively recovers temporal shifts, supporting its use for temporal alignment in TVPDs. Fig. 10 illustrates the practical relevance of the CED for motif search by aligning an input TVPD to one of its own subsequences. The CED-induced alignment correctly retrieves the TVPD and subsequence correspondence and synchronizes the Δ -subdivisions (matched subdivisions share identical time stamps), thereby validating CED for motif search in TVPDs.

Tab. 1 reports the clustering results. On the MDS-based clustering baseline, CED is consistently on par with, or superior to, competing dissimilarities; notably, on Asteroid Impact

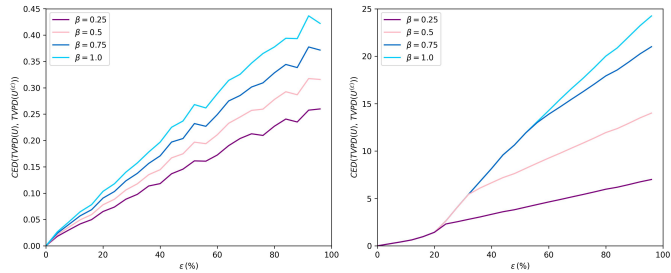


Fig. 12. Empirical robustness of the CED to an additive noise ε : *temporal-only* noise (left) and *spatial-only* noise (right), for several values of the parameter β . For the temporal-only noise (left), the curves grow approximately linearly. For the spatial-only noise (right), the distance increase follows four phases (discussed in the main text). Across both settings, β tunes the tolerance to noise—the slopes and breakpoint shifts as β varies.

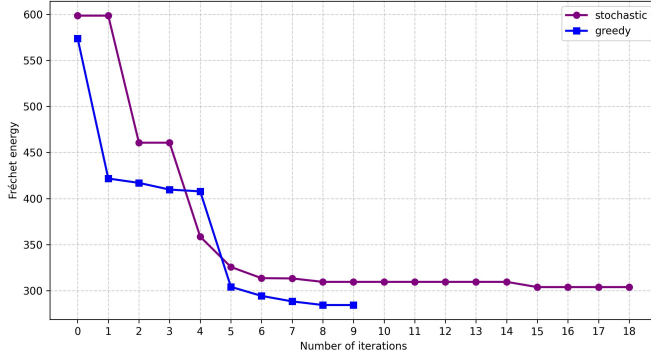


Fig. 13. Convergence of the Fréchet energy across iterations during the computation of a CED barycenter for 16 synthetic input TVPDs. In both cases, the objective decreases and then stabilizes, indicating convergence to a CED barycenter of the 16 TVPDs (returned as the final output).

it is the only one to achieve zero errors with respect to the ground truth. With CED-clustering, the ground-truth partition is always recovered by at least one of the two variants (stochastic or greedy), whereas the MDS-based pipeline misclassifies on VESTEC for every dissimilarity. Taken together, the MDS-based results support the use of CED as a distance for TVPD analysis, and the CED-clustering results validate the stochastic and greedy variants as effective methods for clustering TVPDs.

B. Time performance

Tab. 2 reports the practical time performance of our implementation for $\text{CED}_{\alpha,1}^{\Delta}$ barycenter computation, for both the stochastic and the greedy variants. We observe that the running time depends on the number of input TVPDs in the sample, N , and on the average number of persistence pairs per input TVPD, $P = n^{\Delta} \cdot p$ (where n^{Δ} denotes the average number of Δ -subdivisions per input TVPD in the sample and p the average number of persistence pairs per Δ -subdivision of its piecewise-constant approximation). Indeed, each iteration of our barycenter algorithm requires N CED-geodesic computations and $N \cdot (k - 1)$ CED distance computations for the greedy version (for a step size $\rho_s = 1/k$), and a single CED-geodesic computation for the stochastic version. To carry out the dynamic programming (Sec. III-E) used to compute each $\text{CED}_{\alpha,1}^{\Delta}$ (or each $\text{CED}_{\alpha,1}^{\Delta}$ geodesic) between

Table 2. Running times (in seconds, 5 run average) for the barycenter computation using our *greedy* and *stochastic* variants. Here, N is the number of input TVPDs in the sample, and $P = n^{\Delta} \cdot p$ is the average number of persistence pairs per input TVPD, where n^{Δ} denotes the average number of Δ -subdivisions per input TVPD and p the average number of persistence pairs per Δ -subdivision (in the piecewise-constant approximation). The execution times show that the greedy variant scales with both P and N , whereas the stochastic variant scales primarily with P .

Dataset	N	n^{Δ}	$P = n^{\Delta} \cdot p$	Greedy	Stochastic
Asteroid Impact	6	40.56	1,313,868	19,834.21	3,731.03
Sea Surface Height	8	50	82,680	4,036.67	1,661.90
VESTEC	4	120	36,242	722.46	903.81

two input TVPDs X and Y from the sample, one must first compute the distance d_{Δ}^{α} between every pair of Δ -subdivisions of \tilde{X}^{Δ} and \tilde{Y}^{Δ} . If I denotes the number of persistence pairs in a Δ -subdivision of \tilde{X}^{Δ} and J that of \tilde{Y}^{Δ} , then computing d_{Δ}^{α} between them with an exact assignment algorithm takes $\mathcal{O}((I+J)^3)$. The computation of $\text{CED}_{\alpha,1}^{\Delta}$ between X and Y is then performed by dynamic programming over the Δ -subdivisions of \tilde{X}^{Δ} and \tilde{Y}^{Δ} , yielding a time complexity $\mathcal{O}(N_X^{\Delta} \cdot N_Y^{\Delta})$. Once $\text{CED}_{\alpha,1}^{\Delta}(X, Y)$ has been computed, to place oneself somewhere on their CED-geodesic costs at most $\mathcal{O}((N_X^{\Delta} + N_Y^{\Delta}) \cdot P)$. Consequently, the end-to-end cost of one iteration is on the order of $\mathcal{O}\left((k \cdot N)((n^{\Delta})^2 \cdot (8p^3+1) + n^{\Delta} \cdot 2p)\right)$ for the greedy algorithm and $\mathcal{O}((n^{\Delta})^2 \cdot (8p^3+1) + n^{\Delta} \cdot 2p)$ for the stochastic algorithm. This explains the increase in running time observed for the stochastic variant from the VESTEC to the SSH dataset—its complexity is independent of N and depends only on P , which grows by slightly less than a factor of two, while the runtime grows by slightly more. By contrast, the greedy variant exhibits a marked increase, consistent with its additional scaling in N .

C. Limitations

A practical limitation of CED is its runtime when used within a clustering pipeline, which entails many barycenter evaluations—especially for samples with a large average number of persistence pairs per TVPDs P . Indeed, as shown in Tab. 2, barycenter times on acquired datasets are substantial and scale roughly with P for both the stochastic and the greedy variants. However, several strategies can drastically reduce the cost of each CED computation—and thus the total time required for clustering. First, following Vidal et al. [32], one can efficiently approximate the Wasserstein distance between two persistence diagrams by discarding pairs below a given persistence threshold, which significantly lowers P (and therefore the barycenter runtime) while preserving the signal carried by salient features. Second, locality constraints such as the Sakoe–Chiba band [76], originally proposed for DTW, can be directly adapted to CED: restricting the warping path to a diagonal band and computing costs only inside it reduces the dynamic programming complexity from $\mathcal{O}(n \cdot m)$ to $\mathcal{O}(n \cdot w)$ (band half-width w), leading to substantial speedups for the CED computation, and therefore the barycenter runtime—at the expense of possibly missing large optimal assignments.

Another limitation, of a theoretical nature but with practical implications, is that our construction of $\text{CED}_{\alpha,\beta}^{\Delta}$ -geodesics is

currently restricted to the case $\beta = 1$; extending it to other values of β is left for future work.

Finally, another limitation is the reliance on a common subdivision step when comparing two input TVPDs via CED. When their temporal extents differ significantly, any choice of shared subdivision step Δ induces a nontrivial lower bound on the CED between them, proportional (through the penalty parameter β) to the difference in their durations: a long TVPD P can only be matched to a much shorter one Q up to a large number of unmatched Δ -subdivisions of P , each incurring a positive deletion cost. In such cases, the distance reflects not only differences in topological patterns but also differences in temporal length, which may or may not be desirable depending on the application. In scenarios where one wishes to discount such temporal-length effects, a proper value of β needs to be adjusted. However, as mentioned above, this is only available for distance computation, and not for geodesics or barycenters.

VIII. CONCLUSION

In this paper we presented the *Continuous Edit Distance*, a geodesic, elastic distance for TVPDs. We established metric and geodesic properties, derived efficient dynamic-programming routines to evaluate the CED, and provided an explicit *delete*→*substitute*→*insert* construction of CED-geodesics. On top of this, we proposed two practical barycenter solvers—stochastic and greedy—with monotone Fréchet-energy decrease and simple stopping rules, and we released a C++ implementation within TTK.

Empirically, CED is robust to additive perturbations (approximately linear response to temporal jitter; piecewise-linear to spatial noise), yields interpretable alignments that recover temporal shifts and enable motif search. When used within a k -means-style pipeline on acquired datasets (sea-surface height, VESTEC, asteroid impact), CED delivers clustering quality on par with or superior to standard elastic dissimilarities, and our CED-based clustering attains the ground truth with at least one of the two barycenter variants.

A practical limitation is runtime in clustering pipelines, where many barycenter evaluations are required for samples with large average numbers of persistence pairs. We outlined straightforward accelerations: persistence thresholding to shrink diagram sizes while preserving the signal carried by salient features, and locality constraints (e.g., Sakoe–Chiba bands) to reduce dynamic-programming cost.

Future work includes multi-step-ahead forecasting with CED as the training objective, enabling early-warning and counterfactual topological analysis of time-varying phenomena that commonly exhibit temporal dilation and shifts (e.g., ocean dynamics, atmospheric processes, functional brain connectivity). We also plan a practical CED-based linearization of the TVPD space—mapping neighborhoods to low-dimensional coordinates—so that standard tools (dimensionality reduction, trend analysis) are directly applicable to TVPDs. Finally, a perspective is to improve computational efficiency by exploiting parallelism in our barycenter solvers, in particular for the greedy geodesic descent scheme, where the candidates

sampled along geodesics from the current iterate to each input TVPD can be evaluated independently.

Overall, CED equips TVPD analysis with a principled distance, interpretable geodesics, and practical barycenters enabling standard geometric workflows (alignment, averaging, clustering) directly in the space of TVPDs.

ACKNOWLEDGMENTS

This work is partially supported by the European Commission grant ERC-2019-COG “TORI” (ref. 863464, <https://erc-tori.github.io/>).

REFERENCES

- [1] H. Edelsbrunner and J. Harer, *Computational Topology: An Introduction*, 01 2010.
- [2] H. Edelsbrunner, D. Letscher, and A. Zomorodian, “Topological persistence and simplification,” *Discrete and Computational Geometry*, 2002.
- [3] H. Carr, J. Snoeyink, and U. Axen, “Computing contour trees in all dimensions,” in *Symp. on Dis. Alg.*, 2000.
- [4] C. Gueunet, P. Fortin, J. Jomier, and J. Tierny, “Task-Based Augmented Contour Trees with Fibonacci Heaps,” *IEEE Trans. Parallel Distrib. Syst.*, 2019.
- [5] S. Parsa, “A Deterministic $o(m \log m)$ Time Algorithm for the Reeb Graph,” in *Symposium on Computational Geometry*, 2012.
- [6] C. Gueunet, P. Fortin, J. Jomier, and J. Tierny, “Task-based Augmented Reeb Graphs with Dynamic ST-Trees,” in *Eurographics Symposium on Parallel Graphics and Visualization*, 2019.
- [7] L. De Floriani, U. Fugacci, F. Iuricich, and P. Magillo, “Morse complexes for shape segmentation and homological analysis: discrete models and algorithms,” *Computer Graphics Forum*, 2015.
- [8] A. Gyulassy, P. Bremer, and V. Pascucci, “Shared-Memory Parallel Computation of Morse-Smale Complexes with Improved Accuracy,” *IEEE Trans. Vis. and Comp. Graph. (Proc. of IEEE VIS)*, 2018.
- [9] P. Bremer, G. H. Weber, J. Tierny, V. Pascucci, M. S. Day, and J. B. Bell, “A topological framework for the interactive exploration of large scale turbulent combustion,” in *IEEE eScience*, 2009, pp. 247–254.
- [10] A. Gyulassy, P. Bremer, R. Grout, H. Kolla, J. Chen, and V. Pascucci, “Stability of Dissipation Elements: A case study in combustion,” *EuroVis: Proc. of Eurographics Conference on Visualization*, 2014.
- [11] D. Maljovec, B. Wang, P. Rosen, A. Alfonsi, G. Pastore, C. Rabiti, and V. Pascucci, “Rethinking sensitivity analysis of nuclear simulations with topology,” in *IEEE Pacific Vis*, 2016.
- [12] M. Soler, M. Petitfrère, G. Darche, M. Plainchault, B. Conche, and J. Tierny, “Ranking viscous finger simulations to an acquired ground truth with topology-aware matchings,” in *2019 IEEE 9th Symposium on Large Data Analysis and Visualization (LDAV)*. IEEE, 2019, pp. 62–72.
- [13] J. Kasten, J. Reininghaus, I. Hotz, and H. Hege, “Two-Dimensional Time-Dependent Vortex Regions Based on the Acceleration Magnitude,” *IEEE Trans. Vis. and Comp. Graph.*, 2011.
- [14] F. Nauleau, F. Vivodtzev, T. Bridel-Bertomeu, H. Beaugendre, and J. Tierny, “Topological Analysis of Ensembles of Hydrodynamic Turbulent Flows – An Experimental Study,” in *IEEE Symposium on Large Data Analysis and Visualization*, 2022.
- [15] M. Olejniczak and J. Tierny, “Topological data analysis of vortices in the magnetically-induced current density in lih molecule,” *Phys. Chem. Chem. Phys.*, vol. 25, pp. 5942–5947, 2023.
- [16] T. Daniel, M. Olejniczak, and J. Tierny, “Bondmatcher: H-bond stability analysis in molecular systems,” *IEEE Trans. Vis. and Comp. Graph. (Proc. of IEEE VIS)*, 2025.
- [17] T. Sousbie, “The Persistent Cosmic Web and its Filamentary Structure: Theory and Implementations,” *Royal Astronomical Society*, 2011.
- [18] N. Shivashankar, P. Pranav, V. Natarajan, R. van de Weygaert, E. P. Bos, and S. Rieder, “Felix: A topology based framework for visual exploration of cosmic filaments,” *IEEE Trans. Vis. and Comp. Graph.*, 2016.
- [19] A. Vintescu, F. Dupont, G. Lavoué, P. Memari, and J. Tierny, “Conformal factor persistence for fast hierarchical cone extraction,” in *Eurographics (short papers)*, A. Peytavie and C. Bosch, Eds., 2017, pp. 57–60.
- [20] F. Chazal, L. J. Guibas, S. Y. Oudot, and P. Skraba, “Persistence-Based Clustering in Riemannian Manifolds,” *Journal of the ACM*, 2013.
- [21] H. Doraiswamy, J. Tierny, P. J. S. Silva, L. G. Nonato, and C. T. Silva, “TopoMap: A 0-dimensional Homology Preserving Projection of High-Dimensional Data,” *IEEE Trans. Vis. and Comp. Graph. (Proc. of IEEE VIS)*, 2020.

[22] D. Cohen-Steiner, H. Edelsbrunner, and D. Morozov, "Vines and vineyards by updating persistence in linear time," in *Proceedings of the twenty-second annual symposium on Computational geometry*, 2006, pp. 119–126.

[23] M. G. Bergomi and A. Baratè, "Homological persistence in time series: an application to music classification," *Journal of Mathematics and Music*, vol. 14, no. 2, pp. 204–221, 2020.

[24] J. Yoo, E. Y. Kim, Y. M. Ahn, and J. C. Ye, "Topological persistence vineyard for dynamic functional brain connectivity during resting and gaming stages," *Journal of neuroscience methods*, vol. 267, pp. 1–13, 2016.

[25] E. Chávez, G. Navarro, R. Baeza-Yates, and J. L. Marroquín, "Searching in metric spaces," *ACM computing surveys (CSUR)*, vol. 33, no. 3, pp. 273–321, 2001.

[26] P.-F. Marteau, "Time warp edit distance with stiffness adjustment for time series matching," *IEEE transactions on pattern analysis and machine intelligence*, vol. 31, no. 2, pp. 306–318, 2008.

[27] T. Cover and P. Hart, "Nearest neighbor pattern classification," *IEEE transactions on information theory*, vol. 13, no. 1, pp. 21–27, 1967.

[28] G. E. Carlsson, F. Mémoli *et al.*, "Characterization, stability and convergence of hierarchical clustering methods," *J. Mach. Learn. Res.*, vol. 11, no. Apr, pp. 1425–1470, 2010.

[29] T. Hastie, R. Tibshirani, J. Friedman *et al.*, "The elements of statistical learning," 2009.

[30] P. T. Fletcher, C. Lu, S. M. Pizer, and S. Joshi, "Principal geodesic analysis for the study of nonlinear statistics of shape," *IEEE transactions on medical imaging*, vol. 23, no. 8, pp. 995–1005, 2004.

[31] M. Pont, J. Vidal, and J. Tierny, "Principal geodesic analysis of merge trees (and persistence diagrams)," *IEEE Transactions on Visualization and Computer Graphics*, vol. 29, no. 2, pp. 1573–1589, 2022.

[32] J. Vidal, J. Budin, and J. Tierny, "Progressive wasserstein barycenters of persistence diagrams," *IEEE transactions on visualization and computer graphics*, vol. 26, no. 1, pp. 151–161, 2019.

[33] L. Chen and R. Ng, "On the marriage of l_p -norms and edit distance," in *Proceedings of the Thirtieth international conference on Very large data bases-Volume 30*, 2004, pp. 792–803.

[34] C. Villani *et al.*, *Optimal transport: old and new*. Springer, 2008, vol. 338.

[35] L. Ambrosio, N. Gigli, and G. Savaré, *Gradient flows: in metric spaces and in the space of probability measures*. Springer Science & Business Media, 2008.

[36] Y. Mileyko, S. Mukherjee, and J. Harer, "Probability measures on the space of persistence diagrams," *Inverse Problems*, vol. 27, no. 12, p. 124007, 2011.

[37] D. Cohen-Steiner, H. Edelsbrunner, and J. Harer, "Stability of persistence diagrams," in *Proceedings of the twenty-first annual symposium on Computational geometry*, 2005, pp. 263–271.

[38] K. Turner, Y. Mileyko, S. Mukherjee, and J. Harer, "Fréchet means for distributions of persistence diagrams," 2013. [Online]. Available: <https://arxiv.org/abs/1206.2790>

[39] T. Lacombe, M. Cuturi, and S. Oudot, "Large scale computation of means and clusters for persistence diagrams using optimal transport," *Advances in Neural Information Processing Systems*, vol. 31, 2018.

[40] E. Munch, K. Turner, P. Bendich, S. Mukherjee, J. Mattingly, and J. Harer, "Probabilistic fréchet means for time varying persistence diagrams," 2015.

[41] M. M. Fréchet, "Sur quelques points du calcul fonctionnel," *Rendiconti del Circolo Matematico di Palermo (1884-1940)*, vol. 22, no. 1, pp. 1–72, 1906.

[42] H. Alt and M. Godau, "Computing the fréchet distance between two polygonal curves," *International Journal of Computational Geometry & Applications*, vol. 5, no. 01n02, pp. 75–91, 1995.

[43] A. Driemel and S. Har-Peled, "Jaywalking your dog: computing the fréchet distance with shortcuts," *SIAM Journal on Computing*, vol. 42, no. 5, pp. 1830–1866, 2013.

[44] V. I. Levenshtein *et al.*, "Binary codes capable of correcting deletions, insertions, and reversals," in *Soviet physics doklady*, vol. 10, no. 8. Soviet Union, 1966, pp. 707–710.

[45] G. Navarro, "A guided tour to approximate string matching," *ACM computing surveys (CSUR)*, vol. 33, no. 1, pp. 31–88, 2001.

[46] D. Gusfield, "Algorithms on strings, trees, and sequences: Computer science and computational biology," *Acm Sigact News*, vol. 28, no. 4, pp. 41–60, 1997.

[47] H. Sakoe and S. Chiba, "Dynamic programming algorithm optimization for spoken word recognition," *IEEE transactions on acoustics, speech, and signal processing*, vol. 26, no. 1, pp. 43–49, 2003.

[48] D. J. Berndt and J. Clifford, "Using dynamic time warping to find patterns in time series," in *Proceedings of the 3rd international conference on knowledge discovery and data mining*, 1994, pp. 359–370.

[49] T. M. Rath and R. Manmatha, "Word image matching using dynamic time warping," in *2003 IEEE Computer Society Conference on Computer Vision and Pattern Recognition, 2003. Proceedings.*, vol. 2. IEEE, 2003, pp. II–II.

[50] J. Vial, H. Noçairi, P. Sassi, S. Mallipati, G. Cognon, D. Thiébaut, B. Teillet, and D. N. Rutledge, "Combination of dynamic time warping and multivariate analysis for the comparison of comprehensive two-dimensional gas chromatograms: application to plant extracts," *Journal of Chromatography A*, vol. 1216, no. 14, pp. 2866–2872, 2009.

[51] L. Gupta, D. L. Molfese, R. Tammana, and P. G. Simos, "Nonlinear alignment and averaging for estimating the evoked potential," *IEEE transactions on biomedical engineering*, vol. 43, no. 4, pp. 348–356, 1996.

[52] F. Petitjean, A. Ketterlin, and P. Gançarski, "A global averaging method for dynamic time warping, with applications to clustering," *Pattern recognition*, vol. 44, no. 3, pp. 678–693, 2011.

[53] F. Petitjean and P. Gançarski, "Summarizing a set of time series by averaging: From steiner sequence to compact multiple alignment," *Theoretical Computer Science*, vol. 414, no. 1, pp. 76–91, 2012.

[54] D. Schultz and B. Jain, "Nonsmooth analysis and subgradient methods for averaging in dynamic time warping spaces," *Pattern recognition*, vol. 74, pp. 340–358, 2018.

[55] D. Zhang, W. Zuo, D. Zhang, H. Zhang, and N. Li, "Classification of pulse waveforms using edit distance with real penalty," *EURASIP Journal on Advances in Signal Processing*, vol. 2010, pp. 1–8, 2010.

[56] A. Bagnall, J. Lines, A. Bostrom, J. Large, and E. Keogh, "The great time series classification bake off: a review and experimental evaluation of recent algorithmic advances," *Data mining and knowledge discovery*, vol. 31, pp. 606–660, 2017.

[57] J. Serra and J. L. Arcos, "An empirical evaluation of similarity measures for time series classification," *Knowledge-Based Systems*, vol. 67, pp. 305–314, 2014.

[58] X. Tang, J. Gu, Z. Shen, and P. Chen, "A flight profile clustering method combining twed with k-means algorithm for 4d trajectory prediction," in *2015 Integrated Communication, Navigation and Surveillance Conference (ICNS)*. IEEE, 2015, pp. S3–1.

[59] M. Cuturi and M. Blondel, "Soft-dtw: a differentiable loss function for time-series," in *International conference on machine learning*. PMLR, 2017, pp. 894–903.

[60] M. Tagliaferri, P. Barnouin, H. Wei, E. Bach, C. O. Paschereit, and M. Bohon, "Applications of soft-dtw for time series data averaging inside a rotating detonation combustor," in *AIAA AVIATION 2023 Forum*, 2023, p. 4143.

[61] Y. Ma, Y. Tang, Y. Zeng, T. Ding, and Y. Liu, "An n400 identification method based on the combination of soft-dtw and transformer," *Frontiers in Computational Neuroscience*, vol. 17, p. 1120566, 2023.

[62] S. Y. Oudot, *Persistence theory: from quiver representations to data analysis*. American Mathematical Society Providence, 2015, vol. 209.

[63] H. Edelsbrunner, J. Harer, and A. Zomorodian, "Hierarchical morse complexes for piecewise linear 2-manifolds," in *Proceedings of the seventeenth annual symposium on Computational geometry*, 2001, pp. 70–79.

[64] H. Edelsbrunner and E. P. Mücke, "Simulation of simplicity: a technique to cope with degenerate cases in geometric algorithms," *ACM Transactions on Graphics (tog)*, vol. 9, no. 1, pp. 66–104, 1990.

[65] R. Bellman, "Dynamic programming," *science*, vol. 153, no. 3731, pp. 34–37, 1966.

[66] R. Taylor, A. Chourasia, D. Whalen, and M. L. Norman, "The IEEE scivis contest," <http://sciviscontest.ieeevis.org/2008/>, 2008.

[67] R. Imahori, I. B. Rojo, and T. Günther, "Visualization and analysis of deep water asteroid impacts," in *2018 IEEE Scientific Visualization Conference (SciVis)*. IEEE, 2018, pp. 85–96.

[68] S. Lloyd, "Least squares quantization in pcm," *IEEE transactions on information theory*, vol. 28, no. 2, pp. 129–137, 1982.

[69] A. K. Jain, "Data clustering: 50 years beyond k-means," *Pattern recognition letters*, vol. 31, no. 8, pp. 651–666, 2010.

[70] M. Flatken, A. Podobas, R. Fellegara, A. Basermann, J. Holke, D. Knapp, M. Kontak, C. Krullikowski, M. Nolde, N. Brown *et al.*, "Vestec: Visual exploration and sampling toolkit for extreme computing," *IEEE Access*, vol. 11, pp. 87 805–87 834, 2023.

[71] J. Tierny, G. Favelier, J. A. Levine, C. Gueunet, and M. Michaux, "The Topology ToolKit," *IEEE Trans. Vis. and Comp. Graph. (Proc. of IEEE VIS)*, 2017, <https://topology-tool-kit.github.io/>.

- [72] T. Bin Masood, J. Budin, M. Falk, G. Favelier, C. Garth, C. Gueunet, P. Guillou, L. Hofmann, P. Hristov, A. Kamakshidasan, C. Kappe, P. Klacansky, P. Laurin, J. Levine, J. Lukasczyk, D. Sakurai, M. Soler, P. Steneteg, J. Tierny, W. Usher, J. Vidal, and M. Wozniak, “An Overview of the Topology ToolKit,” in *TopoInVis*, 2019.
- [73] E. Le Guillou, M. Will, P. Guillou, J. Lukasczyk, P. Fortin, C. Garth, and J. Tierny, “TTK is Getting MPI-Ready,” *IEEE Trans. Vis. and Comp. Graph.*, 2024.
- [74] P. Guillou, J. Vidal, and J. Tierny, “Discrete Morse sandwich: Fast computation of persistence diagrams for scalar data – an algorithm and a benchmark,” 2023. [Online]. Available: <https://arxiv.org/abs/2206.13932>
- [75] E. L. Guillou, P. Fortin, and J. Tierny, “Distributed discrete Morse sandwich: Efficient computation of persistence diagrams for massive scalar data,” *IEEE Trans. Parallel Distrib. Syst.*, 2025.
- [76] E. Keogh and C. A. Ratanamahatana, “Exact indexing of dynamic time warping,” *Knowledge and information systems*, vol. 7, no. 3, pp. 358–386, 2005.
- [77] V. I. Bogachev and M. A. S. Ruas, *Measure theory*. Springer, 2007, vol. 1, no. 1.
- [78] V. I. Bogachev, *Measure Theory*. Springer, 2007, vol. 2.
- [79] G. Favelier, N. Faraj, B. Summa, and J. Tierny, “Persistence atlas for critical point variability in ensembles,” 2018. [Online]. Available: <https://arxiv.org/abs/1807.11212>
- [80] M. Pont, J. Vidal, J. Delon, and J. Tierny, “Wasserstein distances, geodesics and barycenters of merge trees,” *IEEE Transactions on Visualization and Computer Graphics*, vol. 28, no. 1, pp. 291–301, 2021.

APPENDIX

APPENDIX A

MEASURE THEORY PRELIMINARIES

We used concepts from measure theory in the formalization of the CED and the elements to which it applies; we therefore succinctly recall some necessary definitions and results. We refer the reader to the textbook [77] for a measure theory exposition.

Let X be a set. A family \mathcal{M} of subsets of X is called a σ -algebra on X if it satisfies the following properties: (i) $X \in \mathcal{M}$; (ii) If $A \in \mathcal{M}$, then $(X \setminus A) \in \mathcal{M}$; (iii) If $A_n \in \mathcal{M}$ for every $n \in \mathbb{N}$, then $\bigcup_{n \in \mathbb{N}} A_n \in \mathcal{M}$. The elements of \mathcal{M} are referred to as the measurable sets of X , and the ordered pair (X, \mathcal{M}) is called a measurable space.

For F a family of subsets of a set X , we define $\sigma(F)$ as the intersection of the σ -algebras \mathcal{M} on X that contain F , and call $\sigma(F)$ the σ -algebra generated by F ; it is the smallest σ -algebra on X that contains F .

If (X, d) is a metric space, the Borel σ -algebra on X is the σ -algebra, denoted $\mathcal{B}(X)$, generated by the open balls of X : $\mathcal{B}(X) = \sigma(\{B(x, r) \mid x \in X, r > 0\})$, with $B(x, r) = \{y \in X, d(x, y) < r\}$.

Considering that (X, \mathcal{M}) and (Y, \mathcal{N}) are measurable spaces, an application $f : X \rightarrow Y$ is said to be measurable with respect to \mathcal{M} and \mathcal{N} if $f^{-1}(A) \in \mathcal{M}$ for all $A \in \mathcal{N}$. In this case, we also say that $f : (X, \mathcal{M}) \rightarrow (Y, \mathcal{N})$ is measurable.

Moreover, for (X, d) and (Y, d') two metric spaces, a result of measure theory is that a continuous application $f : X \rightarrow Y$ is then measurable with respect to $\mathcal{B}(X)$ and $\mathcal{B}(Y)$. When the choice of metrics is not clear from the context, we will say that $f : (X, d) \rightarrow (Y, d')$ is continuous, in order to make continuity with respect to d and d' explicit.

Unless otherwise specified, a function $f : X \rightarrow Y$ is said to be measurable if it is measurable with respect to $\mathcal{B}(X)$ and $\mathcal{B}(Y)$.

Fix (X, \mathcal{M}) a measurable space. A function $\mu : \mathcal{M} \rightarrow [0, +\infty]$ is a positive measure if $\mu(\emptyset) = 0$, and for any countable family $(A_n)_{n \in \mathbb{N}}$ of pairwise disjoint sets in \mathcal{M} , we have $\mu(\bigcup_{n \in \mathbb{N}} A_n) = \sum_{n \in \mathbb{N}} \mu(A_n)$. The triple (X, \mathcal{M}, μ) is called a measure space.

There exists a unique positive measure λ on $(\mathbb{R}, \mathcal{B}(\mathbb{R}))$, called Lebesgue measure, such that $\lambda([a, b]) = \lambda((a, b]) = \lambda([a, b)) = \lambda((a, b)) = b - a$ for all $a, b \in \mathbb{R}$ with $a < b$.

Let (X, \mathcal{M}, μ) be a measure space. A set $A \subset X$ is defined as negligible if $A \in \mathcal{M}$ and $\mu(A) = 0$. The measure μ is said to be complete if every subset of a negligible set is also measurable and negligible. Suppose $\mathcal{Z}(\mathcal{M})$ be the collection of all sets $E \subset X$ for which there exist $A, B \in \mathcal{M}$ such that $A \subset E \subset B$ and $\mu(B \setminus A) = 0$. Define $\mu^*(E) = \mu(A)$. Then $\mathcal{Z}(\mathcal{M})$ is a σ -algebra on X , μ^* is a complete measure extending μ , and $(X, \mathcal{Z}(\mathcal{M}), \mu^*)$ is called the completion of \mathcal{M} for μ . In practice, we still denote μ^* by μ .

Let Y be a metric space. If $I \in \mathcal{B}(\mathbb{R})$, we said a map $f : I \rightarrow Y$ is Lebesgue-measurable if it is measurable with respect to $\mathcal{Z}(\mathcal{B}(\mathbb{R})|_I)$, the completion of $\mathcal{B}(\mathbb{R})|_I$ for the Lebesgue measure λ , and $\mathcal{B}(Y)$, that is, $f^{-1}(B) \in \mathcal{Z}(\mathcal{B}(\mathbb{R})|_I)$ for every $B \in \mathcal{B}(Y)$. In this case, we also say that $f : (I, \mathcal{B}(\mathbb{R})|_I) \rightarrow (Y, \mathcal{B}(Y))$ is Lebesgue-measurable. As a classical result, if $f : I \rightarrow Y$ is continuous, then f is measurable. Moreover, another result is that if $f : I \rightarrow Y$ is measurable, then f is Lebesgue-measurable. So, if $f : I \rightarrow Y$ is continuous, then f is Lebesgue-measurable.

APPENDIX B

PROOFS

Remark. All the abstract results proved in this section apply in particular to the space (\mathcal{D}_2, W_2) of persistence diagrams with finite 2-th moment (implicitly assumed in the main manuscript), endowed with the 2-Wasserstein distance, which is a geodesic Polish metric

space [36], [38] (in particular separable). In the main manuscript, we moreover take $A \subset E$ to be a singleton, so that for every $x \in E$ the set $\{y \in A : d(x, y) = d(x, A)\}$ is non-empty (indeed, it coincides with A itself). Hence all the standing assumptions on (E, d) and on A are automatically satisfied in the setting used in the main manuscript and for the experiments, and the results of the present section apply directly to that case.

Let (E, d) be a non-empty separable metric space, provided with its Borel sigma-algebra $\mathcal{B}(E)$, and let $\alpha \in (0, 1)$, $B \in (0, 1]$, and $A \subsetneq E$ be non-empty.

Set $\Delta \in (0, +\infty)$, and let \mathcal{S}^Δ be the space of applications F from a subset

$$\text{dom } F = \bigcup_{i \in \{1, \dots, N_F^\Delta\}} I_i^F \subset \mathbb{R}$$

to E , with $N_F^\Delta \in \mathbb{N}^*$, and $(I_i^F)_{i \in \{1, \dots, N_F^\Delta\}}$ a disjoint family of intervals of \mathbb{R} , such that:

- $\forall i \in \{1, \dots, N_F^\Delta\}$, $\sup I_i^F - \inf I_i^F = \Delta$,
- $\forall (i, i') \in \{1, \dots, N_F^\Delta\}^2$, $\forall (x, x') \in I_i^F \times I_{i'}^F$, $i < i' \Rightarrow x < x'$,
- $\forall t \in \text{dom } F$, $d(F(t), A) > 0$,
- $\forall i \in \{1, \dots, N_F^\Delta\}$, $F|_{I_i^F} : (I_i^F, \mathcal{Z}(\mathcal{B}(\mathbb{R})|_{I_i^F})) \rightarrow (E, \mathcal{B}(E))$ is measurable, where $\mathcal{Z}(\mathcal{B}(\mathbb{R})|_{I_i^F})$ is the completion of $\mathcal{B}(\mathbb{R})|_{I_i^F}$ for λ , the Lebesgue measure,
- $\forall i \in \{1, \dots, N_F^\Delta\}$, $\text{diam}(\text{Im}(F|_{I_i^F})) < \infty$.

We will omit the superscript Δ in the notation N_F^Δ whenever no ambiguity arises. Let $(F, G) \in (\mathcal{S}^\Delta)^2$, $i \in \{1, \dots, N_F\}$, $j \in \{1, \dots, N_G\}$.

We denote $F_i := F|_{I_i^F}$, and we call F_i a Δ -subdivision.

We consider that two Δ -subdivisions F_i, G_j are equal if:

- $\inf I_i^F = \inf I_j^G$,
- $\sup I_i^F = \sup I_j^G$,
- $\lambda(\{x \in I_i^F \cap I_j^G \mid F_i(x) \neq G_j(x)\}) = 0$.

We denote s^Δ the Δ -subdivision space.

In a similar way, let $(F, G) \in (\mathcal{S}^\Delta)^2$, with $N_F = N_G$, we consider that F, G are equal if, $\forall i \in \{1, \dots, N_F\}$, $F_i = G_i$. More generally, two measurable applications F and G from $\mathcal{X} \subset \mathbb{R}$ to E are considered equal in our framework whenever $\lambda(\{x \in \mathcal{X}, F(x) \neq G(x)\}) = 0$.

Remark : Moreover if,

$$F_i : (I_i^F, \mathcal{Z}(\mathcal{B}(\mathbb{R})|_{I_i^F})) \rightarrow (E, \mathcal{B}(E))$$

with $\inf I_i^F = c$, $\sup I_i^F = d$, $(c, d) \in \mathbb{R}^2$, $I_i^F \neq [c, d]$, we can use instead \tilde{F}_i (still denoted F_i in practice):

$$([c, d], \mathcal{Z}(\mathcal{B}(\mathbb{R})|_{[c, d]})) \rightarrow (E, \mathcal{B}(E))$$

measurable and defined as, $\forall t \in (c, d)$, $\tilde{F}_i(t) = F_i(t)$, $\tilde{F}_i(c) = x$, $\tilde{F}_i(d) = y$, with x, y some elements of E .

Indeed, let us suppose $F \in \mathcal{S}^\Delta$, with $I_i^F \neq [c, d]$, for $(c, d, i) \in \mathbb{R}^2 \times \{1, \dots, N_F\}$

If $A \in \mathcal{B}(E)$,

$$\tilde{F}_i^{-1}(A) = \begin{cases} F_i^{-1}(A) \cup \{c, d\} & \text{if } x \in A \text{ and } y \in A, \\ F_i^{-1}(A) \cup \{c\} & \text{if } x \in A \text{ and } y \notin A, \\ F_i^{-1}(A) \cup \{d\} & \text{if } x \notin A \text{ and } y \in A, \\ F_i^{-1}(A) & \text{if } x \notin A \text{ and } y \notin A. \end{cases}$$

with $F_i^{-1}(A) \in \mathcal{Z}(\mathcal{B}(I_i^F))$, then with $F_i^{-1}(A) \in \mathcal{Z}(\mathcal{B}([c, d]))$. Moreover, $\{c\}, \{d\}, \{c, d\} \in \mathcal{Z}(\mathcal{B}([c, d]))$, then

$$F_i^{-1}(A) \cup \{c\} \in \mathcal{Z}(\mathcal{B}([c, d])), \quad F_i^{-1}(A) \cup \{d\} \in \mathcal{Z}(\mathcal{B}([c, d]))$$

$$F_i^{-1}(A) \cup \{c, d\} \in \mathcal{Z}(\mathcal{B}([c, d]))$$

And so,

$$\tilde{F}_i : ([c, d], \mathcal{Z}(\mathcal{B}(\mathbb{R})|_{[c, d]})) \longrightarrow (E, \mathcal{B}(E))$$

is measurable and $\tilde{F}_i = F_i$.

Similarly, if $F_i : (I_i^F, \mathcal{Z}(\mathcal{B}(\mathbb{R})|_{I_i^F})) \longrightarrow (E, \mathcal{B}(E))$,

with $\inf I_i^F = c, \sup I_i^F = d, (c, d) \in \mathbb{R}^2, I_i^F \neq (c, d)$, we can use instead \tilde{F}_i (still denoted F_i in practice) :

$$((c, d), \mathcal{Z}(\mathcal{B}(\mathbb{R})|_{(c, d)})) \longrightarrow (E, \mathcal{B}(E))$$

measurable and defined as $\forall t \in (c, d), \tilde{F}_i(t) = F_i(t)$.

Indeed, let us suppose $F \in \mathcal{S}^\Delta$, with $I_i^F \neq (c, d)$, for $(c, d, i) \in \mathbb{R}^2 \times \{1, \dots, N_F\}$

If $A \in \mathcal{B}(E)$,

$$\text{we have } \tilde{F}_i^{-1}(A) = F_i^{-1}(A) \cap (c, d)$$

with $F_i^{-1}(A) \in \mathcal{Z}(\mathcal{B}(I_i^F))$.

Then $F_i^{-1}(A) \cap (c, d) \in \mathcal{Z}(\mathcal{B}((c, d)))$ and $\tilde{F}_i^{-1}(A) \in \mathcal{Z}(\mathcal{B}((c, d)))$.

Finally,

$$\tilde{F}_i : ((c, d), \mathcal{Z}(\mathcal{B}(\mathbb{R})|_{(c, d)})) \longrightarrow (E, \mathcal{B}(E))$$

is measurable and $\tilde{F}_i = F_i$.

So, in the next we can assume that I_i^F is open, or closed, as we need.

We therefore now assume for the next that if $F \in \mathcal{S}^\Delta$, then $\forall i \in \{1, \dots, N_F\}, I_i^F$ is open.

Proposition B.1. Let $(P, Q) \in (\mathcal{S}^\Delta)^2$, and $(i, j) \in \{1, \dots, N_P\} \times \{1, \dots, N_Q\}$.

We denote:

$$\begin{aligned} a_i &:= \inf(I_i^P), & b_i &:= \sup(I_i^P), \\ c_j &:= \inf(I_j^Q), & d_j &:= \sup(I_j^Q). \end{aligned}$$

Then the application,

$$W_\alpha^{P_i, Q_j} : (I_i^P, \mathcal{Z}(\mathcal{B}(\mathbb{R})|_{I_i^P})) \longrightarrow (\mathbb{R}, \mathcal{B}(\mathbb{R}))$$

$$t \mapsto W_\alpha^{P_i, Q_j}(t) = (1 - \alpha) \cdot d(P(t), Q(t + c_j - a_i)) + \alpha \cdot |c_j - a_i|$$

is measurable, and Lebesgue-integrable.

Proof. The application

$$U : (I_i^P, \mathcal{Z}(\mathcal{B}(\mathbb{R})|_{I_i^P})) \longrightarrow (I_j^Q, \mathcal{Z}(\mathcal{B}(\mathbb{R})|_{I_j^Q}))$$

is measurable.

$$\text{Indeed, let } M \in \mathcal{Z}(\mathcal{B}(\mathbb{R})|_{I_j^Q}),$$

then $M = A \cup N$ with $A \in \mathcal{B}(\mathbb{R})|_{I_j^Q}$ and N a negligible part of $\mathcal{B}(\mathbb{R})|_{I_j^Q}$,

Then

$$U^{-1}(A \cup N) = U^{-1}(A) \cup U^{-1}(N).$$

Since,

$$\begin{aligned} U : (I_i^P, \mathcal{B}(\mathbb{R})|_{I_i^P}) &\longrightarrow (I_j^Q, \mathcal{B}(\mathbb{R})|_{I_j^Q}) \\ t &\mapsto t + c_j - a_i \end{aligned}$$

is measurable, as continuous function, $\forall K \in \mathcal{B}(\mathbb{R})|_{I_j^Q}$,

$$U^{-1}(K) \in \mathcal{B}(\mathbb{R})|_{I_i^P}.$$

So,

$$U^{-1}(A) \in \mathcal{B}(\mathbb{R})|_{I_i^P}.$$

Moreover, N is a negligible part of $\mathcal{B}(\mathbb{R})|_{I_j^Q}$, then because λ is invariant by translation,

$$\exists T \in \mathcal{B}(\mathbb{R})|_{I_j^Q}, N \subset T, \lambda(T) = 0 \Rightarrow U^{-1}(N) \subset U^{-1}(T)$$

$$\lambda(U^{-1}(T)) = 0, \text{ with } U^{-1}(T) \in \mathcal{B}(\mathbb{R})|_{I_i^P} \text{ (Because,}$$

$$\begin{aligned} U : (I_i^P, \mathcal{B}(\mathbb{R})|_{I_i^P}) &\longrightarrow (I_j^Q, \mathcal{B}(\mathbb{R})|_{I_j^Q}) \\ t &\mapsto t + c_j - a_i \end{aligned}$$

is continuous).

So $U^{-1}(M)$ is the union of a element of $\mathcal{B}(\mathbb{R})|_{I_i^P}$ and a negligible part of $\mathcal{B}(\mathbb{R})|_{I_i^P}$, then

$$U^{-1}(M) \in \mathcal{Z}(\mathcal{B}(\mathbb{R})|_{I_i^P}).$$

$$\begin{aligned} \text{And } U : (I_i^P, \mathcal{Z}(\mathcal{B}(\mathbb{R})|_{I_i^P})) &\rightarrow (I_j^Q, \mathcal{Z}(\mathcal{B}(\mathbb{R})|_{I_j^Q})) \\ t &\mapsto t + c_j - a_i \end{aligned}$$

is measurable.

$$\text{Also } P|_{I_i^P} : (I_i^P, \mathcal{Z}(\mathcal{B}(\mathbb{R})|_{I_i^P})) \longrightarrow (E, \mathcal{B}(E)) \text{ and } Q|_{I_j^Q} :$$

$$(I_j^Q, \mathcal{Z}(\mathcal{B}(\mathbb{R})|_{I_j^Q})) \longrightarrow (E, \mathcal{B}(E)) \text{ are measurable by definition.}$$

Then the application

$$\tilde{Q} = (Q|_{I_j^Q} \circ U) : (I_i^P, \mathcal{Z}(\mathcal{B}(\mathbb{R})|_{I_i^P})) \longrightarrow (E, \mathcal{B}(E))$$

is measurable as composition of measurable applications.

$$\begin{aligned} \text{The application } V &: (I_i^P, \mathcal{Z}(\mathcal{B}(\mathbb{R})|_{I_i^P})) \rightarrow (E^2, \mathcal{B}(E) \otimes \mathcal{B}(E)) \end{aligned}$$

$$t \mapsto V(t) = (P(t), \tilde{Q}(t))$$

has its component-wise applications measurable, and the target sigma-algebra is the sigma-algebra product, then V is measurable.

Because d is continuous (as a distance) on T the topology product of (E, d) and (E, d) , then

$$d : (E^2, \sigma(T)) \rightarrow (\mathbb{R}, \mathcal{B}(\mathbb{R})) \text{ is measurable,}$$

where we denote $\sigma(T)$ the sigma-algebra generated by T .

Because $\sigma(T) = \mathcal{B}(E) \otimes \mathcal{B}(E)$ (since E is separable), and d is measurable for $\sigma(T)$, then d is measurable for $\mathcal{B}(E) \otimes \mathcal{B}(E)$.

Since

$$V : (I_i^P, \mathcal{Z}(\mathcal{B}(\mathbb{R})|_{I_i^P})) \rightarrow (E^2, \mathcal{B}(E) \otimes \mathcal{B}(E))$$

and

$$d : (E^2, \mathcal{B}(E) \otimes \mathcal{B}(E)) \rightarrow (\mathbb{R}, \mathcal{B}(\mathbb{R})) \text{ are measurable,}$$

then

$$\widetilde{W} := d \circ V : (I_i^P, \mathcal{Z}(\mathcal{B}(\mathbb{R})|_{I_i^P})) \rightarrow (\mathbb{R}, \mathcal{B}(\mathbb{R}))$$

is measurable.

Then $W = (1-\alpha) \cdot \widetilde{W}$ is measurable, as a product of a measurable function by a constant.

$$G : (\mathbb{R} \times \mathbb{R}, \mathcal{B}(\mathbb{R}) \otimes \mathcal{B}(\mathbb{R})) \rightarrow (\mathbb{R}, \mathcal{B}(\mathbb{R}))$$

$$(x, y) \mapsto x + y$$

is measurable, as continuous function for

$$\mathcal{B}(\mathbb{R} \otimes \mathbb{R}) = \mathcal{B}(\mathbb{R}) \otimes \mathcal{B}(\mathbb{R}) \quad \text{since } \mathbb{R} \text{ is separable.}$$

Because, $I_i^P \in \mathcal{Z}(\mathcal{B}(\mathbb{R})|_{I_i^P})$, then

$$H : (I_i^P, \mathcal{Z}(\mathcal{B}(\mathbb{R})|_{I_i^P})) \rightarrow (\mathbb{R}, \mathcal{B}(\mathbb{R}))$$

$$t \mapsto \alpha \cdot |c_j - a_i|$$

is measurable.

Then,

$$W_\alpha^{P_i, Q_j} : (I_i^P, \mathcal{Z}(\mathcal{B}(\mathbb{R})|_{I_i^P})) \rightarrow (\mathbb{R}, \mathcal{B}(\mathbb{R}))$$

$$t \mapsto G(W(t), H(t))$$

is measurable as composition of measurable functions.

$$\forall t \in I_i^P,$$

$$0 \leq W_\alpha^{P_i, Q_j}(t) \leq (1-\alpha)(d(P(\frac{a_i + b_i}{2}), Q(\frac{c_j + d_j}{2})) + \text{diam}(\text{Im}(P|_{I_i^P})) + \text{diam}(\text{Im}(Q|_{I_j^Q}))) + \alpha \cdot |c_j - a_i| \quad (2)$$

(by triangular inequality of d). Then $W_\alpha^{P_i, Q_j}$ is Lebesgue-integrable.

□

Proposition B.2. Let $P \in \mathcal{S}^\Delta$, and $i \in \{1, \dots, N_P\}$. We denote $a_i = \inf(I_i^P)$, $b_i = \sup(I_i^P)$.

Then the application,

$$S_\alpha^{P_i} : (I_i^P, \mathcal{Z}(\mathcal{B}(\mathbb{R})|_{I_i^P})) \rightarrow (\mathbb{R}, \mathcal{B}(\mathbb{R}))$$

$$t \mapsto S_\alpha^{P_i}(t) = (1-\alpha) \cdot d(P(t), A)$$

is measurable, and Lebesgue-integrable.

Proof. The application

$$d(\cdot, A) : (E, d) \rightarrow (\mathbb{R}, |\cdot|)$$

$$x \mapsto d(x, A)$$

is continuous, because 1-Lipschitz (as a distance to a subset function in a metric space), so

$$d(\cdot, A) : (E, \mathcal{B}(E)) \rightarrow (\mathbb{R}, \mathcal{B}(\mathbb{R}))$$

$$x \mapsto d(x, A)$$

is measurable.

Since

$$P|_{I_i^P} : (I_i^P, \mathcal{Z}(\mathcal{B}(\mathbb{R})|_{I_i^P})) \rightarrow (E, \mathcal{B}(E))$$

is measurable, then

$$\tilde{S} := d(\cdot, A) \circ P|_{I_i^P}$$

is measurable, as composition of measurable functions.

Then, $S_\alpha^{P_i} = (1-\alpha) \cdot \tilde{S}$ is measurable as a product of a measurable function by a constant.

Finally, $\forall t \in I_i^P$,

$$0 \leq S_\alpha^{P_i}(t) \leq (1-\alpha) \cdot \left(d\left(P\left(\frac{a_i + b_i}{2}\right), A\right) + \text{diam}(\text{Im}(P|_{I_i^P})) \right) \quad (3)$$

so $S_\alpha^{P_i}$ is Lebesgue-integrable. □

Definition B.3. Let $(\rho, q) \in (s^\Delta)^2$.

Then $\exists (P, Q) \in (\mathcal{S}^\Delta)^2$, $\exists (i, j) \in \{1, \dots, N_P\} \times \{1, \dots, N_Q\}$, such that $\rho = P_i$ and $q = Q_j$.

Let's denote

$$\begin{aligned} a_i &= \inf(I_i^P), & b_i &= \sup(I_i^P), \\ c_j &= \inf(I_j^Q), & d_j &= \sup(I_j^Q). \end{aligned}$$

We define

$$D_\Delta^\alpha(\rho, q) = D_\Delta^\alpha(P_i, Q_j) := \int_{a_i}^{b_i} W_\alpha^{P_i, Q_j}(t) dt$$

and

$$D_\Delta^\alpha(\rho, A) = D_\Delta^\alpha(P_i, A) := \int_{a_i}^{b_i} S_\alpha^{P_i}(t) dt$$

Lemma B.4. Let $(\rho, q, r) \in (s^\Delta)^3$.

So $\exists (P, Q, R) \in (\mathcal{S}^\Delta)^3$, $\exists (i, j, k) \in \{1, \dots, N_P\} \times \{1, \dots, N_Q\} \times \{1, \dots, N_R\}$, such that $\rho = P_i$, $q = Q_j$, $r = R_k$

Then we have,

- $\forall i \in \{1, \dots, N_P\}$, $\forall j \in \{1, \dots, N_Q\}$, $D_\Delta^\alpha(P_i, Q_j) = D_\Delta^\alpha(Q_j, P_i)$

- $\forall (i, j, k) \in \{1, \dots, N_P\} \times \{1, \dots, N_Q\} \times \{1, \dots, N_R\}$,

$$D_\Delta^\alpha(P_i, Q_j) + D_\Delta^\alpha(Q_j, R_k) \geq D_\Delta^\alpha(P_i, R_k)$$

- $\forall (i, j) \in \{1, \dots, N_P\} \times \{1, \dots, N_Q\}$, $P_i = Q_j \Leftrightarrow D_\Delta^\alpha(P_i, Q_j) = 0$

- $\forall (i, j) \in \{1, \dots, N_P\} \times \{1, \dots, N_Q\}$, $D_\Delta^\alpha(P_i, Q_j) \geq 0$

And so, $(s^\Delta, D_\Delta^\alpha)$ is a metric space.

Proof. Let's denote $a_i = \inf(I_i^P)$, $b_i = \sup(I_i^P)$, $c_j = \inf(I_j^Q)$, $d_j = \sup(I_j^Q)$, $e_k = \inf(I_k^R)$, and $f_k = \sup(I_k^R)$.

$$(I_i^P, \mathcal{Z}(\mathcal{B}(\mathbb{R})|_{I_i^P})) \longrightarrow (\mathbb{R}, \mathcal{B}(\mathbb{R}))$$

$$t \mapsto (1 - \alpha) \cdot d(P(t), Q(t + c_j - a_i)) + \alpha \cdot |c_j - a_i|$$

is measurable and Lebesgue-integrable (see B.1), and

$$(0, 1) \longrightarrow (a_i, b_i) \text{ is a } C^1\text{-diffeomorphism.}$$

$$t \mapsto a_i \cdot (1 - t) + b_i \cdot t$$

Moreover,

$$(I_j^Q, \mathcal{Z}(\mathcal{B}(\mathbb{R})|_{I_j^Q})) \longrightarrow (\mathbb{R}, \mathcal{B}(\mathbb{R}))$$

$$t \mapsto (1 - \alpha) \cdot d(Q(t), P(t + a_i - c_j)) + \alpha \cdot |a_i - c_j|$$

is measurable and Lebesgue-integrable, and

$$(0, 1) \longrightarrow (c_j, d_j) \text{ is a } C^1\text{-diffeomorphism.}$$

$$t \mapsto c_j \cdot (1 - t) + d_j \cdot t$$

Then, using Lebesgue integration by substitution theorem,

$$\begin{aligned} & \bullet D_\Delta^\alpha(P_i, Q_j) \\ &= \int_{a_i}^{b_i} [(1 - \alpha) \cdot d(P(t), Q(t + c_j - a_i)) \\ &+ \alpha \cdot |c_j - a_i|] dt \\ &= (b_i - a_i) \cdot \int_0^1 [(1 - \alpha) \cdot d(P(a_i \cdot (1 - t) + b_i \cdot t), \\ &Q(a_i \cdot (1 - t) + b_i \cdot t + c_j - a_i)) + \alpha \cdot |c_j - a_i|] dt \\ &= \Delta \cdot \int_0^1 [(1 - \alpha) \cdot d(P(a_i \cdot (1 - t) + b_i \cdot t), \\ &Q((b_i - a_i) \cdot t + c_j)) + \alpha \cdot |c_j - a_i|] dt \\ &= \Delta \cdot \int_0^1 [(1 - \alpha) \cdot d(P(a_i \cdot (1 - t) + b_i \cdot t), \\ &Q(c_j \cdot (1 - t) + d_j \cdot t)) + \alpha \cdot |c_j - a_i|] dt \\ &= \Delta \cdot \int_0^1 [(1 - \alpha) \cdot d(Q(c_j \cdot (1 - t) + d_j \cdot t), \\ &P(a_i \cdot (1 - t) + b_i \cdot t)) + \alpha \cdot |a_i - c_j|] dt \\ &= |d_j - c_j| \cdot \int_0^1 [(1 - \alpha) \cdot d(Q(c_j \cdot (1 - t) + d_j \cdot t), \\ &P((b_i - a_i) \cdot t + a_i)) + \alpha \cdot |a_i - c_j|] dt \\ &= |d_j - c_j| \cdot \int_0^{d_j} [(1 - \alpha) \cdot d(Q(c_j \cdot (1 - t) + d_j \cdot t), \\ &P((d_j - c_j) \cdot t + a_i)) + \alpha \cdot |a_i - c_j|] dt \\ &= \int_{c_j}^{d_j} [(1 - \alpha) \cdot d(Q(t), P(t + a_i - c_j)) + \\ &\alpha \cdot |a_i - c_j|] dt \\ &= D_\Delta^\alpha(Q_j, P_i) \end{aligned} \tag{4}$$

$$\begin{aligned} & \bullet D_\Delta^\alpha(P_i, Q_j) + D_\Delta^\alpha(Q_j, R_k) \\ &= \Delta \cdot \int_0^1 [(1 - \alpha) \cdot d(P(a_i \cdot (1 - t) + b_i \cdot t), \\ &Q(c_j \cdot (1 - t) + d_j \cdot t)) + \alpha \cdot |c_j - a_i|] dt \\ &+ \Delta \cdot \int_0^1 [(1 - \alpha) \cdot d(Q(c_j \cdot (1 - t) + d_j \cdot t), \\ &R(e_k \cdot (1 - t) + f_k \cdot t)) + \alpha \cdot |e_k - c_j|] dt \\ &= \Delta \cdot \int_0^1 [(1 - \alpha) \cdot (d(P(a_i \cdot (1 - t) + b_i \cdot t), \\ &Q(c_j \cdot (1 - t) + d_j \cdot t)) \\ &+ d(Q(c_j \cdot (1 - t) + d_j \cdot t), \\ &R(e_k \cdot (1 - t) + f_k \cdot t))) + \alpha \cdot (|c_j - a_i| + |e_k - c_j|)] dt \\ &\geq \Delta \cdot \int_0^1 [(1 - \alpha) \cdot d(P(a_i \cdot (1 - t) + b_i \cdot t), \\ &R(e_k \cdot (1 - t) + f_k \cdot t)) + \alpha \cdot |e_k - a_i|] dt \\ &= D_\Delta^\alpha(P_i, R_k) \quad (\text{by triangular inequality of } d \text{ and } |\cdot|) \end{aligned} \tag{5}$$

- If $P_i = Q_j$, then

$$\begin{aligned} & D_\Delta^\alpha(P_i, Q_j) \\ &= \Delta \cdot \int_0^1 [(1 - \alpha) \cdot d(P(a_i \cdot (1 - t) + b_i \cdot t), \\ &Q(c_j \cdot (1 - t) + d_j \cdot t)) + \alpha \cdot |c_j - a_i|] dt \\ &= \Delta \cdot \int_0^1 [(1 - \alpha) \cdot d(P(a_i \cdot (1 - t) + b_i \cdot t), \\ &Q(a_i \cdot (1 - t) + b_i \cdot t)) + \alpha \cdot |a_i - a_i|] dt \\ &= \Delta \cdot \int_0^1 [(1 - \alpha) \cdot d(P(a_i \cdot (1 - t) + b_i \cdot t), \\ &Q(a_i \cdot (1 - t) + b_i \cdot t))] dt \\ &= \Delta \cdot (1 - \alpha) \cdot \int_0^1 d(P(a_i \cdot (1 - t) + b_i \cdot t), \\ &Q(a_i \cdot (1 - t) + b_i \cdot t)) dt \\ &= \Delta \cdot (1 - \alpha) \cdot \int_0^1 0 \cdot dt = 0 \quad (\text{Since} \\ &\lambda(\{x \in I_i^P \cap I_j^Q \text{ such that } P_i(x) \neq Q_j(x)\}) = 0, \\ &\text{then } \lambda(\{t \in [0, 1] \text{ such that } d(P(a_i \cdot (1 - t) + b_i \cdot t), \\ &Q(a_i \cdot (1 - t) + b_i \cdot t)) \neq 0\}) = 0) \end{aligned} \tag{6}$$

- If $D_\Delta^\alpha(P_i, Q_j) = 0$, then

$$\begin{aligned} & \Delta \cdot \int_0^1 [(1 - \alpha) \cdot d(P(a_i \cdot (1 - t) + b_i \cdot t), \\ &Q(c_j \cdot (1 - t) + d_j \cdot t)) + \alpha \cdot |c_j - a_i|] dt = 0, \end{aligned} \tag{7}$$

which implies, $a_i = c_j$ (and so $b_i = d_j$), and

$$\begin{aligned} & \lambda(\{t \in (0, 1) \text{ such that } d(P(a_i \cdot (1 - t) + b_i \cdot t), \\ &Q(a_i \cdot (1 - t) + b_i \cdot t)) \neq 0\}) = 0, \end{aligned} \tag{8}$$

Thus

$$\lambda(\{x \in I_i^P \cap I_j^Q \text{ such that } P_i(x) \neq Q_j(x)\}) = 0,$$

and $a_i = c_j$, $b_i = d_j$, then finally,

$$P_i = Q_j.$$

□

Lemma B.5. Let $(\rho, q) \in (s^\Delta)^2$,

so $\exists (P, Q) \in (\mathcal{S}^\Delta)^2$, $\exists (i, j) \in \{1, \dots, N_P\} \times \{1, \dots, N_Q\}$, such that $\rho = P_i$, $q = Q_j$.

We have,

$$D_{\Delta}^{\alpha}(P_i, A) + D_{\Delta}^{\alpha}(P_i, Q_j) \geq D_{\Delta}^{\alpha}(Q_j, A)$$

Proof. With the same notation as above,

$$\begin{aligned} D_{\Delta}^{\alpha}(P_i, A) + D_{\Delta}^{\alpha}(P_i, Q_j) &= \int_{a_i}^{b_i} (1-\alpha) \cdot d(P(t), A) dt + \int_{a_i}^{b_i} ((1-\alpha) \cdot d(P(t), Q(t+c_j - a_i)) + \alpha |c_j - a_i|) dt \\ &\geq \int_{a_i}^{b_i} (1-\alpha) \cdot d(P(t), A) dt + \int_{a_i}^{b_i} ((1-\alpha) \cdot d(P(t), Q(t+c_j - a_i))) dt \\ &= \int_{a_i}^{b_i} (1-\alpha) \cdot [d(P(t), A) + d(P(t), Q(t+c_j - a_i))] dt \\ &\geq \int_{a_i}^{b_i} (1-\alpha) \cdot d(Q(t+c_j - a_i), A) dt \end{aligned}$$

(Because in a metric space (E, d) with $A \subset E$, we have $\forall (x, y) \in E^2$, $d(x, y) + d(y, A) \geq d(x, A)$, indeed $d(\cdot, A)$ is 1-Lipschitz)

$$= \int_{c_j}^{d_j} (1-\alpha) \cdot d(Q(t), A) dt = D_{\Delta}^{\alpha}(Q_j, A),$$

by Lebesgue integral substitution theorem, with the C^1 -diffeomorphism,

$$\varphi : (c_j, d_j) \longrightarrow (a_i, b_i), \quad t \longmapsto t + a_i - c_j$$

and the measurable function,

$$((a_i, b_i), \mathcal{Z}(\mathcal{B}(\mathbb{R})|_{(a_i, b_i)})) \longrightarrow (\mathbb{R}, \mathcal{B}(\mathbb{R})),$$

$$t \longmapsto (1-\alpha) \cdot d(Q(t+c_j - a_i), A)$$

as composition of $\mathcal{S}_{\alpha}^{Q_j}$ (see B.2) and \mathcal{U} . \square

If $P \in \mathcal{S}^{\Delta}$, thanks to the imposed conditions, we can unambiguously denote P as a sequence $(P_i)_{1 \leq i \leq N_P}$. Moreover, if $N \in \{1, \dots, N_P\}$, then $(P_i)_{1 \leq i \leq N}$ stay obviously in \mathcal{S}^{Δ} .

Definition B.6. Set $(P, Q) \in (\mathcal{S}^{\Delta})^2$. We call Δ -partial assignment (we omit the Δ when the context is clear) between P and Q any function f from $\text{dom } f \subset \{1, 2, \dots, N_P\}$ to $\text{Im } f \subset \{1, 2, \dots, N_Q\}$, such that f is strictly increasing, i.e. $\forall (i, j) \in (\text{dom } f)^2$, $i < j \Rightarrow f(i) < f(j)$. We denote $\mathcal{A}^{\Delta}(P, Q)$ the set of the partial assignments between P and Q in \mathcal{S}^{Δ} , we can see that specifying an $f \in \mathcal{A}^{\Delta}(P, Q)$ directly yields an assignment $f^{-1} \in \mathcal{A}^{\Delta}(Q, P)$.

Then, the $\text{CED}_{\alpha, \beta}^{\Delta}$ between $P = (P_i)_{1 \leq i \leq N_P}$ and $Q = (Q_j)_{1 \leq j \leq N_Q}$ is defined as:

$$\begin{aligned} \text{CED}_{\alpha, \beta}^{\Delta}(P, Q) &= \min_{f \in \mathcal{A}^{\Delta}(P, Q)} \text{cost}_{(P, Q)}^{\Delta}(f) := \\ &\min_{f \in \mathcal{A}^{\Delta}(P, Q)} \left(\sum_{i \in \text{dom } f} D_{\Delta}^{\alpha}(P_i, Q_{f(i)}) \right. \\ &\quad + \sum_{i \notin \text{dom } f} \beta \cdot D_{\Delta}^{\alpha}(P_i, A) \quad (3) \\ &\quad \left. + \sum_{j \notin \text{Im } f} \beta \cdot D_{\Delta}^{\alpha}(Q_j, A) \right) \quad (4) \end{aligned}$$

Proposition B.7. Let $0 < \Delta_1, \Delta_2 < +\infty$ be such that $\Delta_2 = k \Delta_1$ for some integer $k \geq 1$. Let $(P, Q) \in \mathcal{S}^{\Delta_2} \times \mathcal{S}^{\Delta_2}$. Then $(P, Q) \in \mathcal{S}^{\Delta_1} \times \mathcal{S}^{\Delta_1}$ and

$$\text{CED}_{\alpha, \beta}^{\Delta_1}(P, Q) \leq \text{CED}_{\alpha, \beta}^{\Delta_2}(P, Q). \quad (9)$$

Proof. By definition of \mathcal{S}^{Δ_2} , the domain of P (resp. Q) is a finite union of consecutive intervals of length Δ_2 , which we call Δ_2 -subdivisions. Since $\Delta_2 = k \Delta_1$, each such Δ_2 -subdivision can be partitioned into k consecutive intervals of length Δ_1 . Thus (P, Q) also admit a representation in $\mathcal{S}^{\Delta_1} \times \mathcal{S}^{\Delta_1}$.

Let

$$g \in \mathcal{A}^{\Delta_2}(P, Q)$$

be a partial assignment achieving $\text{CED}_{\alpha, \beta}^{\Delta_2}(P, Q)$, that is

$$\text{CED}_{\alpha, \beta}^{\Delta_2}(P, Q) = \text{cost}_{(P, Q)}^{\Delta_2}(g). \quad (10)$$

We now construct a refined partial assignment $g' \in \mathcal{A}^{\Delta_1}(P, Q)$ as follows. Each Δ_2 -subdivision of P (resp. Q) is split into k consecutive Δ_1 -subdivisions. For every matched pair $(i, g(i))$ of Δ_2 -subdivisions, we match, within the corresponding blocks, the ℓ -th Δ_1 -subdivision of P to the ℓ -th Δ_1 -subdivision of Q , for $\ell = 1, \dots, k$. For Δ_2 -subdivisions that are unmatched in g (deletions or insertions), we declare the corresponding k Δ_1 -subdivisions unmatched in g' . Because g is strictly increasing and the refinement inside each block preserves the order, g' is strictly increasing as well, hence $g' \in \mathcal{A}^{\Delta_1}(P, Q)$.

It remains to compare the costs. Let

$$P_i \quad \text{and} \quad Q_j$$

be two matched Δ_2 -subdivisions in g , with time intervals

$$I_i^P = (a, b), \quad I_j^Q = (c, d),$$

so that $b - a = d - c = \Delta_2$. By definition of the local distance $D_{\Delta_2}^{\alpha}$, we have

$$\begin{aligned} D_{\Delta_2}^{\alpha}(P_i, Q_j) &= \int_a^b ((1-\alpha) W_2(P(t), Q(t+c-a)) + \alpha |c-a|) dt. \end{aligned} \quad (11)$$

On the refined grid with step Δ_1 , the interval (a, b) is partitioned into

$$\begin{aligned} (a_0, a_1], \quad (a_1, a_2], \quad \dots, \quad (a_{k-1}, a_k), \\ a_0 = a, \quad a_k = b, \quad a_{\ell+1} - a_{\ell} = \Delta_1, \end{aligned} \quad (12)$$

and similarly (c, d) into

$$\begin{aligned} (c_0, c_1], \quad (c_1, c_2], \quad \dots, \quad (c_{k-1}, c_k), \\ c_0 = c, \quad c_k = d, \quad c_{\ell+1} - c_{\ell} = \Delta_1, \end{aligned} \quad (13)$$

with $c_{\ell} - c = a_{\ell} - a$ for all ℓ . For each $\ell \in \{0, \dots, k-1\}$, the corresponding Δ_1 -subdivisions $P^{(\ell)}, Q^{(\ell)}$ have time intervals $(a_{\ell}, a_{\ell+1})$ and $(c_{\ell}, c_{\ell+1})$. Applying the definition of $D_{\Delta_1}^{\alpha}$ to this pair gives

$$\begin{aligned} D_{\Delta_1}^{\alpha}(P^{(\ell)}, Q^{(\ell)}) &= \int_{a_{\ell}}^{a_{\ell+1}} ((1-\alpha) W_2(P(t), Q(t+c_{\ell}-a_{\ell})) \\ &\quad + \alpha |c_{\ell}-a_{\ell}|) dt. \end{aligned} \quad (14)$$

Since $c_{\ell} - a_{\ell} = (c + (a_{\ell} - a)) - a_{\ell} = c - a$, (14) simplifies to

$$\begin{aligned} D_{\Delta_1}^{\alpha}(P^{(\ell)}, Q^{(\ell)}) &= \int_{a_{\ell}}^{a_{\ell+1}} ((1-\alpha) W_2(P(t), Q(t+c-a)) \\ &\quad + \alpha |c-a|) dt. \end{aligned} \quad (15)$$

Summing (15) over $\ell = 0, \dots, k-1$ and using the additivity of the integral over the partition of (a, b) yields

$$\begin{aligned} \sum_{\ell=0}^{k-1} D_{\Delta_1}^{\alpha}(P^{(\ell)}, Q^{(\ell)}) &= \int_a^b ((1-\alpha) W_2(P(t), Q(t+c-a)) \\ &\quad + \alpha |c-a|) dt = D_{\Delta_2}^{\alpha}(P_i, Q_j). \end{aligned} \quad (16)$$

An entirely similar computation holds for the deletion and insertion terms, defined via $D_\Delta^\alpha(\cdot, A)$. For instance, consider a deletion of a Δ_2 -subdivision P_i with time interval $I_i^P = (a, b)$. By definition,

$$D_{\Delta_2}^\alpha(P_i, A) = \int_a^b (1 - \alpha) W_2(P(t), A) dt. \quad (17)$$

On the refined grid with step Δ_1 , the interval (a, b) is partitioned into $(a_0, a_1], \dots, (a_{k-1}, a_k)$ as above, and the corresponding Δ_1 -subdivisions $P^{(\ell)}$ have time intervals $(a_\ell, a_{\ell+1})$. For each $\ell \in \{0, \dots, k-1\}$, we have

$$D_{\Delta_1}^\alpha(P^{(\ell)}, A) = \int_{a_\ell}^{a_{\ell+1}} (1 - \alpha) W_2(P(t), A) dt. \quad (18)$$

Summing (18) over ℓ and using the additivity of the integral over the partition of (a, b) yields

$$\begin{aligned} \sum_{\ell=0}^{k-1} D_{\Delta_1}^\alpha(P^{(\ell)}, A) &= \int_a^b (1 - \alpha) W_2(P(t), A) dt \\ &= D_{\Delta_2}^\alpha(P_i, A). \end{aligned} \quad (19)$$

The case of insertions is handled in the same way, by applying the definition of $D_\Delta^\alpha(\cdot, A)$ to a Δ_2 -subdivision Q_j and its refinement into Δ_1 -subdivisions $Q^{(\ell)}$. Hence, the total deletion and insertion costs are preserved when passing from Δ_2 to Δ_1 .

Therefore, the total cost of the refined assignment g' in \mathcal{S}^{Δ_1} satisfies

$$\text{cost}_{(P, Q)}^{\Delta_1}(g') = \text{cost}_{(P, Q)}^{\Delta_2}(g) = \text{CED}_{\alpha, \beta}^{\Delta_2}(P, Q).$$

By minimality of $\text{CED}_{\alpha, \beta}^{\Delta_1}$ over $\mathcal{A}^{\Delta_1}(P, Q)$, we obtain

$$\text{CED}_{\alpha, \beta}^{\Delta_1}(P, Q) \leq \text{cost}_{(P, Q)}^{\Delta_1}(g') = \text{CED}_{\alpha, \beta}^{\Delta_2}(P, Q),$$

which proves the claim. \square

Definition B.8. Let $P = (P_i)_{1 \leq i \leq N_P} \in \mathcal{S}^\Delta$, $Q = (Q_j)_{1 \leq j \leq N_Q} \in \mathcal{S}^\Delta$. In this subsection, we will note for $v = (x, y) \in \mathbb{R}^2$, $v_1 = x$, $v_2 = y$, $\delta_\Delta^{\alpha, \beta}(v) = \delta_\Delta^{\alpha, \beta}((P_i)_{0 \leq i \leq v_1}, (Q_j)_{0 \leq j \leq v_2})$. Then, we define recursively, $\forall K \in \{1, \dots, N_P\}$, $\forall K' \in \{1, \dots, N_Q\}$,

$$\begin{aligned} \delta_\Delta^{\alpha, \beta}(K, K') &= \min \left\{ \delta_\Delta^{\alpha, \beta}(K-1, K') + \beta \cdot D_\Delta^\alpha(P_K, A), \right. \\ \delta_\Delta^{\alpha, \beta}(K-1, K'-1) &+ D_\Delta^\alpha(P_K, Q_{K'}), \\ \left. \delta_\Delta^{\alpha, \beta}(K, K'-1) + \beta \cdot D_\Delta^\alpha(Q_{K'}, A) \right\} \end{aligned}$$

with initialization $\delta_\Delta^{\alpha, \beta}(0, 0) = 0, \forall K \in \{1, \dots, N_P\}$, $\delta_\Delta^{\alpha, \beta}(K, 0) = \delta_\Delta^{\alpha, \beta}(K-1, 0) + \beta \cdot D_\Delta^\alpha(P_K, A)$, and $\forall K' \in \{1, \dots, N_Q\}$, $\delta_\Delta^{\alpha, \beta}(0, K') = \delta_\Delta^{\alpha, \beta}(0, K'-1) + \beta \cdot D_\Delta^\alpha(Q_{K'}, A)$.

Moreover, once the recursive computation of $\delta_\Delta^{\alpha, \beta}((P_i)_{0 \leq i \leq N_P}, (Q_j)_{0 \leq j \leq N_Q})$ has been carried out, we define recursively, with initializations $A_0 = \emptyset$, $B_0 = (N_P, N_Q)$,

- $B_{z+1} = B_z - (1, 0)$ if $\delta_\Delta^{\alpha, \beta}(B_z) = \delta_\Delta^{\alpha, \beta}(B_z - (1, 0)) + \beta \cdot D_\Delta^\alpha(P_{B_{z_1}}, A)$,
- $B_{z+1} = B_z - (1, 1)$ if $\delta_\Delta^{\alpha, \beta}(B_z) = \delta_\Delta^{\alpha, \beta}(B_z - (1, 1)) + D_\Delta^\alpha(P_{B_{z_1}}, Q_{B_{z_2}})$,
- $B_{z+1} = B_z - (0, 1)$ if $\delta_\Delta^{\alpha, \beta}(B_z) = \delta_\Delta^{\alpha, \beta}(B_z - (0, 1)) + \beta \cdot D_\Delta^\alpha(Q_{B_{z_2}}, A)$,
- $A_{z+1} = A_z \cup B_z$ if $B_{z+1} = B_z - (1, 1)$,
- $A_{z+1} = A_z$ if $B_{z+1} = B_z - (1, 0)$,
- $A_{z+1} = A_z$ if $B_{z+1} = B_z - (0, 1)$.

We stop when $B_Z = (0, 0)$ for some $Z \in \mathbb{N}$.

Proposition B.9. Let $(P, Q) \in \mathcal{S}^\Delta$. Then

$$\delta_\Delta^{\alpha, \beta}((P_i)_{0 \leq i \leq N_P}, (Q_j)_{0 \leq j \leq N_Q}) = \text{CED}_{\alpha, \beta}^{\Delta_2}(P, Q).$$

Proof. Let $\mathcal{I} = N_P$ and $\mathcal{J} = N_Q$. We prove the proposition by induction on $\mathcal{I} + \mathcal{J}$.

— Suppose that $\mathcal{I} = 1$, and $\mathcal{J} = 1$.

$$\begin{aligned} \delta_\Delta^{\alpha, \beta}(1, 1) &= \min \left(\delta_\Delta^{\alpha, \beta}(0, 1) + \beta \cdot D_\Delta^\alpha(P_1, A), \right. \\ \delta_\Delta^{\alpha, \beta}(0, 0) &+ D_\Delta^\alpha(P_1, Q_1), \\ \left. \delta_\Delta^{\alpha, \beta}(1, 0) + \beta \cdot D_\Delta^\alpha(Q_1, A) \right) \\ &= \min \left(\beta \cdot D_\Delta^\alpha(Q_1, A) + \beta \cdot D_\Delta^\alpha(P_1, A), \right. \\ D_\Delta^\alpha(P_1, Q_1), \beta \cdot D_\Delta^\alpha(P_1, A) &+ \beta \cdot D_\Delta^\alpha(Q_1, A) \left. \right) \\ &= \min_{f \in \mathcal{A}^\Delta(P, Q)} \text{cost}_{(P, Q)}^\Delta(f) = \text{CED}_{\alpha, \beta}^{\Delta_2}(P, Q). \end{aligned}$$

Then the proposition is true for $\mathcal{I} = 1$, and $\mathcal{J} = 1$.

— Suppose that the proposition is true for all indices $(\mathcal{I}', \mathcal{J}')$ with $\mathcal{I}' + \mathcal{J}' < \mathcal{I} + \mathcal{J}$.

Firstly, note that:

$$\begin{aligned} \mathcal{A}^\Delta(P, Q) &= \left\{ f \in \mathcal{A}^\Delta(P, Q) \mid f(\mathcal{I}) = \mathcal{J} \right\} \\ &\cup \left\{ f \in \mathcal{A}^\Delta(P, Q) \mid \mathcal{I} \notin \text{dom}(f) \right\} \\ &\cup \left\{ f \in \mathcal{A}^\Delta(P, Q) \mid \mathcal{J} \notin \text{Im}(f) \right\}. \end{aligned} \quad (20)$$

(i) Assume that the optimal Δ -partial assignment f between P and Q belongs to $\{f \in \mathcal{A}^\Delta(P, Q) \mid f(\mathcal{I}) = \mathcal{J}\}$.

Then

$$\begin{aligned} \text{CED}_{\alpha, \beta}^\Delta(P, Q) &= \text{cost}_{(P, Q)}^\Delta(f) \\ &= \text{cost}_{((P_i)_{1 \leq i \leq \mathcal{I}-1}, (Q_j)_{1 \leq j \leq \mathcal{J}-1})}^\Delta(f^{(\mathcal{I}, \mathcal{J})*}) + D_\Delta^\alpha(P_\mathcal{I}, Q_\mathcal{J}) \end{aligned} \quad (21)$$

with $f^{(\mathcal{I}, \mathcal{J})*}$ the Δ -partial assignment between $(P_i)_{1 \leq i \leq \mathcal{I}-1}$ and $(Q_j)_{1 \leq j \leq \mathcal{J}-1}$ obtained from f by removing the substitution of $P_\mathcal{I}$ to $Q_\mathcal{J}$ from f . Thus $f^{(\mathcal{I}, \mathcal{J})*}$ is the optimal Δ -partial assignment between $(P_i)_{1 \leq i \leq \mathcal{I}-1}$ and $(Q_j)_{1 \leq j \leq \mathcal{J}-1}$. Indeed if this were not the case, and if $g \neq f^{(\mathcal{I}, \mathcal{J})*}$ were the optimal Δ -partial assignment between $(P_i)_{1 \leq i \leq \mathcal{I}-1}$ and $(Q_j)_{1 \leq j \leq \mathcal{J}-1}$, then g to which we add the substitution of $P_\mathcal{I}$ by $Q_\mathcal{J}$ would have a cost lower than f , which would contradict that f is the optimal assignment between P and Q .

Then

$$\begin{aligned} \text{CED}_{\alpha, \beta}^\Delta((P_i)_{1 \leq i \leq \mathcal{I}-1}, (Q_j)_{1 \leq j \leq \mathcal{J}-1}) &= \\ &= \text{cost}_{((P_i)_{1 \leq i \leq \mathcal{I}-1}, (Q_j)_{1 \leq j \leq \mathcal{J}-1})}^\Delta(f^{(\mathcal{I}, \mathcal{J})*}) \end{aligned} \quad (22)$$

and so

$$\begin{aligned} \text{CED}_{\alpha, \beta}^\Delta(P, Q) &= \text{CED}_{\alpha, \beta}^\Delta((P_i)_{1 \leq i \leq \mathcal{I}-1}, (Q_j)_{1 \leq j \leq \mathcal{J}-1}) \\ &+ D_\Delta^\alpha(P_\mathcal{I}, Q_\mathcal{J}). \end{aligned} \quad (23)$$

Thus,

$$\begin{aligned} \delta_\Delta^{\alpha, \beta}(\mathcal{I}, \mathcal{J}) &= \min \left\{ \delta_\Delta^{\alpha, \beta}(\mathcal{I}-1, \mathcal{J}) + \beta \cdot D_\Delta^\alpha(P_\mathcal{I}, A), \right. \\ \delta_\Delta^{\alpha, \beta}(\mathcal{I}-1, \mathcal{J}-1) &+ D_\Delta^\alpha(P_\mathcal{I}, Q_\mathcal{J}), \\ \left. \delta_\Delta^{\alpha, \beta}(\mathcal{I}, \mathcal{J}-1) + \beta \cdot D_\Delta^\alpha(Q_\mathcal{J}, A) \right\} \end{aligned} \quad (24)$$

$$\begin{aligned} &= \min \left\{ \delta_\Delta^{\alpha, \beta}(\mathcal{I}-1, \mathcal{J}) + \beta \cdot D_\Delta^\alpha(P_\mathcal{I}, A), \right. \\ \text{CED}_{\alpha, \beta}^\Delta((P_i)_{1 \leq i \leq \mathcal{I}-1}, (Q_j)_{1 \leq j \leq \mathcal{J}-1}) &+ D_\Delta^\alpha(P_\mathcal{I}, Q_\mathcal{J}), \\ \delta_\Delta^{\alpha, \beta}(\mathcal{I}, \mathcal{J}-1) + \beta \cdot D_\Delta^\alpha(Q_\mathcal{J}, A) \left. \right\} \text{(by induction)} \end{aligned} \quad (25)$$

$$\begin{aligned} &= \min \left\{ \delta_\Delta^{\alpha, \beta}(\mathcal{I}-1, \mathcal{J}) + \beta \cdot D_\Delta^\alpha(P_\mathcal{I}, A), \right. \\ \text{CED}_{\alpha, \beta}^\Delta(P, Q) &+ D_\Delta^\alpha(P_\mathcal{I}, Q_\mathcal{J}), \\ \delta_\Delta^{\alpha, \beta}(\mathcal{I}, \mathcal{J}-1) + \beta \cdot D_\Delta^\alpha(Q_\mathcal{J}, A) \left. \right\} \leq \text{CED}_{\alpha, \beta}^\Delta(P, Q) \end{aligned} \quad (26)$$

(ii) Assume that the optimal Δ -partial assignment f between P and Q belongs to $\{f \in \mathcal{A}^\Delta(P, Q) \text{ such that } \mathcal{I} \notin \text{dom}(f)\}$.

Then

$$\text{CED}_{\alpha,\beta}^\Delta(P, Q) = \text{cost}_{(P, Q)}^\Delta(f) \quad (27)$$

$$= \text{cost}_{((P_i)_{1 \leq i \leq \mathcal{I}-1}, (Q_j)_{1 \leq j \leq \mathcal{J}})}^\Delta(f^{\mathcal{I}^*}) + \beta \cdot D_\Delta^\alpha(P_{\mathcal{I}}, A), \quad (28)$$

with $f^{\mathcal{I}^*}$ the Δ -partial assignment between $(P_i)_{1 \leq i \leq \mathcal{I}-1}$ and $(Q_j)_{1 \leq j \leq \mathcal{J}}$ obtained from f by removing the deletion of $P_{\mathcal{I}}$ from f . Thus $f^{\mathcal{I}^*}$ is the optimal Δ -partial assignment between $(P_i)_{1 \leq i \leq \mathcal{I}-1}$ and $(Q_j)_{1 \leq j \leq \mathcal{J}}$. Indeed if this were not the case, and if $g \neq f^{\mathcal{I}^*}$ were the optimal Δ -partial assignment between $(P_i)_{1 \leq i \leq \mathcal{I}-1}$ and $(Q_j)_{1 \leq j \leq \mathcal{J}}$, then g to which we add the deletion of $P_{\mathcal{I}}$ would have a cost lower than f , which would contradict that f is the optimal assignment between P and Q .

Then

$$\begin{aligned} \text{CED}_{\alpha,\beta}^\Delta(P, Q) &= \text{CED}_{\alpha,\beta}^\Delta((P_i)_{1 \leq i \leq \mathcal{I}-1}, (Q_j)_{1 \leq j \leq \mathcal{J}}) \\ &\quad + \beta \cdot D_\Delta^\alpha(P_{\mathcal{I}}, A). \end{aligned} \quad (29)$$

Thus,

$$\begin{aligned} \delta_\Delta^{\alpha,\beta}(\mathcal{I}, \mathcal{J}) &= \min \left\{ \delta_\Delta^{\alpha,\beta}(\mathcal{I}-1, \mathcal{J}) + \beta \cdot D_\Delta^\alpha(P_{\mathcal{I}}, A), \right. \\ &\quad \delta_\Delta^{\alpha,\beta}(\mathcal{I}-1, \mathcal{J}-1) + D_\Delta^\alpha(P_{\mathcal{I}}, Q_{\mathcal{J}}), \\ &\quad \left. \delta_\Delta^{\alpha,\beta}(\mathcal{I}, \mathcal{J}-1) + \beta \cdot D_\Delta^\alpha(Q_{\mathcal{J}}, A) \right\} \end{aligned} \quad (30)$$

$$\begin{aligned} &= \min \left\{ \text{CED}_{\alpha,\beta}^\Delta((P_i)_{1 \leq i \leq \mathcal{I}-1}, (Q_j)_{1 \leq j \leq \mathcal{J}}) \right. \\ &\quad \left. + \beta \cdot D_\Delta^\alpha(P_{\mathcal{I}}, A), \delta_\Delta^{\alpha,\beta}(\mathcal{I}-1, \mathcal{J}-1) + D_\Delta^\alpha(P_{\mathcal{I}}, Q_{\mathcal{J}}), \right. \\ &\quad \left. \delta_\Delta^{\alpha,\beta}(\mathcal{I}, \mathcal{J}-1) + \beta \cdot D_\Delta^\alpha(Q_{\mathcal{J}}, A) \right\} \text{ (by induction)} \end{aligned} \quad (31)$$

$$\begin{aligned} &= \min \left\{ \text{CED}_{\alpha,\beta}^\Delta(P, Q), \right. \\ &\quad \left. \delta_\Delta^{\alpha,\beta}(\mathcal{I}-1, \mathcal{J}-1) + D_\Delta^\alpha(P_{\mathcal{I}}, Q_{\mathcal{J}}), \right. \\ &\quad \left. \delta_\Delta^{\alpha,\beta}(\mathcal{I}, \mathcal{J}-1) + \beta \cdot D_\Delta^\alpha(Q_{\mathcal{J}}, A) \right\} \end{aligned} \quad (32)$$

$$\begin{aligned} &\leq \text{CED}_{\alpha,\beta}^\Delta(P, Q). \end{aligned} \quad (33)$$

(iii) Assume that the optimal Δ -partial assignment f between P and Q belongs to $\{f \in \mathcal{A}^\Delta(P, Q) \text{ such that } \mathcal{J} \notin \text{Im}(f)\}$.

$$\text{CED}_{\alpha,\beta}^\Delta(P, Q) = \text{cost}_{(P, Q)}^\Delta(f) \quad (34)$$

$$\begin{aligned} &= \text{cost}_{((P_i)_{1 \leq i \leq \mathcal{I}}, (Q_j)_{1 \leq j \leq \mathcal{J}-1})}^\Delta(f^{\mathcal{J}^*}) \\ &\quad + \beta \cdot D_\Delta^\alpha(Q_{\mathcal{J}}, A) \end{aligned} \quad (35)$$

with $f^{\mathcal{J}^*}$ the Δ -partial assignment between $(P_i)_{1 \leq i \leq \mathcal{I}}$ and $(Q_j)_{1 \leq j \leq \mathcal{J}-1}$ obtained from f by removing the insertion of $Q_{\mathcal{J}}$ from f . Thus $f^{\mathcal{J}^*}$ is the optimal Δ -partial assignment between $(P_i)_{1 \leq i \leq \mathcal{I}}$ and $(Q_j)_{1 \leq j \leq \mathcal{J}-1}$. Indeed if this were not the case, and if $g \neq f^{\mathcal{J}^*}$ were the optimal Δ -partial assignment between $(P_i)_{1 \leq i \leq \mathcal{I}}$ and $(Q_j)_{1 \leq j \leq \mathcal{J}-1}$, then g to which we add the insertion of $Q_{\mathcal{J}}$ would have a cost lower than f , which would contradict that f is the optimal assignment between P and Q .

$$\begin{aligned} \text{CED}_{\alpha,\beta}^\Delta(P, Q) &= \text{CED}_{\alpha,\beta}^\Delta((P_i)_{1 \leq i \leq \mathcal{I}}, (Q_j)_{1 \leq j \leq \mathcal{J}-1}) \\ &\quad + \beta \cdot D_\Delta^\alpha(Q_{\mathcal{J}}, A). \end{aligned} \quad (36)$$

Then,

$$\begin{aligned} \delta_\Delta^{\alpha,\beta}(\mathcal{I}, \mathcal{J}) &= \min \left\{ \delta_\Delta^{\alpha,\beta}(\mathcal{I}-1, \mathcal{J}) \right. \\ &\quad \left. + \beta \cdot D_\Delta^\alpha(P_{\mathcal{I}}, A), \delta_\Delta^{\alpha,\beta}(\mathcal{I}-1, \mathcal{J}-1) + D_\Delta^\alpha(P_{\mathcal{I}}, Q_{\mathcal{J}}), \right. \\ &\quad \left. \delta_\Delta^{\alpha,\beta}(\mathcal{I}, \mathcal{J}-1) + \beta \cdot D_\Delta^\alpha(Q_{\mathcal{J}}, A) \right\} \end{aligned} \quad (37)$$

$$\begin{aligned} &= \min \left\{ \delta_\Delta^{\alpha,\beta}(\mathcal{I}-1, \mathcal{J}) + \beta \cdot D_\Delta^\alpha(P_{\mathcal{I}}, A), \right. \\ &\quad \left. \delta_\Delta^{\alpha,\beta}(\mathcal{I}-1, \mathcal{J}-1) + D_\Delta^\alpha(P_{\mathcal{I}}, Q_{\mathcal{J}}), \right. \\ &\quad \left. \text{CED}_{\alpha,\beta}^\Delta((P_i)_{1 \leq i \leq \mathcal{I}}, (Q_j)_{1 \leq j \leq \mathcal{J}-1}) + \beta \cdot D_\Delta^\alpha(Q_{\mathcal{J}}, A) \right\} \end{aligned} \quad (38)$$

$$\begin{aligned} &= \min \left\{ \delta_\Delta^{\alpha,\beta}(\mathcal{I}-1, \mathcal{J}) + \beta \cdot D_\Delta^\alpha(P_{\mathcal{I}}, A), \right. \\ &\quad \left. \delta_\Delta^{\alpha,\beta}(\mathcal{I}-1, \mathcal{J}-1) + D_\Delta^\alpha(P_{\mathcal{I}}, Q_{\mathcal{J}}), \text{CED}_{\alpha,\beta}^\Delta(P, Q) \right\} \\ &\leq \text{CED}_{\alpha,\beta}^\Delta(P, Q) \end{aligned} \quad (39)$$

(i) Conversely, if

$$\delta_\Delta^{\alpha,\beta}(\mathcal{I}, \mathcal{J}) = \delta_\Delta^{\alpha,\beta}(\mathcal{I}-1, \mathcal{J}) + \beta \cdot D_\Delta^\alpha(P_{\mathcal{I}}, A), \quad (40)$$

then by induction

$$\begin{aligned} \delta_\Delta^{\alpha,\beta}(\mathcal{I}, \mathcal{J}) &= \text{CED}_{\alpha,\beta}^\Delta((P_i)_{1 \leq i \leq \mathcal{I}-1}, (Q_j)_{1 \leq j \leq \mathcal{J}}) \\ &\quad + \beta \cdot D_\Delta^\alpha(P_{\mathcal{I}}, A) \end{aligned} \quad (41)$$

$$\begin{aligned} &= \text{cost}_{((P_i)_{1 \leq i \leq \mathcal{I}-1}, (Q_j)_{1 \leq j \leq \mathcal{J}})}^\Delta(f^{\mathcal{I}^*}) \\ &\quad + \beta \cdot D_\Delta^\alpha(P_{\mathcal{I}}, A) \end{aligned} \quad (42)$$

with $f^{\mathcal{I}^*}$ the optimal Δ -partial assignment between $(P_i)_{1 \leq i \leq \mathcal{I}-1}$ and $(Q_j)_{1 \leq j \leq \mathcal{J}}$. Then append to $f^{\mathcal{I}^*}$ the deletion of $P_{\mathcal{I}}$ resulting to a partial assignment between P and Q with cost equal to

$$\begin{aligned} &\text{cost}_{((P_i)_{1 \leq i \leq \mathcal{I}}, (Q_j)_{1 \leq j \leq \mathcal{J}})}^\Delta(f^{\mathcal{I}^*}) + \beta \cdot D_\Delta^\alpha(P_{\mathcal{I}}, A) \\ &= \delta_\Delta^{\alpha,\beta}(\mathcal{I}, \mathcal{J}) \end{aligned} \quad (43)$$

thus

$$\delta_\Delta^{\alpha,\beta}(\mathcal{I}, \mathcal{J}) \geq \min_{f \in \mathcal{A}^\Delta(P, Q)} \text{cost}_{(P, Q)}^\Delta(f) = \text{CED}_{\alpha,\beta}^\Delta(P, Q) \quad (44)$$

(ii) If

$$\delta_\Delta^{\alpha,\beta}(\mathcal{I}, \mathcal{J}) = \delta_\Delta^{\alpha,\beta}(\mathcal{I}-1, \mathcal{J}-1) + D_\Delta^\alpha(P_{\mathcal{I}}, Q_{\mathcal{J}}), \quad (45)$$

then by induction,

$$\begin{aligned} \delta_\Delta^{\alpha,\beta}(\mathcal{I}, \mathcal{J}) &= \text{CED}_{\alpha,\beta}^\Delta((P_i)_{1 \leq i \leq \mathcal{I}-1}, (Q_j)_{1 \leq j \leq \mathcal{J}-1}) \\ &\quad + D_\Delta^\alpha(P_{\mathcal{I}}, Q_{\mathcal{J}}) \end{aligned} \quad (46)$$

$$\begin{aligned} &= \text{cost}_{((P_i)_{1 \leq i \leq \mathcal{I}-1}, (Q_j)_{1 \leq j \leq \mathcal{J}-1})}^\Delta(f^{(\mathcal{I}, \mathcal{J})^*}) \\ &\quad + D_\Delta^\alpha(P_{\mathcal{I}}, Q_{\mathcal{J}}) \end{aligned} \quad (47)$$

with $f^{(\mathcal{I}, \mathcal{J})^*}$ the optimal Δ -partial assignment between $(P_i)_{1 \leq i \leq \mathcal{I}-1}$ and $(Q_j)_{1 \leq j \leq \mathcal{J}-1}$. Then append to $f^{(\mathcal{I}, \mathcal{J})^*}$ the substitution of $P_{\mathcal{I}}$ by $Q_{\mathcal{J}}$, resulting to a partial assignment between P and Q with cost equal to

$$\begin{aligned} &\text{cost}_{((P_i)_{1 \leq i \leq \mathcal{I}}, (Q_j)_{1 \leq j \leq \mathcal{J}})}^\Delta(f^{(\mathcal{I}, \mathcal{J})^*}) + D_\Delta^\alpha(P_{\mathcal{I}}, Q_{\mathcal{J}}) \\ &= \delta_\Delta^{\alpha,\beta}(\mathcal{I}, \mathcal{J}), \end{aligned} \quad (48)$$

thus

$$\delta_\Delta^{\alpha,\beta}(\mathcal{I}, \mathcal{J}) \geq \min_{f \in \mathcal{A}^\Delta(P, Q)} \text{cost}_{(P, Q)}^\Delta(f) = \text{CED}_{\alpha,\beta}^\Delta(P, Q). \quad (49)$$

(iii) If

$$\delta_\Delta^{\alpha,\beta}(\mathcal{I}, \mathcal{J}) = \delta_\Delta^{\alpha,\beta}(\mathcal{I}, \mathcal{J}-1) + \beta \cdot D_\Delta^\alpha(Q_{\mathcal{J}}, A), \quad (50)$$

then by induction,

$$\delta_{\Delta}^{\alpha,\beta}(\mathcal{I}, \mathcal{J}) = \text{CED}_{\alpha,\beta}^{\Delta}\left((P_i)_{1 \leq i \leq \mathcal{I}}, (Q_j)_{1 \leq j \leq \mathcal{J}-1}\right) + \beta \cdot D_{\Delta}^{\alpha}(Q_{\mathcal{J}}, A), \quad (51)$$

$$= \text{cost}_{\Delta}^{\Delta}\left((P_i)_{1 \leq i \leq \mathcal{I}}, (Q_j)_{1 \leq j \leq \mathcal{J}-1}\right)(f^{\mathcal{J}^*}) + \beta \cdot D_{\Delta}^{\alpha}(Q_{\mathcal{J}}, A), \quad (52)$$

with $f^{\mathcal{J}^*}$ the optimal Δ -partial assignment between $(P_i)_{1 \leq i \leq \mathcal{I}}$ and $(Q_j)_{1 \leq j \leq \mathcal{J}-1}$. Then append to $f^{\mathcal{J}^*}$ the insertion of $Q_{\mathcal{J}}$ resulting to a partial assignment between P and Q with cost equal to

$$\text{cost}_{\Delta}^{\Delta}\left((P_i)_{1 \leq i \leq \mathcal{I}}, (Q_j)_{1 \leq j \leq \mathcal{J}}\right)(f^{\mathcal{J}^*}) + \beta \cdot D_{\Delta}^{\alpha}(Q_{\mathcal{J}}, A) = \delta_{\Delta}^{\alpha,\beta}(\mathcal{I}, \mathcal{J}), \quad (53)$$

thus

$$\delta_{\Delta}^{\alpha,\beta}(\mathcal{I}, \mathcal{J}) \geq \min_{f \in \mathcal{A}^{\Delta}(P, Q)} \text{cost}_{\Delta}^{\Delta}(P, Q)(f) = \text{CED}_{\alpha,\beta}^{\Delta}(P, Q). \quad (54)$$

Thus if the proposition is true for all indices $(\mathcal{I}', \mathcal{J}')$ with $\mathcal{I}' + \mathcal{J}' < \mathcal{I} + \mathcal{J}$, then the proposition is true for indices \mathcal{I} and \mathcal{J} . \square

Theorem B.10. *The space $(\mathcal{S}^{\Delta}, \text{CED}_{\alpha,\beta}^{\Delta})$ is a metric space.*

Proof. • Triangle inequality

We will prove triangle inequality by induction on $M = I + J + K$.

- The triangle inequality is true for $M = 0$ since $\delta_{\Delta}^{\alpha,\beta}((P_i)_{0 \leq i \leq 0}, (R_k)_{0 \leq k \leq 0}) = 0 \geq 0 + 0 = \delta_{\Delta}^{\alpha,\beta}((P_i)_{0 \leq i \leq 0}, (Q_j)_{0 \leq j \leq 0}) + \delta_{\Delta}^{\alpha,\beta}((Q_j)_{0 \leq j \leq 0}, (R_k)_{0 \leq k \leq 0})$
- Suppose the triangle inequality is true for all $n \in \{0, \dots, M-1\}$ for some $M > 0$. For simplicity, we will denote $(P_I) = (P_i)_{0 \leq i \leq I}, (Q_J) = (Q_j)_{0 \leq j \leq J}, (R_K) = (R_k)_{0 \leq k \leq K}$. Then we have different cases :

1st case :

$$\text{If } \delta_{\Delta}^{\alpha,\beta}((P_I), (Q_J)) = \delta_{\Delta}^{\alpha,\beta}((P_{I-1}), (Q_J)) + \beta \cdot D_{\Delta}^{\alpha}(P_I, A). \text{ Then } \delta_{\Delta}^{\alpha,\beta}((P_I), (Q_J)) + \delta_{\Delta}^{\alpha,\beta}((Q_J), (R_K)) = \delta_{\Delta}^{\alpha,\beta}((P_{I-1}), (Q_J)) + \delta_{\Delta}^{\alpha,\beta}((Q_J), (R_K)) + \beta \cdot D_{\Delta}^{\alpha}(P_I, A) \geq \delta_{\Delta}^{\alpha,\beta}((P_{I-1}), (R_K)) + \beta \cdot D_{\Delta}^{\alpha}(P_I, A) \text{ (by triangular inequality of } \delta_{\Delta}^{\alpha,\beta} \text{ until } M-1)$$

$$\geq \delta_{\Delta}^{\alpha,\beta}((P_I), (R_K)) \text{ (by the recursive definition of } \delta_{\Delta}^{\alpha,\beta} \text{)}$$

2nd case :

$$\text{If } \begin{cases} \delta_{\Delta}^{\alpha,\beta}((P_I), (Q_J)) = \delta_{\Delta}^{\alpha,\beta}((P_I), (Q_{J-1})) \\ + \beta \cdot D_{\Delta}^{\alpha}(Q_J, A) \\ \delta_{\Delta}^{\alpha,\beta}((Q_J), (R_K)) = \delta_{\Delta}^{\alpha,\beta}((Q_{J-1}), (R_{K-1})) \\ + D_{\Delta}^{\alpha}(Q_J, R_K) \end{cases}$$

$$\text{Then } \delta_{\Delta}^{\alpha,\beta}((P_I), (Q_J)) + \delta_{\Delta}^{\alpha,\beta}((Q_J), (R_K)) \geq (\delta_{\Delta}^{\alpha,\beta}((P_I), (Q_{J-1})) + \delta_{\Delta}^{\alpha,\beta}((Q_{J-1}), (R_{K-1}))) + (\beta \cdot D_{\Delta}^{\alpha}(Q_J, A) + D_{\Delta}^{\alpha}(Q_J, R_K)) \geq (\delta_{\Delta}^{\alpha,\beta}((P_I), (Q_{J-1})) + \delta_{\Delta}^{\alpha,\beta}((Q_{J-1}), (R_{K-1}))) + \beta \cdot (D_{\Delta}^{\alpha}(Q_J, A) + D_{\Delta}^{\alpha}(Q_J, R_K))$$

$$\geq (\delta_{\Delta}^{\alpha,\beta}((P_I), (R_{K-1}))) + \beta \cdot (D_{\Delta}^{\alpha}(Q_J, A) + D_{\Delta}^{\alpha}(Q_J, R_K)) \text{ (by triangular inequality of } \delta_{\Delta}^{\alpha,\beta} \text{ until } M-1)$$

$$\geq (\delta_{\Delta}^{\alpha,\beta}((P_I), (R_{K-1}))) + \beta \cdot D_{\Delta}^{\alpha}(R_K, A) \text{ (by Lemma B.5)} \geq \delta_{\Delta}^{\alpha,\beta}((P_I), (R_K))$$

3rd case :

$$\text{If } \begin{cases} \delta_{\Delta}^{\alpha,\beta}((P_I), (Q_J)) = \delta_{\Delta}^{\alpha,\beta}((P_{I-1}), (Q_{J-1})) \\ + D_{\Delta}^{\alpha}(P_I, Q_J) \\ \delta_{\Delta}^{\alpha,\beta}((Q_J), (R_K)) = \delta_{\Delta}^{\alpha,\beta}((Q_{J-1}), (R_{K-1})) \\ + D_{\Delta}^{\alpha}(Q_J, R_K) \end{cases}$$

$$\text{Then } \delta_{\Delta}^{\alpha,\beta}((P_I), (Q_J)) + \delta_{\Delta}^{\alpha,\beta}((Q_J), (R_K)) \geq \delta_{\Delta}^{\alpha,\beta}((P_{I-1}), (Q_{J-1})) + \delta_{\Delta}^{\alpha,\beta}((Q_{J-1}), (R_{K-1})) + D_{\Delta}^{\alpha}(P_I, Q_J) + D_{\Delta}^{\alpha}(Q_J, R_K) \geq \delta_{\Delta}^{\alpha,\beta}((P_{I-1}), (R_{K-1})) + D_{\Delta}^{\alpha}(P_I, R_K) \text{ (by triangular}$$

inequality of $\delta_{\Delta}^{\alpha,\beta}$ (until $M-1$) and D_{Δ}^{α})

$\geq \delta_{\Delta}^{\alpha,\beta}((P_I), (R_K))$
Then other cases are trivial or equivalent by symmetry to the first three cases.

- Symmetry and positivity

Since the distance D_{Δ}^{α} is symmetric and positive, it is easy to show by induction that $\delta_{\Delta}^{\alpha,\beta}$ is symmetric and positive.

- $P = Q \Rightarrow \text{CED}_{\alpha,\beta}^{\Delta}(P, Q) = 0$

By the identity partial assignment,

$$\begin{aligned} \text{CED}_{\alpha,\beta}^{\Delta}(P, Q) &\leq \text{cost } id = D_{\Delta}^{\alpha}(P_1, Q_1) + \dots \\ &+ D_{\Delta}^{\alpha}(P_{N_P^{\Delta}}, Q_{N_Q^{\Delta}}) \\ &= 0 + \dots + 0 \\ &= 0 \end{aligned}$$

where id is the identity partial assignment $\{(1, 1), \dots, (N_P^{\Delta}, N_Q^{\Delta})\}$.

- $\text{CED}_{\alpha,\beta}^{\Delta}(P, Q) = 0 \Rightarrow P = Q$

Suppose $\text{CED}_{\alpha,\beta}^{\Delta}(P, Q) = 0$.

Then, $\text{CED}_{\alpha,\beta}^{\Delta}(P, Q) = \text{cost}_{\Delta}^{\Delta}(P, Q)(f)$ for f a optimal partial assignment of (P, Q) . Since $\text{CED}_{\alpha,\beta}^{\Delta}(P, Q) = 0$, f doesn't have any deletion or insertion (because $D_{\Delta}^{\alpha}(P_i, A) > 0$ and $D_{\Delta}^{\alpha}(Q_j, A) > 0$ by definition of TVPDs). Then $N_P^{\Delta} = N_Q^{\Delta}$ and $f = \{(1, 1), \dots, (N_P^{\Delta}, N_P^{\Delta})\}$. Hence, $\forall i \in \{1, \dots, N_P^{\Delta}\}$, $D_{\Delta}^{\alpha}(P_i, Q_i) = 0$ and thus, $\forall i \in \{1, \dots, N_P^{\Delta}\}$, $P_i = Q_i$. Finally, $P = Q$. \square

Lemma B.11. *Let $P \in \mathcal{S}^{\Delta}$ and $Q \in \mathcal{S}^{\Delta}$. Then:*

- 1) *The backtracking procedure starting from $B_0 = (N_P, N_Q)$ and constructing $(B_z)_z$ by steps $(-1, 0)$, $(-1, -1)$, or $(0, -1)$ as specified, terminates after a finite number of steps at $B_Z = (0, 0)$ for some $Z \in \mathbb{N}$.*
- 2) *The set $f := A_Z$ is a Δ -partial assignment between P and Q , i.e. $f \in \mathcal{A}^{\Delta}(P, Q)$.*
- 3) *The cost of f satisfies*

$$\text{cost}_{\Delta}^{\Delta}(P, Q)(f) = \delta_{\Delta}^{\alpha,\beta}((P_i)_{0 \leq i \leq N_P}, (Q_j)_{0 \leq j \leq N_Q}),$$

so that f achieves the minimum in the definition of $\text{CED}_{\alpha,\beta}^{\Delta}(P, Q)$, and in particular

$$\text{CED}_{\alpha,\beta}^{\Delta}(P, Q) = \text{cost}_{\Delta}^{\Delta}(P, Q)(f).$$

Proof. Let us write $B_z = (i_z, j_z)$. By construction of the backtracking: each step replaces B_z by $B_{z+1} = B_z - (1, 0)$, or $B_{z+1} = B_z - (1, 1)$, or $B_{z+1} = B_z - (0, 1)$. Hence

$$i_{z+1} \leq i_z, \quad j_{z+1} \leq j_z, \quad i_{z+1} + j_{z+1} \leq i_z + j_z - 1,$$

so the quantity $i_z + j_z$ strictly decreases at each step. Since i_z, j_z are nonnegative (at every step, (i_z, j_z) is a valid entry of the dynamic-programming table, so $0 \leq i_z \leq N_P$ and $0 \leq j_z \leq N_Q$. In particular, i_z and j_z are nonnegative integers) and we start from $(i_0, j_0) = (N_P, N_Q)$, this process must stop in finitely many steps, and the only possible limit in \mathbb{N}^2 is $(0, 0)$. This proves (1).

Next, by definition, A_z is obtained from A_{z-1} by adding the current index pair $B_{z-1} = (i_{z-1}, j_{z-1})$ if and only if the step from B_{z-1} to B_z is a diagonal move $(-1, -1)$; in the other two cases (deletion or insertion) the set A_z is left unchanged. Thus A_Z is exactly the set of index pairs (i_z, j_z) along the backtracking path for which a diagonal step is taken.

Along this path, the indices (i_z, j_z) are strictly decreasing in both coordinates when a diagonal step is taken. Reading these pairs in reverse order (from $(0, 0)$ to (N_P, N_Q)) therefore yields a family of pairs with strictly increasing first and second coordinates. Hence $f = A_Z$ is the graph of a strictly increasing map from a subset of $\{1, \dots, N_P\}$ to a subset of $\{1, \dots, N_Q\}$, i.e. $f \in \mathcal{A}^{\Delta}(P, Q)$. This proves (2).

We prove point (3) by induction on the backtracking index z . Recall that the backtracking produces a sequence (B_z) with $B_z = (i_z, j_z)$, starting from $(i_0, j_0) = (N_P, N_Q)$ and ending at

$(i_z, j_z) = (0, 0)$, and at each step z we choose B_{z+1} so that one of the three defining equalities of the dynamic-programming recursion holds, namely

$$\begin{aligned}\delta_{\Delta}^{\alpha, \beta}(i_z, j_z) &= \delta_{\Delta}^{\alpha, \beta}(i_z - 1, j_z) + \beta \cdot D_{\Delta}^{\alpha}(P_{i_z}, A), \\ \delta_{\Delta}^{\alpha, \beta}(i_z, j_z) &= \delta_{\Delta}^{\alpha, \beta}(i_z - 1, j_z - 1) + D_{\Delta}^{\alpha}(P_{i_z}, Q_{j_z}), \\ \delta_{\Delta}^{\alpha, \beta}(i_z, j_z) &= \delta_{\Delta}^{\alpha, \beta}(i_z, j_z - 1) + \beta \cdot D_{\Delta}^{\alpha}(Q_{j_z}, A),\end{aligned}$$

according to whether the step is a deletion, a substitution, or an insertion.

For each $z \in \{0, \dots, Z - 1\}$, let lc_z denote this *local cost* (deletion, insertion, or substitution) incurred when moving from B_z to B_{z+1} . Rearranging the corresponding equality, we obtain

$$\delta_{\Delta}^{\alpha, \beta}(i_z, j_z) = \delta_{\Delta}^{\alpha, \beta}(i_{z+1}, j_{z+1}) + \text{lc}_z.$$

We now prove by induction on $k \in \{0, \dots, Z\}$ that

$$\delta_{\Delta}^{\alpha, \beta}(i_0, j_0) = \delta_{\Delta}^{\alpha, \beta}(i_k, j_k) + \sum_{z=0}^{k-1} \text{lc}_z,$$

with the convention that the sum is zero for $k = 0$.

- The equality is true for $k = 0$, since both sides reduce to $\delta_{\Delta}^{\alpha, \beta}(i_0, j_0)$.
- Assume the statement holds for some $k < Z$. Using the relation above for $z = k$, we have

$$\delta_{\Delta}^{\alpha, \beta}(i_k, j_k) = \delta_{\Delta}^{\alpha, \beta}(i_{k+1}, j_{k+1}) + \text{lc}_k.$$

Plugging this into the induction hypothesis yields

$$\delta_{\Delta}^{\alpha, \beta}(i_0, j_0) = \delta_{\Delta}^{\alpha, \beta}(i_{k+1}, j_{k+1}) + \sum_{z=0}^k \text{lc}_z,$$

which is exactly the desired formula at rank $k + 1$. This completes the induction.

Taking $k = Z$ and using the initialization $\delta_{\Delta}^{\alpha, \beta}(0, 0) = 0$ gives

$$\delta_{\Delta}^{\alpha, \beta}(N_P, N_Q) = \sum_{z=0}^{Z-1} \text{lc}_z.$$

By construction of f during backtracking, this sum of local costs coincides with $\text{cost}_{(P, Q)}^{\Delta}(f)$, which proves

$$\text{cost}_{(P, Q)}^{\Delta}(f) = \delta_{\Delta}^{\alpha, \beta}(N_P, N_Q),$$

and therefore point (3) of the lemma. \square

Proposition B.12. Let $F \in C^{\Delta}$.

Then for every $\varepsilon \in \mathbb{R}_+^*$, there exists $\tilde{F}^{\eta(\varepsilon)} \in PC^{\Delta}$ such that $\text{CED}_{\alpha, \beta}^{\Delta}(F, \tilde{F}^{\eta(\varepsilon)}) < \varepsilon$.

Proof. Let $F : \text{dom } F = \bigcup_{i \in \{1, \dots, N_F^{\Delta}\}} I_i^F \rightarrow E$, be one continuous TVPD of S^{Δ} , that is $F \in C^{\Delta}$. Let $i \in \{1, \dots, N_F^{\Delta}\}$, then F_i can be extended continuously to the closure $\overline{I_i^F}$, yielding the extension F'_i ; because $\overline{I_i^F}$ is compact, then F'_i is uniformly continuous on that set. Then $\forall \varepsilon > 0, \exists \eta_i > 0, \forall (t, s) \in \overline{I_i^F}, |t - s| < \eta_i \implies d(F'_i(t), F'_i(s)) < \varepsilon$. Let $\varepsilon > 0$, then $\forall i \in \{1, \dots, N_F^{\Delta}\}$, there exists $\eta_i > 0$, such that, $\forall (t, s) \in I_i^F, |t - s| < \eta_i \implies d(F_i(t), F_i(s)) < \varepsilon / (\mu(\text{dom } F) \cdot (1 - \alpha))$. Fixing $\eta' = \min_{i \in \{1, \dots, N_F^{\Delta}\}} \eta_i$, let $k_{\Delta} \in \mathbb{N}^*$, such that $\Delta / k_{\Delta} < \eta'$, and define $\eta = \Delta / k_{\Delta}$. For every $i \in \{1, \dots, N_F^{\Delta}\}$, let $M_i \in \mathbb{N}$, such that $\inf I_i^F + M_i \cdot \eta = \sup I_i^F$, and denote $\tilde{F}_i : \overline{I_i^F} \rightarrow E$ the piecewise-constant application defined by $\tilde{F}_i(t) = F'_i(a_{i,n}), \forall t \in [a_{i,n}, a_{i,n+1}]$, with $a_{i,n} = \inf I_i^F + n \cdot \eta$, for $n = 0, \dots, M_i$. Denoting \tilde{F}_i the restriction of \tilde{F}_i on I_i^F , and gluing all the \tilde{F}_i together, for every $i \in \{1, \dots, N_F^{\Delta}\}$, we obtain the piecewise-constant approximation $\tilde{F} : \text{dom } F \rightarrow E$ of

F . Obviously $\tilde{F} \in S^{\Delta}$ as a simple function on each I_i^F , moreover we have $\forall t \in \text{dom } F, d(F(t), \tilde{F}(t)) < \varepsilon / (\mu(\text{dom } F) \cdot (1 - \alpha))$, which implies $\text{CED}_{\alpha, \beta}^{\Delta}(F, \tilde{F}) \leq \sum_{i \in \{1, \dots, N_F^{\Delta}\}} D_{\Delta}^{\alpha}(F_i, \tilde{F}_i) < N_F^{\Delta} \cdot \Delta \cdot (1 - \alpha) \cdot (\varepsilon / (\mu(\text{dom } F) \cdot (1 - \alpha))) = \mu(\text{dom } F) \cdot (1 - \alpha) \cdot \varepsilon / (\mu(\text{dom } F) \cdot (1 - \alpha)) = \varepsilon$. \square

Proposition B.13. Let

$$V_n = (X_n, t_n)_{0 \leq n \leq N_V}$$

be a sequence in $E \times \mathbb{R}$, with $t_0 < t_1 < \dots < t_{N_V}$. For each $n \in \{0, \dots, N_V - 1\}$, let $\gamma_n : [0, 1] \rightarrow E$ be a constant-speed d -geodesic satisfying $\gamma_n(0) = X_n$ and $\gamma_n(1) = X_{n+1}$. Define $F : [t_0, t_{N_V}] \rightarrow E$ by

$$F(t) = \gamma_n(\lambda_n(t)), \quad \text{for } t \in [t_n, t_{n+1}),$$

where

$$\lambda_n(t) = \frac{t - t_n}{t_{n+1} - t_n} \in [0, 1],$$

and set $F(t_{N_V}) = X_{N_V}$.

Let

$$K_V = \max_{0 \leq n \leq N_V - 1} \frac{d(X_n, X_{n+1})}{t_{n+1} - t_n}.$$

Then, for all $t, t' \in [t_0, t_{N_V}]$,

$$d(F(t), F(t')) \leq K_V \cdot |t' - t|.$$

In particular, F is K_V -Lipschitz as a map $([t_0, t_{N_V}], |\cdot|) \rightarrow (E, d)$.

Proof. Fix $n \in \{0, \dots, N_V - 1\}$ and let $t, t' \in [t_n, t_{n+1})$. Since γ_n is a constant-speed geodesic for d , we have

$$d(\gamma_n(u), \gamma_n(v)) = |u - v| \cdot d(X_n, X_{n+1})$$

for all $u, v \in [0, 1]$. By construction of F ,

$$F(t) = \gamma_n(\lambda_n(t)), \quad F(t') = \gamma_n(\lambda_n(t')).$$

Moreover, at the breakpoint t_{n+1} we have

$$F(t_{n+1}) = X_{n+1} = \gamma_n(1) = \gamma_n(\lambda_n(t_{n+1})),$$

since

$$\lambda_n(t_{n+1}) = \frac{t_{n+1} - t_n}{t_{n+1} - t_n} = 1.$$

So, the identity

$$F(t) = \gamma_n(\lambda_n(t))$$

also holds when $t = t_{n+1}$. Thus, $\forall t, t' \in [t_n, t_{n+1}]$,

$$\begin{aligned}d(F(t), F(t')) &= |\lambda_n(t) - \lambda_n(t')| \cdot d(X_n, X_{n+1}) \\ &= \frac{|t - t'|}{t_{n+1} - t_n} d(X_n, X_{n+1}) \\ &\leq K_V \cdot |t - t'|.\end{aligned}$$

For arbitrary $t, t' \in [t_0, t_{N_V}]$ with $t < t'$, let $t = \tau_0 < \tau_1 < \dots < \tau_r = t'$ be a subdivision obtained by intersecting $[t, t']$ with the breakpoints $\{t_n\}_n$. Applying the previous bound on each subinterval and using the triangle inequality,

$$\begin{aligned}d(F(t), F(t')) &\leq \sum_{k=0}^{r-1} d(F(\tau_k), F(\tau_{k+1})) \\ &\leq \sum_{k=0}^{r-1} K_V \cdot |\tau_{k+1} - \tau_k| \\ &= K_V \cdot |t' - t|.\end{aligned}$$

This holds for all t, t' , which concludes the proof. \square

For the geodesic constructions that follow, we further assume that (E, d) is a geodesic Polish space, and we slightly relax the definition

of \mathcal{S}^Δ . We define $\bar{\mathcal{S}}^\Delta$ as the space of functions F satisfying all conditions of \mathcal{S}^Δ except the condition " $\forall t \in \text{dom } F, d(F(t), A) > 0$ ". Similarly, \bar{s}^Δ denotes the corresponding space of Δ -subdivisions. On $\bar{\mathcal{S}}^\Delta$, we define the equivalence relation $P \sim Q \Leftrightarrow \text{CED}_{\alpha,\beta}^\Delta(P, Q) = 0$, and we work on the quotient metric space $(\bar{\mathcal{S}}^\Delta / \sim, \text{CED}_{\alpha,\beta}^\Delta)$. Indeed, all preceding results extend trivially to this setting. The original space \mathcal{S}^Δ embeds naturally into $\bar{\mathcal{S}}^\Delta / \sim$ via $P \mapsto [P]$, preserving CED distances, hence for simplicity, we continue to denote this space by \mathcal{S}^Δ and the distance by $\text{CED}_{\alpha,\beta}^\Delta$ in what follows.

Theorem B.14. *Let $P \in \mathcal{S}^\Delta, Q \in \mathcal{S}^\Delta$.*

If (E, d) is a geodesic Polish space, then $\forall i \in \{1, \dots, N_P\}, \forall j \in \{1, \dots, N_Q\}$,

$$\forall T \in (0, 1),$$

$$\exists G_{i,j}^T \in \mathcal{S}^\Delta : \left(I_{i,j}^T, \mathcal{Z}(\mathcal{B}(\mathbb{R})|_{I_{i,j}^T}) \right) \longrightarrow (E, \mathcal{B}(E))$$

measurable, such that for λ -almost every $t \in I_i^P$,

$$G_{i,j}^T(t + \inf I_{i,j}^T - a_i) \in \{G(P(t), Q(t + c_j - a_i))(T)\} \subset E,$$

where we denote $a_i = \inf(I_i^P)$, $b_i = \sup(I_i^P)$, $c_j = \inf(I_j^Q)$, $d_j = \sup(I_j^Q)$,

$$\inf I_{i,j}^T = (1 - T) \cdot a_i + T \cdot c_j,$$

$$\sup I_{i,j}^T = (1 - T) \cdot b_i + T \cdot d_j$$

and $G(P(t), Q(t + c_j - a_i))$ a d -geodesic from $P(t)$ to $Q(t + c_j - a_i)$ as defined in Sec. IV-A of the main manuscript.

Proof. Let $\text{Geod}(E)$ denote the space of geodesics in E (see Sec. IV-A of the main manuscript). Define $\text{Geod}^*(E) = \{\gamma \in \text{Geod}(E) : \forall (s, t) \in [0, 1]^2, d(\gamma(s), \gamma(t)) = |s - t| \cdot d(\gamma(0), \gamma(1))\}$. We endow $\text{Geod}^*(E)$ with the uniform norm to make it a Souslin space.

Let $i \in \{1, \dots, N_P\}, j \in \{1, \dots, N_Q\}, T \in (0, 1)$, and Ψ the multivalued function from $E \times E$ to the set of nonempty subsets of $\text{Geod}^*(E)$, defined as,

$$\begin{aligned} \forall (y_1, y_2) \in E \times E, \Psi(y_1, y_2) \\ = \{\gamma \in \text{Geod}^*(E) : \gamma(0) = y_1, \gamma(1) = y_2\}. \end{aligned} \quad (55)$$

Let's denote $\Gamma_\Psi = \{((x, y), \gamma) \in E^2 \times \text{Geod}^*(E) : \gamma \in \Psi(x, y)\}$ its graph; then Γ_Ψ is closed in $(E \times E \times \text{Geod}^*(E), \mathcal{T}_{(E \times E \times \text{Geod}^*(E))})$, where \mathcal{T} denote the product topology. Indeed, let $((x_n, y_n), \gamma_n)_{n \in \mathbb{N}}$ a sequence in Γ_Ψ converging to $((x, y), \gamma) \in E^2 \times \text{Geod}^*(E)$. Then,

$$\begin{aligned} \lim_{n \rightarrow +\infty} d(x_n, x) &= \lim_{n \rightarrow +\infty} d(y_n, y) \\ &= \lim_{n \rightarrow +\infty} \sup_{t \in [0, 1]} d(\gamma_n(t), \gamma(t)) = 0. \end{aligned} \quad (56)$$

So, because E is closed,

$$\lim_{n \rightarrow +\infty} x_n = x \in E, \quad \lim_{n \rightarrow +\infty} y_n = y \in E, \quad (57)$$

moreover by uniform convergence, in particular,

$$\lim_{n \rightarrow +\infty} \gamma_n(0) = \gamma(0), \quad \lim_{n \rightarrow +\infty} \gamma_n(1) = \gamma(1). \quad (58)$$

Since $\gamma_n(0) = x_n \rightarrow x$ and $\gamma_n(1) = y_n \rightarrow y$, we obtain by uniqueness of the limit in a metric space,

$$\gamma(0) = x, \quad \gamma(1) = y. \quad (59)$$

Each γ_n is a constant-speed geodesic joining x_n to y_n , that is,

$$\forall (s, t) \in [0, 1]^2, \quad d(\gamma_n(s), \gamma_n(t)) = |s - t| \cdot d(x_n, y_n). \quad (60)$$

As a distance on E , $d(\cdot, \cdot)$ is continuous. Moreover, $E \times E$ is a metrizable space, then we have the sequential characterization of limits, and $\lim_{n \rightarrow +\infty} x_n = x, \lim_{n \rightarrow +\infty} y_n = y$, so

$$\lim_{n \rightarrow +\infty} d(x_n, y_n) = d(x, y). \quad (61)$$

Likewise, the uniform convergence of γ_n to γ implies, for every $(s, t) \in [0, 1]^2$,

$$\lim_{n \rightarrow +\infty} \gamma_n(s) = \gamma(s), \quad \lim_{n \rightarrow +\infty} \gamma_n(t) = \gamma(t), \quad (62)$$

thus,

$$\lim_{n \rightarrow +\infty} d(\gamma_n(s), \gamma_n(t)) = d(\gamma(s), \gamma(t)). \quad (63)$$

Given (60), (61), and (63), we obtain for every $(s, t) \in [0, 1]^2$,

$$d(\gamma(s), \gamma(t)) = |s - t| d(x, y), \quad (64)$$

that is, $\gamma \in \Psi(x, y)$. Finally $x \in E, y \in E, \gamma \in \Psi(x, y)$ so $((x, y), \gamma) \in \Gamma_\Psi$. Thus Γ_Ψ is closed (indeed $E \times E \times \text{Geod}^*(E)$ is a metrizable space, as a finite product of metrizable spaces, and hence first-countable) for the product topology, and then a Borel of $\mathcal{B}(E \times E \times \text{Geod}^*(E))$.

Moreover, $E \times E$ is a Polish space (as a finite product of Polish spaces) and so a Souslin space; also, $\text{Geod}^*(E)$ is a Souslin space; thus $E \times E \times \text{Geod}^*(E)$ is a Souslin space as a finite product of Souslin spaces.

Since Γ_Ψ is a Borel subset of the Souslin space $E \times E \times \text{Geod}^*(E)$, Γ_Ψ is a Souslin set. Then, there exists a map $f : E \times E \longrightarrow \text{Geod}^*(E)$ that is measurable with respect to, the σ -algebra $\sigma(\mathcal{S}_{E \times E})$ generated by all Souslin sets in $E \times E$, and $\mathcal{B}(\text{Geod}^*(E))$, such that $f(\omega) \in \Psi(\omega), \forall \omega \in E \times E$ [78, Thm. 6.9.2].

Let us remember that the application

$$\begin{aligned} V : (I_i^P, \mathcal{Z}(\mathcal{B}(\mathbb{R})|_{I_i^P})) &\longrightarrow (E^2, \mathcal{B}(E) \otimes \mathcal{B}(E)), \\ t &\longmapsto V(t) = (P(t), Q(t + c_j - a_i)) \end{aligned}$$

is measurable. Recall also that $\mathcal{B}(E) \otimes \mathcal{B}(E) = \mathcal{B}(E \times E)$, since E is separable.

We denote $\mu = \lambda \circ V^{-1}$, the push-forward measure on $(E \times E, \mathcal{B}(E \times E))$, where λ is the Lebesgue measure on $(I_i^P, \mathcal{Z}(\mathcal{B}(\mathbb{R})|_{I_i^P}))$. Moreover, we denote $(E \times E, \mathcal{Z}(\mathcal{B}(E \times E)))$ the completion of $(E \times E, \mathcal{B}(E \times E))$ for μ . Since $E \times E$ is a Polish space, any Souslin set of $E \times E$ is an analytic set. Also, because any analytic set is universally measurable, and μ is a complete measure on $(E \times E, \mathcal{Z}(\mathcal{B}(E \times E)))$ that measures all Borel sets of $E \times E$, then

$$\sigma(\mathcal{S}_{E \times E}) \subset \mathcal{Z}(\mathcal{B}(E \times E)), \quad (65)$$

and so

$$f : (E \times E, \mathcal{Z}(\mathcal{B}(E \times E))) \longrightarrow (\text{Geod}^*(E), \mathcal{B}(\text{Geod}^*(E)))$$

is measurable.

Additionally, there exists a measurable function

$$g : (E \times E, \mathcal{B}(E \times E)) \longrightarrow (\text{Geod}^*(E), \mathcal{B}(\text{Geod}^*(E)))$$

μ -a.s equal to f .

Indeed, first we remark that since $\text{Geod}^*(E)$ is metric and separable, then $\text{Geod}^*(E)$ has a countable base $\{A_i\}_{i \in \mathbb{N}}$ and so $\mathcal{B}(\text{Geod}^*(E)) = \sigma(\{A_i\}_{i \in \mathbb{N}})$.

Let $A_i \in \{A_i\}_{i \in \mathbb{N}}, f^{-1}(A_i) \in \mathcal{Z}(\mathcal{B}(E \times E))$, then $\exists B_{A_i} \in \mathcal{B}(E \times E)$, and $\exists N_{A_i} \subset E \times E$ a negligible part of $(E \times E, \mathcal{B}(E \times E))$ such that

$$f^{-1}(A_i) = B_{A_i} \cup N_{A_i}.$$

Let us denote $N' = \bigcup_{i \in \mathbb{N}} N_{A_i}$, then $N' \in \mathcal{Z}(\mathcal{B}(E \times E))$ and

$$\mu(N') = \mu \left(\bigcup_{i \in \mathbb{N}} N_{A_i} \right) \leq \sum_{i=0}^{\infty} \mu(N_{A_i}) = \sum_{i=0}^{\infty} 0 = 0. \quad (66)$$

Since $N' \in \mathcal{Z}(\mathcal{B}(E \times E))$, then $\exists(M, N) \in \mathcal{B}(E \times E)^2$ such that $M \subset N' \subset N$ and $\mu(N - M) = 0$. Because $M \subset N'$ and $\mu(N') = 0$, then $\mu(M) \leq 0$, so $\mu(M) = 0$. Also, $\mu(N) = \mu(M) + \mu(N - M) = \mu(M) + 0 = 0$. Then we have $N' \subset N$, $N \in \mathcal{B}(E \times E)$, $\mu(N) = 0$.

We define

$$g : (E \times E, \mathcal{B}(E \times E)) \longrightarrow (\text{Geod}^*(E), \mathcal{B}(\text{Geod}^*(E)))$$

such that

$$g(x) = \begin{cases} f(x) & \text{if } x \in (E \times E) \setminus N, \\ y_0 & \text{if } x \in N, \end{cases}$$

with $y_0 \in \text{Geod}^*(E)$ an arbitrary fixed element.

Let $A_i \in \{A_i\}_{i \in \mathbb{N}}$, we have $g^{-1}(A_i) = (g^{-1}(A_i) \cap N^c) \cup (g^{-1}(A_i) \cap N)$. For $x \in N^c$, $g(x) = f(x)$, then

$$\begin{aligned} g^{-1}(A_i) \cap N^c &= f^{-1}(A_i) \cap N^c = (B_{A_i} \cup N_{A_i}) \cap N^c \\ &= (B_{A_i} \cap N^c) \cup (N_{A_i} \cap N^c) \\ &= (B_{A_i} \cap N^c) \cup \emptyset \\ &= B_{A_i} \cap N^c \in \mathcal{B}(E \times E). \end{aligned} \quad (67)$$

For $x \in N$, $g(x) = y_0$, then

$$g^{-1}(A_i) \cap N = \begin{cases} N & \text{if } y_0 \in A_i, \\ \emptyset & \text{if } y_0 \notin A_i, \end{cases} \quad (68)$$

thus in any case $g^{-1}(A_i) \cap N \in \mathcal{B}(E \times E)$.

Finally, $(g^{-1}(A_i) \cap N^c) \cup (g^{-1}(A_i) \cap N) \in \mathcal{B}(E \times E)$ and $g^{-1}(A_i) \in \mathcal{B}(E \times E)$, then

$$g : (E \times E, \mathcal{B}(E \times E)) \longrightarrow (\text{Geod}^*(E), \mathcal{B}(\text{Geod}^*(E)))$$

is measurable.

For each $\theta \in [0, 1]$, the evaluation map

$$e_\theta : \text{Geod}^*(E) \rightarrow E, \quad \gamma \mapsto \gamma(\theta),$$

is continuous. Indeed, let $(\gamma_n)_{n \in \mathbb{N}}$ be a sequence in $\text{Geod}^*(E)$ that converges uniformly to γ . Fix $\varepsilon > 0$. Since (γ_n) converges uniformly to γ , there exists $N(\varepsilon) \in \mathbb{N}$ such that for all $n \geq N(\varepsilon)$,

$$d(\gamma_n(\theta), \gamma(\theta)) \leq \sup_{s \in [0, 1]} d(\gamma_n(s), \gamma(s)) < \varepsilon,$$

hence e_θ is continuous. As a continuous map,

$$e_T : (\text{Geod}^*(E), \mathcal{B}(\text{Geod}^*(E))) \rightarrow (E, \mathcal{B}(E)), \quad \gamma \mapsto \gamma(t),$$

is measurable. So, as a composition of measurable maps,

$$m_T = e_T \circ g : (E \times E, \mathcal{B}(E \times E)) \longrightarrow (E, \mathcal{B}(E)),$$

is measurable.

Because $m_T : (E \times E, \mathcal{B}(E \times E)) \longrightarrow (E, \mathcal{B}(E))$ and $V : (I_i^P, \mathcal{Z}(\mathcal{B}(\mathbb{R})|_{I_i^P})) \longrightarrow (E^2, \mathcal{B}(E \times E))$, $t \mapsto V(t) = (P(t), Q(t + c_j - a_i))$ are measurable, then $m_T \circ V : (I_i^P, \mathcal{Z}(\mathcal{B}(\mathbb{R})|_{I_i^P})) \longrightarrow (E, \mathcal{B}(E))$ is measurable. Also, the map

$$\begin{aligned} \tilde{U} : (I_{i,j}^T, \mathcal{Z}(\mathcal{B}(\mathbb{R})|_{I_{i,j}^T})) &\longrightarrow (I_i^P, \mathcal{Z}(\mathcal{B}(\mathbb{R})|_{I_i^P})) \\ t &\mapsto t + a_i - (1 - T) \cdot a_i - T \cdot c_j \end{aligned}$$

is measurable (for the same reasons as U). Then finally,

$$G_{i,j}^T = (m_T \circ V) \circ \tilde{U}$$

is measurable and so

$$G_{i,j}^T \in s^\Delta. \quad (69)$$

Lemma B.15. Let $P \in \mathcal{S}^\Delta$. If (E, d) is a geodesic Polish space, A closed and $\forall x \in E$, $\{y \in A, d(x, y) = d(x, A)\}$ is non-empty.

Then $\forall i \in \{1, \dots, N_P\}$, there exists a measurable function $p^i : (I_i^P, \mathcal{Z}(\mathcal{B}(\mathbb{R})|_{I_i^P})) \longrightarrow (E, \mathcal{B}(E))$, such that for λ -almost every $t \in I_i^P$, $p^i(t) \in \{y \in A, d(P_i(t), y) = d(P_i(t), A)\}$.

Proof. For clarity, we present the proof together with that of the next theorem. \square

Theorem B.16. Let $P \in \mathcal{S}^\Delta$. If (E, d) is a geodesic Polish space, A closed and $\forall x \in E$, $\{y \in A, d(x, y) = d(x, A)\}$ is non-empty.

Then $\forall i \in \{1, \dots, N_P\}$,

$$\forall T \in (0, 1),$$

$$\exists G_i^T \in s^\Delta : (I_i^P, \mathcal{Z}(\mathcal{B}(\mathbb{R})|_{I_i^P})) \longrightarrow (E, \mathcal{B}(E))$$

measurable, such that for λ -almost every $t \in I_i^P$,

$$G_i^T(t) \in \{G(P(t), p^i(t))(T)\}.$$

where $G(P(t), p^i(t))$ a d -geodesic from $P(t)$ to $p^i(t)$ as defined in Sec. IV-A of the main manuscript.

Proof. Let $i \in \{1, \dots, N_P\}$, and let Π the multivalued function from E to the set of non-empty subsets of E , defined as $\forall x \in E$,

$$\Pi(x) = \{y \in A, \text{ such that } d(x, y) = d(x, A)\}$$

Let's denote Γ_Π its graph, then Γ_Π is closed in $(E \times E, \mathcal{B}(E \times E))$

Indeed, we have

$$\Gamma_\Pi = \{(x, y) \in E^2, y \in A, d(x, y) = d(x, A)\}$$

Let $(x_n, y_n)_{n \in \mathbb{N}}$ a sequence in Γ_Π converging to $(x, y) \in E \times E$. Then,

$$\lim_{n \rightarrow +\infty} d(x_n, x) = \lim_{n \rightarrow +\infty} d(y_n, y) = 0$$

and so

$$\lim_{n \rightarrow +\infty} x_n = x, \quad \lim_{n \rightarrow +\infty} y_n = y$$

Moreover $y \in A$ because A is closed in (E, d) first-countable space (because metric), and because $\forall n \in \mathbb{N}, y_n \in A$.

Also, $d(x_n, y_n) = d(x_n, A)$ because

$$(x_n, y_n) \in \Gamma_\Pi$$

Then

$$\lim_{n \rightarrow +\infty} d(x_n, y_n) = \lim_{n \rightarrow +\infty} d(x_n, A)$$

So, because $d(\cdot, \cdot)$ and $d(\cdot, A)$ are continuous (because (E, d) is metric, then $d(\cdot, \cdot)$ is continuous and $d(\cdot, A)$ is 1-Lipschitz, and hence continuous) and $\lim_{n \rightarrow +\infty} x_n = x$, and $\lim_{n \rightarrow +\infty} y_n = y$, then $d(x, y) = d(x, A)$ by the sequential characterization of limits in metrizable spaces.

Finally, we have $(x, y) \in \Gamma_\Pi$ and so Γ_Π is closed in E^2 for the product topology, and then $\Gamma_\Pi \in \mathcal{B}(E^2)$.

Moreover E is a Polish space, then E^2 is a Polish space, and so a Souslin space.

Since Γ_Π is a Borel subset of the Souslin space E^2 , Γ_Π is a Souslin set.

Then, there exists a mapping

$$\tilde{\rho} : E \longrightarrow E \text{ that is measurable}$$

with respect to the σ -algebra $\sigma(\mathcal{S}_E)$ generated by all Souslin sets in E , and $\mathcal{B}(E)$, such that $\tilde{\rho}(\omega) \in \Pi(\omega), \forall \omega \in E$ [78].

Let us remember that the application $P_i : (I_i^P, \mathcal{Z}(\mathcal{B}(\mathbb{R})|_{I_i^P})) \rightarrow (E, \mathcal{B}(E)), t \mapsto P(t)$ is measurable by definition.

We denote $\mu^* = \lambda \circ P_i^{-1}$, the pushforward measure on $(E, \mathcal{B}(E))$, where λ is the Lebesgue measure on $(I_i^P, \mathcal{Z}(\mathcal{B}(\mathbb{R})|_{I_i^P}))$. We denote $(E, \mathcal{Z}(\mathcal{B}(E)))$ the completion of $(E, \mathcal{B}(E))$ for μ^* .

Since E is a Polish space, any Souslin set of E is an analytic set. Also, because any analytic set is universally measurable, and μ^* is a complete measure on $(E, \mathcal{Z}(\mathcal{B}(E)))$ that measures all Borel of E , then $\sigma(\mathcal{S}_E) \subset \mathcal{Z}(\mathcal{B}(E))$, and so $\tilde{\rho} : (E, \mathcal{Z}(\mathcal{B}(E))) \rightarrow (E, \mathcal{B}(E))$ is measurable.

Then there exists a measurable function $\rho : (E, \mathcal{B}(E)) \rightarrow (E, \mathcal{B}(E))$ which is μ^* -a.s. equal to $\tilde{\rho}$ (See the proof in the previous theorem).

So $p_i := \rho \circ P_i$ is measurable, with respect to $(I_i^P, \mathcal{Z}(\mathcal{B}(\mathbb{R})|_{I_i^P}))$, and $(E, \mathcal{B}(E))$, as a composition of measurable functions, and we can apply theorem B.14 with P_i and $p_i = \rho \circ P_i$ (the assumption $p_i \in s^\Delta$ is not needed in order to apply the theorem) to conclude the proof. \square

Remark : Many conditions allow the hypothesis, $\forall x \in E, \{y \in A, d(x, y) = d(x, A)\}$ non-empty, to be satisfied. Some examples are : A compact; $\forall x \in E, A \cap B(x, r+\epsilon)$ compact (with any $\epsilon \in \mathbb{R}_+^*$, and $r = d(x, A)$); (E,d) complete and $\forall x \in E, A \cap B(x, r+\epsilon)$ relatively compact; Heine-Borel E space; E complete connected Riemannian manifold; (E,d) complete length-metric space and locally compact.

Lemma B.17. *If (E, d) is a geodesic Polish space, then $(s^\Delta, D_\Delta^\alpha)$ is a geodesic metric space.*

Proof. Let $\rho, q \in s^\Delta$. Then there exist $P, Q \in \mathcal{S}^\Delta$ and indices $i \in \{1, \dots, N_P\}, j \in \{1, \dots, N_Q\}$ such that $\rho = P_i$ and $q = Q_j$. Write $a_i = \inf(I_i^P), b_i = \sup(I_i^P), c_j = \inf(I_j^Q),$ and $d_j = \sup(I_j^Q)$. By the definition of \mathcal{S}^Δ ,

$$b_i - a_i = d_j - c_j = \Delta.$$

For $T \in (0, 1)$, let $G_{i,j}^T \in s^\Delta$ be given by Theorem B.14, with $\inf I_{i,j}^T = (1-T) \cdot a_i + T \cdot c_j$, and $\sup I_{i,j}^T = (1-T) \cdot b_i + T \cdot d_j$. For $t \in (0, 1)$, set

$$\phi_P(t) = a_i \cdot (1-t) + b_i \cdot t \in I_i^P, \phi_Q(t) = c_j \cdot (1-t) + d_j \cdot t \in I_j^Q.$$

Since $b_i - a_i = d_j - c_j = \Delta$, we have

$$\phi_Q(t) = \phi_P(t) + c_j - a_i, \quad t \in (0, 1).$$

By Theorem B.14, for every $s \in I_i^P$,

$$G_{i,j}^T(s + \inf I_{i,j}^T - a_i) \in \{\gamma(P(s), Q(s + c_j - a_i))(T)\},$$

where $\gamma(x, y)$ denotes a constant-speed d -geodesic in E from x to y (for clarity in the following proof, we will no longer use the letter G to denote d -geodesics). Taking $s = \phi_P(t)$ and using $\phi_P(t) + c_j - a_i = \phi_Q(t)$ gives, for all $t \in (0, 1)$,

$$\begin{aligned} & G_{i,j}^T(\inf I_{i,j}^T \cdot (1-t) + \sup I_{i,j}^T \cdot t) \\ &= G_{i,j}^T((1-T) \cdot \phi_P(t) + T \cdot \phi_Q(t)) \\ &= \gamma(P(\phi_P(t)), Q(\phi_Q(t)))(T). \end{aligned}$$

Now let $0 \leq S < T \leq 1$. For $S, T \in (0, 1)$, by the constant-speed property of γ we obtain, for all $t \in (0, 1)$,

$$\begin{aligned} & d\left(G_{i,j}^S(\inf I_{i,j}^S(1-t) + \sup I_{i,j}^S t), \right. \\ & \quad \left. G_{i,j}^T(\inf I_{i,j}^T(1-t) + \sup I_{i,j}^T t)\right) \\ &= |T - S| d(P(\phi_P(t)), Q(\phi_Q(t))). \end{aligned}$$

Moreover, the left endpoints of $I_{i,j}^S$ and $I_{i,j}^T$ satisfy

$$\begin{aligned} \inf I_{i,j}^T - \inf I_{i,j}^S &= [(1-T) \cdot a_i + T \cdot c_j] \\ &\quad - [(1-S) \cdot a_i + S \cdot c_j] \\ &= (T - S)(c_j - a_i), \end{aligned}$$

so the temporal shift in D_Δ^α between $G_{i,j}^S$ and $G_{i,j}^T$ is $|T - S| \cdot |c_j - a_i|$.

By the definition of D_Δ^α (using the common parametrization $t \mapsto \inf I_{i,j}(1-t) + \sup I_{i,j} t$) we therefore have

$$\begin{aligned} D_\Delta^\alpha(G_{i,j}^S, G_{i,j}^T) &= \Delta \int_0^1 (1-\alpha) d(G_{i,j}^S(\cdots), G_{i,j}^T(\cdots)) dt \\ &+ \alpha \Delta |\inf I_{i,j}^T - \inf I_{i,j}^S| \end{aligned} \tag{70}$$

$$\begin{aligned} &= \Delta \int_0^1 (1-\alpha) |T - S| d(P(\phi_P(t)), Q(\phi_Q(t))) dt \\ &+ \alpha \Delta |T - S| |c_j - a_i| \end{aligned} \tag{71}$$

$$\begin{aligned} &= |T - S| \left[\Delta \int_0^1 (1-\alpha) d(P(\phi_P(t)), Q(\phi_Q(t))) dt \right. \\ &\quad \left. + \alpha \Delta |c_j - a_i| \right] \\ &= |T - S| \cdot D_\Delta^\alpha(P_i, Q_j). \end{aligned} \tag{72}$$

We now extend the definition to the endpoints by setting

$$G_{i,j}^0 := P_i, \quad G_{i,j}^1 := Q_j,$$

and define

$$g_{i,j} : [0, 1] \rightarrow s^\Delta, \quad g_{i,j}(T) = G_{i,j}^T.$$

Then for all $S, T \in [0, 1]$ we have

$$D_\Delta^\alpha(g_{i,j}(S), g_{i,j}(T)) = |T - S| D_\Delta^\alpha(P_i, Q_j),$$

so $g_{i,j}$ is a constant-speed geodesic in $(s^\Delta, D_\Delta^\alpha)$ joining $\rho = P_i$ to $q = Q_j$.

Since $\rho, q \in s^\Delta$ were arbitrary, this shows that $(s^\Delta, D_\Delta^\alpha)$ is a geodesic metric space.

Remark : We used in this proof that, for every $T \in (0, 1)$, and for every $t \in (0, 1)$, we have

$$G_{i,j}^T(\inf I_{i,j}^T \cdot (1-t) + \sup I_{i,j}^T \cdot t) \in \{\gamma(P(a_i \cdot (1-t) + b_i \cdot t), Q(c_j \cdot (1-t) + d_j \cdot t))(T)\}. \tag{73}$$

Indeed, as said previously, set $T \in (0, 1)$, by Theorem B.14, $\forall s \in (a_i, b_i)$ we have

$$\begin{aligned} & G_{i,j}^T(s + \inf I_{i,j}^T - a_i) \\ & \in \{\gamma(P(s), Q(s + c_j - a_i))(T)\}. \end{aligned} \tag{74}$$

Then, because,

$$\phi_P : (0, 1) \rightarrow (a_i, b_i), \quad \phi_P(t) = a_i \cdot (1-t) + b_i \cdot t, \tag{75}$$

$$\phi_Q : (0, 1) \rightarrow (c_j, d_j), \quad \phi_Q(t) = c_j \cdot (1-t) + d_j \cdot t, \tag{76}$$

we have for $t \in (0, 1)$,

$$\begin{aligned}
& G_{i,j}^T(s + \inf I_{i,j}^T - a_i) \\
& \in \{\gamma(P(s), Q(s + c_j - a_i))(T)\} \\
& \implies G_{i,j}^T(\phi_P(t) + ((1-T)a_i + Tc_j) - a_i) \\
& \in \{\gamma(P(\phi_P(t)), Q(\phi_P(t) + c_j - a_i))(T)\} \\
& \implies G_{i,j}^T((1-T)\phi_P(t) + T(c_j + \phi_P(t) - a_i)) \\
& \in \{\gamma(P(\phi_P(t)), Q(c_j + (b_i - a_i)t))(T)\} \\
& \implies G_{i,j}^T((1-T)\phi_P(t) + T(c_j + (b_i - a_i)t)) \\
& \in \{\gamma(P(\phi_P(t)), Q(c_j + (b_i - a_i)t))(T)\} \\
& \implies G_{i,j}^T((1-T)\phi_P(t) + T(c_j + (d_j - c_j)t)) \\
& \in \{\gamma(P(\phi_P(t)), Q(c_j + (d_j - c_j)t))(T)\} \\
& \implies G_{i,j}^T((1-T)\phi_P(t) + T(c_j(1-t) + d_jt)) \\
& \in \{\gamma(P(\phi_P(t)), Q(c_j(1-t) + d_jt))(T)\} \\
& \implies G_{i,j}^T((1-T)\phi_P(t) + T(\phi_Q(t))) \\
& \in \{\gamma(P(\phi_P(t)), Q(\phi_Q(t)))(T)\} \\
& \implies G_{i,j}^T((1-T)(a_i(1-t) + b_i t) + T(c_j(1-t) + d_jt)) \\
& \in \{\gamma(P(\phi_P(t)), Q(\phi_Q(t)))(T)\} \\
& \implies G_{i,j}^T([(1-T)a_i + Tc_j](1-t) + [(1-T)b_i + Td_j]t) \\
& \in \{\gamma(P(\phi_P(t)), Q(\phi_Q(t)))(T)\} \\
& \implies G_{i,j}^T(\inf I_{i,j}^T(1-t) + \sup I_{i,j}^T t) \\
& \in \{\gamma(P(\phi_P(t)), Q(\phi_Q(t)))(T)\}.
\end{aligned}$$

To make the proof more concrete, we now compute the length of $g_{i,j}$ using uniform partitions of $[0, 1]$, indeed let $N \in \mathbb{N}^*$, then

$$\sum_{k=0}^{N-1} D_\Delta^\alpha(G_{i,j}^{k/N}, G_{i,j}^{(k+1)/N}) \quad (77)$$

$$\begin{aligned}
& = \sum_{k=0}^{N-1} \Delta \cdot \int_0^1 (1-\alpha) \cdot d\left(G_{i,j}^{k/N}(\inf I_{i,j}^{k/N} \cdot (1-t) + \sup I_{i,j}^{k/N} \cdot t), G_{i,j}^{(k+1)/N}(\inf I_{i,j}^{(k+1)/N} \cdot (1-t) + \sup I_{i,j}^{(k+1)/N} \cdot t)\right) dt + \alpha \cdot |c_j - a_i| \cdot \frac{\Delta + k \cdot (\Delta - \Delta)}{N} \\
& = \sum_{k=0}^{N-1} \Delta \cdot \int_0^1 (1-\alpha) \cdot \frac{1}{N} d(P(a_i \cdot (1-t) + b_i \cdot t), Q(c_j \cdot (1-t) + d_j \cdot t)) dt + \alpha \cdot \frac{|c_j - a_i|}{N}
\end{aligned} \quad (78)$$

$$\begin{aligned}
& Q(c_j \cdot (1-t) + d_j \cdot t) dt + \alpha \cdot \frac{|c_j - a_i|}{N} \\
& = \sum_{k=0}^{N-1} \frac{1}{N} \cdot D_\Delta^\alpha(P_i, Q_j) = D_\Delta^\alpha(P_i, Q_j).
\end{aligned} \quad (80)$$

Moreover, we have

$$\lim_{N \rightarrow +\infty} D_\Delta^\alpha(G_{i,j}^{k/N}, G_{i,j}^{(k+1)/N}) \quad (81)$$

$$= \lim_{N \rightarrow +\infty} \frac{1}{N} \cdot D_\Delta^\alpha(P_i, Q_j) = 0, \quad (82)$$

Thus finally, with $g_{i,j}$ the map defined by,

$$g_{i,j} : [0, 1] \longrightarrow s^\Delta, \quad T \longmapsto g_{i,j}(T) = G_{i,j}^T,$$

we have $g_{i,j}$ continuous, and

$$\sup \sum_{i=0}^k D_\Delta^\alpha(g_{i,j}(T_i), g_{i,j}(T_{i+1})) = D_\Delta^\alpha(P_i, Q_j), \quad (83)$$

(where the supremum is taken over all $k \in \mathbb{N}^*$, and all sequences $T_0 = 0 < T_1 < \dots < T_k = 1$ in $[0, 1]$), so $g_{i,j}$ is a geodesic. \square

Theorem B.18. If (E, d) is a geodesic Polish space, and $A \subsetneq E$ is closed such that, $\forall x \in E, \{y \in A, d(x, y) = d(x, A)\}$ is non-empty, then

$$(S^\Delta, \text{CED}_{\alpha,1}^\Delta)$$

is a geodesic space.

Proof. Let $P \in S^\Delta, Q \in S^\Delta$, with optimal partial assignment $f \in \mathcal{A}^\Delta(P, Q)$. If $\ell \in [0, L_{1/3}]$, then let $\tilde{G}^\ell = (\tilde{G}_i^\ell)_{1 \leq i \leq N_P^\Delta} \in S^\Delta$ defined by

$$\forall i \in \mathcal{S}_P, \quad \tilde{G}_i^\ell = P_i, \text{ and } \forall i \in \mathcal{D}_P, \quad \tilde{G}_i^\ell = G_i^{\frac{\ell}{L_{1/3}}}, \quad (84)$$

as defined in Theorem B.16 for P_i , from P_i to A (i.e., $p_i = \rho \circ P_i$).

If $\ell = L_{1/3}$, let

$$\tilde{G}^\ell = P \setminus \{P_i, i \in \mathcal{D}_P\}. \quad (85)$$

Let (ℓ_j) be a sequence in $[0, L_{1/3}]$ such that

$$\ell_0 = 0 < \ell_1 < \dots < \ell_K = L_{1/3}.$$

Then,

$$\begin{aligned}
& \sum_{j=0}^{K-1} \text{CED}_{\alpha,1}^\Delta(\tilde{G}^{\ell_j}, \tilde{G}^{\ell_{j+1}}) \\
& \leq \sum_{j=0}^{K-2} \sum_{i=0}^{N_P^\Delta} D_\Delta^\alpha(\tilde{G}_i^{\ell_j}, \tilde{G}_i^{\ell_{j+1}}) + \sum_{i \in \mathcal{D}_P} D_\Delta^\alpha(\tilde{G}_i^{\ell_{K-1}}, A).
\end{aligned} \quad (86)$$

Moreover,

$$\begin{aligned}
& \sum_{j=0}^{K-2} \sum_{i \in \mathcal{D}_P} D_\Delta^\alpha(\tilde{G}_i^{\ell_j}, \tilde{G}_i^{\ell_{j+1}}) + \sum_{i \in \mathcal{D}_P} D_\Delta^\alpha(\tilde{G}_i^{\ell_{K-1}}, A) \\
& = \sum_{j=0}^{K-2} \sum_{i \in \mathcal{D}_P} \frac{\ell_{j+1} - \ell_j}{L_{1/3}} \cdot D_\Delta^\alpha(P_i, A) + \sum_{i \in \mathcal{D}_P} D_\Delta^\alpha(\tilde{G}_i^{\ell_{K-1}}, A) \\
& = \frac{1}{L_{1/3}} \sum_{i \in \mathcal{D}_P} D_\Delta^\alpha(P_i, A) \sum_{j=0}^{K-2} (\ell_{j+1} - \ell_j) \\
& \quad + \sum_{i \in \mathcal{D}_P} \frac{\ell_K - \ell_{K-1}}{L_{1/3}} \cdot D_\Delta^\alpha(P_i, A) \\
& = \frac{1}{L_{1/3}} \sum_{i \in \mathcal{D}_P} \left[D_\Delta^\alpha(P_i, A) \left(\sum_{j=0}^{K-2} (\ell_{j+1} - \ell_j) \right) \right. \\
& \quad \left. + (\ell_K - \ell_{K-1}) \right] \\
& = \frac{1}{L_{1/3}} \sum_{i \in \mathcal{D}_P} D_\Delta^\alpha(P_i, A) \cdot L_{1/3} \\
& = \sum_{i \in \mathcal{D}_P} D_\Delta^\alpha(P_i, A)
\end{aligned}$$

Then,

$$\sup \sum \text{CED}_{\alpha,1}^\Delta(\tilde{G}^{\ell_j}, \tilde{G}^{\ell_{j+1}}) \leq \sum_{i \in \mathcal{D}_P} D_\Delta^\alpha(P_i, A) \quad (87)$$

where the supremum is taken over all $K \in \mathbb{N}^*$, and all sequences $\ell_0 = 0 < \ell_1 < \dots < \ell_K = L_{1/3}$ in $[0, L_{1/3}]$.

Moreover,

$$\begin{aligned}
\sum_{j=0}^{K-1} \text{CED}_{\alpha,1}^{\Delta}(\tilde{G}^{\ell_j}, \tilde{G}^{\ell_{j+1}}) &\geq \text{CED}_{\alpha,1}^{\Delta}(\tilde{G}^0, \tilde{G}^{L_{1/3}}) \\
&= \text{CED}_{\alpha,1}^{\Delta}(P, \tilde{G}^{L_{1/3}}) \\
&= \text{CED}_{\alpha,1}^{\Delta}(P, P \setminus \{P_i, i \in \mathcal{D}_P\}) \\
&= \sum_{i \in \mathcal{D}_P} D_{\Delta}^{\alpha}(P_i, A)
\end{aligned} \tag{88}$$

Indeed, if $f \in \mathcal{A}^{\Delta}(P, Q)$ is optimal, then

$$f^* \in \mathcal{A}^{\Delta}(P, \{Q_{f(i)} \mid i \in \mathcal{S}_P\})$$

defined as

$$\begin{aligned}
f^* : \{1, \dots, N_P^{\Delta}\} &\rightarrow \{j \text{ such that } \exists i \in \{1, \dots, N_P^{\Delta}\}, \\
&\quad j = f(i)\}, \\
&i \mapsto f(i)
\end{aligned} \tag{89}$$

and it is optimal for $(P, \{Q_{f(i)}, i \in \mathcal{S}_P\})$. Indeed, by contradiction, if another one were optimal instead, this would induce an optimal assignment for (P, Q) with a cost smaller than f , which would contradict the fact that f is optimal for (P, Q) .

Moreover, since f^* is optimal for $(P, \{Q_{f(i)}, i \in \mathcal{S}_P\})$, we have

$$\begin{aligned}
f^{**} &\in \mathcal{A}^{\Delta}(P, \tilde{G}^{L_{1/3}}) \text{ defined as} \\
f^{**} : i \in \{1, \dots, N_P^{\Delta}\} &\rightarrow \mathcal{S}_P, \\
&i \mapsto i, \text{ if } i \in \mathcal{S}_P
\end{aligned} \tag{90}$$

and it is optimal. Indeed, f^* is optimal for $(P, \{Q_{f(i)}, i \in \mathcal{S}_P\})$. Thus, for every $i \in \mathcal{S}_P$, if we move $Q_{f(i)}$ towards P_i , then the cost of the assignment decreases and remains optimal; in the limit, we reach P_i , which gives the optimal assignment f^{**} between P and $\tilde{G}^{L_{1/3}}$, with cost

$$\sum_{i \in \mathcal{D}_P} D_{\Delta}^{\alpha}(P_i, A).$$

Thus, we finally obtain

$$\sup \sum_{j=0}^{K-1} \text{CED}_{\alpha,1}^{\Delta}(\tilde{G}^{\ell_j}, \tilde{G}^{\ell_{j+1}}) = \sum_{i \in \mathcal{D}_P} D_{\Delta}^{\alpha}(P_i, A). \tag{91}$$

Moreover, the map

$$G_D : [0, L_{1/3}] \rightarrow \mathcal{S}^{\Delta}, \quad \ell \mapsto \tilde{G}^{\ell}$$

is trivially uniformly continuous by construction, since

$$\begin{aligned}
\lim_{\ell \rightarrow L} \text{CED}_{\alpha,1}^{\Delta}(\tilde{G}^{\ell}, \tilde{G}^L) &\leq \lim_{\ell \rightarrow L} \sum_{i \in \mathcal{D}_P} D_{\Delta}^{\alpha}(\tilde{G}_i^{\ell}, \tilde{G}_i^L) \\
&= \lim_{\ell \rightarrow L} \frac{1}{L_{1/3}} \sum_{i \in \mathcal{D}_P} |\ell - L| D_{\Delta}^{\alpha}(P_i, A) = 0.
\end{aligned} \tag{92}$$

Next, if $\ell \in [L_{1/3}, L_{2/3}]$, then let

$$\begin{aligned}
\tilde{G}^{\ell} &= (\tilde{G}_i^{\ell})_{1 \leq i \leq N_P^{\Delta}, i \in \mathcal{S}_P} \in \mathcal{S}^{\Delta} \quad \text{defined by} \\
\forall i \in \mathcal{S}_P, \quad \tilde{G}_i^{\ell} &= G_{i,f(i)}^{\frac{\ell - L_{1/3}}{L_{2/3} - L_{1/3}}}
\end{aligned}$$

as defined in Theorem B.14, from P_i to $Q_{f(i)}$.

Let $(\ell_j)_{0 \leq j \leq K \in \mathbb{N}^*}$ be a sequence in $[L_{1/3}, L_{2/3}]$ such that

$$\ell_0 = L_{1/3} < \ell_1 < \dots < \ell_K = L_{2/3}.$$

Then,

$$\sum_{j=0}^{K-1} \text{CED}_{\alpha,1}^{\Delta}(\tilde{G}^{\ell_j}, \tilde{G}^{\ell_{j+1}}) \leq \sum_{j=0}^{K-1} \sum_{i \in \mathcal{S}_P} D_{\Delta}^{\alpha}(\tilde{G}_i^{\ell_j}, \tilde{G}_i^{\ell_{j+1}}). \tag{93}$$

Moreover,

$$\begin{aligned}
\sum_{j=0}^{K-1} \sum_{i \in \mathcal{S}_P} D_{\Delta}^{\alpha}(\tilde{G}_i^{\ell_j}, \tilde{G}_i^{\ell_{j+1}}) &= \sum_{j=0}^{K-1} \sum_{i \in \mathcal{S}_P} \left(\frac{\ell_{j+1} - \ell_j}{L_{2/3} - L_{1/3}} \right) D_{\Delta}^{\alpha}(P_i, Q_{f(i)}) \\
&= \frac{1}{L_{2/3} - L_{1/3}} \sum_{i \in \mathcal{S}_P} D_{\Delta}^{\alpha}(P_i, Q_{f(i)}) \sum_{j=0}^{K-1} (\ell_{j+1} - \ell_j) \\
&= \frac{1}{L_{2/3} - L_{1/3}} \sum_{i \in \mathcal{S}_P} D_{\Delta}^{\alpha}(P_i, Q_{f(i)})(L_{2/3} - L_{1/3}) \\
&= \sum_{i \in \mathcal{S}_P} D_{\Delta}^{\alpha}(P_i, Q_{f(i)}).
\end{aligned} \tag{94}$$

Thus,

$$\sup \sum_{j=0}^{K-1} \text{CED}_{\alpha,1}^{\Delta}(\tilde{G}^{\ell_j}, \tilde{G}^{\ell_{j+1}}) \leq \sum_{i \in \mathcal{S}_P} D_{\Delta}^{\alpha}(P_i, Q_{f(i)}). \tag{95}$$

where the supremum is taken over all $K \in \mathbb{N}^*$ and all sequences

$$\ell_0 = L_{1/3} < \ell_1 < \dots < \ell_K = L_{2/3} \quad \text{in } [L_{1/3}, L_{2/3}].$$

Moreover,

$$\begin{aligned}
\sum_{j=0}^{K-1} \text{CED}_{\alpha,1}^{\Delta}(\tilde{G}^{\ell_j}, \tilde{G}^{\ell_{j+1}}) &\geq \text{CED}_{\alpha,1}^{\Delta}(\tilde{G}^{L_{1/3}}, \tilde{G}^{L_{2/3}}) \\
&= \text{CED}_{\alpha,1}^{\Delta}(P \setminus \{P_i, i \in \mathcal{D}_P\}, \\
&\quad \{Q_{f(i)}, i \in \mathcal{S}_P\}) \\
&= \sum_{i \in \mathcal{S}_P} D_{\Delta}^{\alpha}(P_i, Q_{f(i)}),
\end{aligned} \tag{96}$$

again by contradiction.

Then,

$$\sup \sum_{j=0}^{K-1} \text{CED}_{\alpha,1}^{\Delta}(\tilde{G}^{\ell_j}, \tilde{G}^{\ell_{j+1}}) = \sum_{i \in \mathcal{S}_P} D_{\Delta}^{\alpha}(P_i, Q_{f(i)}). \tag{97}$$

Moreover,

$$G_S : [L_{1/3}, L_{2/3}] \rightarrow \mathcal{S}^{\Delta}, \quad \ell \mapsto \tilde{G}^{\ell}$$

is trivially continuous by construction, since

$$\begin{aligned}
\lim_{\ell \rightarrow L} \text{CED}_{\alpha,1}^{\Delta}(\tilde{G}^{\ell}, \tilde{G}^L) &\leq \lim_{\ell \rightarrow L} \sum_{i \in \mathcal{S}_P} D_{\Delta}^{\alpha}(\tilde{G}_i^{\ell}, \tilde{G}_i^L) \\
&= \frac{1}{L_{2/3} - L_{1/3}} \lim_{\ell \rightarrow L} \sum_{i \in \mathcal{S}_P} |\ell - L| D_{\Delta}^{\alpha}(P_i, Q_{f(i)}) \\
&= 0.
\end{aligned} \tag{98}$$

Finally, if $\ell \in (L_{2/3}, L_{3/3}]$, then let

$$\tilde{G}^{\ell} = (\tilde{G}_i^{\ell})_{1 \leq i \leq N_Q^{\Delta}} \in \mathcal{S}^{\Delta} \text{ defined by}$$

$$\forall i \notin \mathcal{I}_Q, \quad \tilde{G}_i^{\ell} = Q_i, \quad \text{and } \forall i \in \mathcal{I}_Q, \quad \tilde{G}_i^{\ell} = G_i^{\frac{\ell - L_{2/3}}{L_{3/3} - L_{2/3}}}$$

as defined in Theorem B.16 for Q_i , but from A (i.e., $p_i = \rho \circ Q_i$) to Q_i .

Let $(\ell_j)_{0 \leq j < K \in \mathbb{N}^*}$ be a sequence in $[L_{2/3}, L_{3/3}]$ such that

$$\ell_0 = L_{2/3} < \ell_1 < \dots < \ell_K = L_{3/3}.$$

Then,

$$\sum_{j=0}^{K-1} \text{CED}_{\alpha,1}^{\Delta}(\tilde{G}^{\ell_j}, \tilde{G}^{\ell_{j+1}}) \leq \sum_{j=1}^{K-1} \sum_{i=0}^{N_Q^{\Delta}} D_{\Delta}^{\alpha}(\tilde{G}_i^{\ell_j}, \tilde{G}_i^{\ell_{j+1}}) + \sum_{i \in \mathcal{I}_Q} D_{\Delta}^{\alpha}(\tilde{G}_i^{\ell_1}, A). \quad (99)$$

$$\begin{aligned} &= \left(\sum_{j=1}^{K-1} \sum_{i \in \mathcal{I}_Q} D_{\Delta}^{\alpha}(\tilde{G}_i^{\ell_j}, \tilde{G}_i^{\ell_{j+1}}) \right) + \sum_{i \in \mathcal{I}_Q} D_{\Delta}^{\alpha}(\tilde{G}_i^{\ell_1}, A) \\ &= \left(\sum_{j=1}^{K-1} \sum_{i \in \mathcal{I}_Q} \frac{(\ell_{j+1} - \ell_j)}{L_{3/3} - L_{2/3}} D_{\Delta}^{\alpha}(Q_i, A) \right) + \sum_{i \in \mathcal{I}_Q} D_{\Delta}^{\alpha}(\tilde{G}_i^{\ell_1}, A) \\ &= \left(\frac{1}{L_{3/3} - L_{2/3}} \sum_{i \in \mathcal{I}_Q} D_{\Delta}^{\alpha}(Q_i, A) \sum_{j=1}^{K-1} (\ell_{j+1} - \ell_j) + \sum_{i \in \mathcal{I}_Q} \frac{\ell_1 - \ell_0}{L_{3/3} - L_{2/3}} D_{\Delta}^{\alpha}(Q_i, A) \right) \\ &= \frac{1}{L_{3/3} - L_{2/3}} \sum_{i \in \mathcal{I}_Q} \left(D_{\Delta}^{\alpha}(Q_i, A) \left(\sum_{j=1}^{K-1} (\ell_{j+1} - \ell_j) + (\ell_1 - \ell_0) \right) \right) \\ &= \sum_{i \in \mathcal{I}_Q} D_{\Delta}^{\alpha}(Q_i, A). \end{aligned}$$

Then

$$\sup \sum_{j=0}^{K-1} \text{CED}_{\alpha,1}^{\Delta}(\tilde{G}^{\ell_j}, \tilde{G}^{\ell_{j+1}}) \leq \sum_{i \in \mathcal{I}_Q} D_{\Delta}^{\alpha}(Q_i, A). \quad (100)$$

where the supremum is taken over all $K \in \mathbb{N}^*$ and all sequences $\ell_0 = L_{2/3} < \ell_1 < \dots < \ell_K = L_{3/3}$ in $[L_{2/3}, L_{3/3}]$.

Moreover,

$$\sum_{j=0}^{K-1} \text{CED}_{\alpha,1}^{\Delta}(\tilde{G}^{\ell_j}, \tilde{G}^{\ell_{j+1}}) \geq \text{CED}_{\alpha,1}^{\Delta}(\tilde{G}^{L_{2/3}}, \tilde{G}^{L_{3/3}}). \quad (101)$$

$$\begin{aligned} &= \text{CED}_{\alpha,1}^{\Delta}(\tilde{G}^{L_{2/3}}, Q) \\ &= \text{CED}_{\alpha,1}^{\Delta}(\{Q_{f(i)} \mid i \in \mathcal{S}_P\}, Q) \\ &= \sum_{i \in \mathcal{I}_Q} D_{\Delta}^{\alpha}(Q_i, A) \end{aligned}$$

(by the same argument as previously).

We thus obtain

$$\sum_{j=0}^{K-1} \text{CED}_{\alpha,1}^{\Delta}(\tilde{G}^{\ell_j}, \tilde{G}^{\ell_{j+1}}) = \sum_{i \in \mathcal{I}_Q} D_{\Delta}^{\alpha}(Q_i, A). \quad (102)$$

Moreover, $G_I : [L_{2/3}, L_{3/3}] \rightarrow \mathcal{S}^{\Delta}$, $\ell \mapsto \tilde{G}^{\ell}$ is continuous, again by the same argument as previously.

By concatenating the three continuous paths G_D , G_S , and G_I , we obtain a continuous path G of length $\text{CED}_{\alpha,1}^{\Delta}(P, Q)$ such that $G(0) = P$ and $G(L_{3/3}) = Q$. \square

APPENDIX C DATA SPECIFICATION

This section catalogues the ensemble datasets used in our study. For each dataset, we report its provenance, the format in which we handle it, any preprocessing applied, and the associated ground-truth classification. All ensembles were obtained from publicly available sources.

To streamline reproducibility, we supply scripts that automatically (i) retrieve the data, (ii) run the TTK pipeline for preprocessing, and (iii) export standardized VTK files embedding the ground-truth labels as VTK “Field Data.” For convenience, we also publish a ready-to-use archive containing the curated ensembles in VTK format. All scripts and curated data are available at: <https://github.com/sebastien-tchitchek/ContinuousEditDistance>. In addition, the code package ships with the full sets of TVPDs computed from these inputs.

A. Asteroid impact

Asteroid Impact (SciVis Contest 2018) comprises six timed PL-scalar fields—YA11, YB11, YC11, YA31, YB31, YC31 sequences—totaling approximately 300 GB. The raw data are available at: <https://oceans11.lanl.gov/deepwaterimpact/>. Each member simulates either a direct ocean impact or an atmospheric airburst whose blast wave interacts with the sea surface. Two asteroid diameters are explored (first digit 1 \rightarrow 100 m; 3 \rightarrow 250 m) and three impact/airburst altitudes A: sea-surface impact; B: explosion at 5 km; C explosion at 10 km). We analyze the matter-density scalar field, which clearly separates asteroid, water, and ambient air. This ensemble is a parameter study; here we examine how the asteroid’s size affects the resulting wave. In our pipeline, salient maxima capture effectively the asteroid and large water splashes; thus, each member is represented as a time series of persistence diagrams of maxima. The ground-truth labels group members by asteroid diameter, so the classification task is to assign each series to its correct diameter class. The ground-truth classification is as follows:

- **Class 1** (3 members): ya11, yb11, yc11
- **Class 2** (3 members): ya31, yb31, yc31

B. Sea surface height

This ensemble contains 48 members provided as 2D regular grids at 1440 \times 720 resolution. Each member is a global sea-surface height observation acquired in January, April, July, and October 2012. The raw data can be found at the following address: https://apdrc.soest.hawaii.edu/erddap/griddap/hawaii_soest_90b3_314d_ab45.html. The ensemble has been used in prior work [32], [79], [80], and corresponding VTK files and persistence diagrams are available at <https://github.com/julesvidal/wasserstein-pd-barycenter>. The features of interest are ocean eddy centers, which are reliably captured by height extrema. Accordingly, each observation can be represented by a persistence-diagram representation of the ssh field. The ground truth groups observations by month—four classes (January, April, July, October) representative of seasons—so the task is to identify, for any given observation, its correct month/season. Concretely in our TVPD setting, we consider the four time series of 12 observations/diagrams (one series per month). Next, each monthly series is further split by taking alternating time stamps (even/odd indices), yielding eight sub-series of six observations each; these naturally cluster into four groups—one per month—each grouping the two sub-series derived from the same month. The ground-truth labels are:

- **Class 1** (2 members): 201201-even, 201201-odd
- **Class 2** (2 members): 201204-even, 201201-odd
- **Class 3** (2 members): 201207-even, 201201-odd
- **Class 4** (2 members): 201210-even, 201201-odd

C. VESTEC

In VESTEC [70], space weather—understood here as the collection of physical phenomena in the solar system, particularly

near Earth, with emphasis on magnetic and radiative effects—is investigated through the analysis of magnetic reconnection events in the magnetosphere. Given the complexity of these processes, only standard theoretic simulations are currently performed. Accordingly, an ensemble of 3D magnetic-reconnection simulations was generated under varied initial conditions, with the project’s goal being to build a simulation-and-analysis pipeline for decision support during catastrophic events. In previous work [70], four simulation runs were executed on the same 3D domain ($128 \times 64 \times 64$) for 2,500 time steps, with distinct input parameter sets (variations of the initial magnetic field and particle types present in the domain). The code used for these simulations is available at: <https://github.com/KTH-HPC/iPIC3D>. For every time step in each run, the persistence diagram of the magnetic-field magnitude were computed, yielding a corpus of 10,000 diagrams archived in a Cinema database. In our TVPDs application context, we embedded these four simulations into three dimensions using multidimensional scaling (MDS); within each run, we then selected a subsequence so that the runs separated clearly into two clusters under the MDS embedding. Specifically, we retained similar subsequences for simulations 1–2 and for simulations 3–4, ensuring that these two groups were well separated. The ground-truth classification is:

- **Class 1** (2 members): VESTEC1, VESTEC2
- **Class 2** (3 members): VESTEC3, VESTEC4

APPENDIX D PARAMETER SETTINGS

This appendix details the parameter settings used in the experiments reported in the main text. Beyond these specific choices, the discussion is intended as a practical guideline for selecting α , Δ , η and β when applying CED to other TVPD datasets.

Parameter settings. In all experiments, we fix $\alpha < 10^{-4}$. This choice is motivated by the fact that, across all datasets considered, temporal distances between time samples in the TVPDs to be compared are several orders of magnitude larger than the W_2 distances between the persistence diagrams composing these TVPDs. Setting α to such a small value lets the Wasserstein term dominate the metric, so that $\text{CED}_{\alpha,\beta}^{\Delta}$ essentially compares TVPDs through their topological content while still respecting their temporal structure. The same value of α was enforced for the other dissimilarity measures (L2, Fréchet, TWED, DTW) in our MDS-based clustering experiment.

As discussed in the main manuscript (see Sec. III-D and Sec. III-G), from a theoretical standpoint the most relevant choice is to take Δ as small as possible, in order to increase the resolution of the assignments, and to set $\eta = \Delta$, which simplifies the computations. However, in practice this has to be balanced against reasonable running times. A simple practical strategy is to fix a target average number of Δ -subdivisions per input TVPD in the sample (e.g., 100), and then choose Δ so that the resulting TVPDs have approximately this average number of subdivisions. In our experiments, we adopt a more data-adaptive protocol in which the number of Δ -subdivisions, and hence the values of Δ and η , adapts to the input data in order to obtain more accurate numerical approximations. For these experiments, the protocol is as follows: for each dataset in our clustering study, we choose a common approximation tolerance $\varepsilon > 0$. We then select a subdivision step Δ satisfying $\Delta < \min_V \frac{\varepsilon}{(1-\alpha) K_V (t_{NV} - t_0)}$, (recall that $\eta \leq \Delta$ by construction) where the minimum is taken over all TVPDs V in the dataset (see Sec. III-G of the main manuscript for the definitions of K_V and t_{NV}), and we set $\eta = \Delta$. This guarantees that, for all input TVPDs in the dataset, the corresponding piecewise-constant approximation incurs a $\text{CED}_{\alpha,\beta}^{\Delta}$ error on the order of ε . To select the tolerance ε for a dataset, we first fixed a moderately small subdivision step Δ (and set $\eta = \Delta$, as discussed above) and computed all the pairwise $\text{CED}_{\alpha,\beta}^{\Delta}$ distances between the input TVPDs in the sample. We then inspected the typical scale of these distances and chose ε as a small fraction of that scale (e.g., significantly smaller than the typical pairwise distance, typically on the order of one fiftieth to one hundredth of that scale in practice,

depending on the available computational resources), so that the error introduced by the piecewise-constant approximation remained small relative to the scale of the $\text{CED}_{\alpha,\beta}^{\Delta}$ distances within the dataset. This procedure yields $\Delta = 0.1$ for sea-surface height, $\Delta = 0.25$ for VESTEC, and $\Delta = 1000$ for asteroid impact.

For the tracking experiments, which were all conducted on the asteroid impact dataset, the subdivision step Δ (and hence η as well, with $\eta = \Delta$) was further reduced in order to increase the resolution of the optimal assignments and to more precisely highlight the accuracy of pattern synchronization achieved by CED, whether in the temporal-shift-recovery ($\Delta = 250$) or pattern-search setting ($\Delta = 500$).

Finally, we fix $\beta = 1$ by default in all experiments, consistently with our geodesic construction, so that all reported results rely on the same CED geometry and are directly comparable.